UNIVERSITÀ DEGLI STUDI DI TRIESTE

UNIVERSITÀ CA' FOSCARI DI VENEZIA

XXXIV CICLO DEL DOTTORATO DI RICERCA IN
CHIMICA

DOTTORATO IN COLLABORAZIONE CON ISTITUTO ITALIANO DI TECNOLOGIA

ZEIN-BASED HYDROPHOBIC COATING: FROM PROMISING PROPERTIES TO FIELD APPLICATION

Settore scientifico-disciplinare: CHIM/12 - CHIMICA DELL'AMBIENTE E DEI BENI CULTURALI

DOTTORANDA

MARGHERITA ZUCCHELLI

COORDINATORE

PROF. ENZO ALESSIO

SUPERVISORI DI TESI

PROF. ELISABETTA ZENDRI

DR. ATHANASSIA ATHANASSIOU

ANNO ACCADEMICO 2020/2021

Contents

Synopsis

The protection of stone materials is one of the most important and critical aspects for the conservation of outdoor architectural monuments. Even though various synthetic polymers have been widely used for the protection of historical monuments it is now clear that their degradation processes lead to serious problems on the treated surfaces and they can hardly be removed. The aim of the present work is to develop new materials as protective coatings for stone cultural heritage. This thesis will focus on the development of an innovative material based on biopolymers and non-toxic solvents. Biopolymers replaced synthetic polymers in many applications and fields (such as food packaging, cosmetics and medicine) due to their good properties of reversibility, biodegradability and eco-sustainability. The application of biopolymers in cultural heritage field is, instead, quite recent and often the products and methodologies are borrowed from other fields. This is the case of zein, the protein used for the production of the developed coating. Zein is mainly used in food packaging and pharmaceutical field but could represent a suitable alternative to meet the requirements for the protection of historical building materials, such as non-toxicity and reversibility.

This study is the result of the close collaboration between the Smart Materials group of Istituto Italiano di Tecnologia (IIT) in Genova, the Center for Cultural Heritage Technology (CCHT@Ca' Foscari), the research group of Dipartimento di Scienze Ambientali, Informatica e Statistica (DAIS) in Università Ca' Foscari of Venezia, and Univeristà degli Studi di Trieste. Polymeric manufacturing and several chemical, physical, and mechanical characterization techniques were carried out in Smart Materials group in IIT. Ca' Foscari team contributed with long-standing knowledge of the building materials and of the specific and crucial requirements of their preservation, which is the base for designing compatible conservation interventions. Trieste University offered several educational events and opportunities for dialogue and exchange. The promising results obtained thanks to this collaboration are summarized and illustrated in the present work, which has been structured as follow:

- The first part (Introduction) is dedicated to illustrate the main characteristics of natural stone for buildings and decoration of architectural monuments in Cultural Heritage; their characteristics and the chemical-physical decay processes, which may occur with the exposure of these materials to weathering factors, are explained. Then, the chapter illustrates the protective treatments reported in literature and the necessity of promoting the use of green materials and methodologies. Finally, in light of all these elements, the aim of the research is illustrated.

- In the second part (Development of a novel zein-based formulation), zein is proposed for the development of a transparent and hydrophobic formulation. Zein characteristics, which guided in its choise for the development of the new material are illustrated. The methodology followed for zein purification and for the preparation of the novel formulation are presented in this part. Moreover, a detailed study of the influence of coating fabrication method on the hydrophobic character of polymeric solution is described, through the study of protein secondary structure.

- In the third part (Investigation of zein formulation performance as a protective), the effectiveness of the developed coating when applied on stone material is evaluated. The methodology used to apply the coating, the choice of the stone substrate and its preparation are presented. The way in which the coating is distributed over the stone, its morphology, adhesion and its thickness are here evaluated. Results in terms of hydrophobicity, water uptake and water vapor permeability are also shown and discussed in in this part.

- The fourth part (Applicability of the zein-based coating) focuses on the actual applicability of the developed material as a protective for buildings and monuments protection. Results of artificial ageing, biocolonisation, biodegradability and removability tests are reported in this part. The tests aimed at verify the long-term serviceability and the possible removability of the treatment in case of need. Moreover a preliminary implementation for a future Life Cycle Assessment of the developed material is proposed.

- The last part summarizes the results obtained throughout this study and outlines possible future developments and applications of this research.

1. Introduction

Natural stone has been used for constructive and artistic purposes since dawn of civilization. The earliest stone structure built by humans dates back at the Stonehenge site, realized approximately around 2500 BC. Despite the vast variety of other building materials appeared in architecture over time, such as bricks, earth materials, gypsum and concrete, the multilateral values' appreciation of stone has not ceased up to the present day. Even though the domination of Portland cement in architecture since the early 20th century inferred the decrease in the usage of natural building materials, the attention to lasting stone beauty and to its proper maintenance has increased in recent years. This is due to the heavy urbanization and industrialization of the last century that led to an acceleration in the deterioration of monuments and statues emphasizing the need of preventive and conservation solutions to preserve architectural heritage [1,2].

The present chapter is a short review, which aims at describing the main degradation processes of stone due to outdoor exposure. Secondly, the chapter is meant to summarize the state of the art of protective treatments for stone with the aim of giving an overview of the most used and tested synthetic polymers. From this introduction, the critical issues associated with the use of synthetic polymers and nanostructured materials will emerge, both in terms of compatibility and durability and in terms of environmental issues linked to their use.

In fact, it is nowadays clear that innovative and more green conservation strategies and materials are required for the preservation of our architectural and monumental heritage [3,4]. For a long time, restorers and conservators have been focusing in searching the most compatible solutions with the materials of the artefacts without taking into account the possible issues for the operators and the environment [5,6]

Then, this introduction aims to present and evaluate the available green and sustainable products and methodologies for protection of buildings and monuments materials.

1.1 Degradation of natural stone

It is known that stone, when placed in different environmental conditions from those where it was formed, naturally tends to degrade; in fact, it is forced to reach new conditions of equilibrium through changes in its characteristics.

This phenomenon is particularly problematic when it involves valuable architectural and artistic works, like masonry of historical buildings and decorative details. The necessity to preserve cultural heritage

integrity stress the need to increase the scientific knowledge on the behavior of these materials, in order to provide suitable solutions for their conservation[7–9].

In this sense, in the process of characterizing stone decay, it is important to underline that similar composition of the stone does not necessarily means same durability and/or behavior with ageing. For example, Istrian stone, Lecce limestone, and Carrara marble are all carbonate materials, but their modes of deterioration depend more on characteristics such as porosity, pore shapes, pore size distribution, and grain size then on their chemical composition. Moreover, the degree of hygric swelling and its strength strongly influence the durability of the stone too. Stone with high porosity, high rate of swelling and low strength will tend to be relatively poor building materials.

Water plays a key role in the various deterioration mechanism to which stones are susceptible, because it can promote degradation by acting as transport medium of several potentially harmful agents [10–12].

The following sections describe the main processes involved in building materials deterioration and promoted by the action of water.

1.1.1 Damages due to air pollution

The problems related to the changes in urban air quality are nowadays universally known. Industrialization, heavy urbanization and anthropogenic activities in general have increased the concentration of pollutants in the urban and rural environment, leading to serious issues not only for human health and environment but also for the buildings and monuments in our cities. Figure 1.1 shows the principal pathways by which airborne pollutants can be transported.

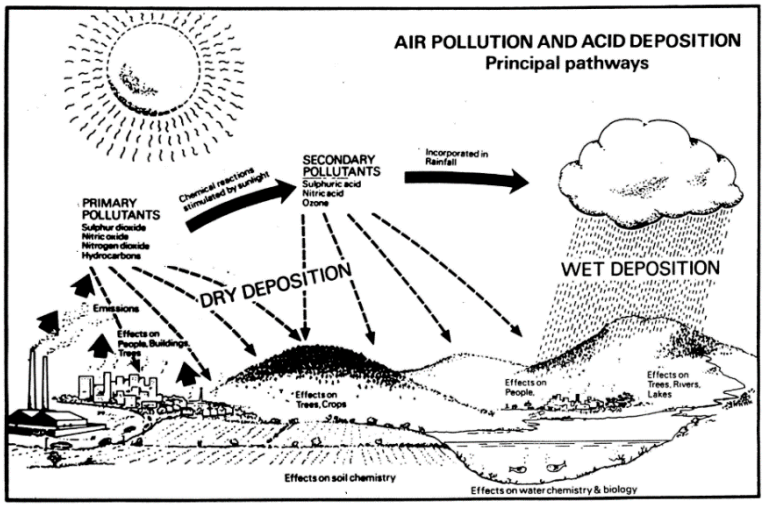

Figure 1.1 Principal pathways due to polluted environments [13].

Carbonate stone, such as limestone, marble and calcareous sandstone are particularly liable to damages due to polluted environments. The increased sulphur dioxide (SO_2) concentration in the atmosphere, resulting from the increased use of fossil fuel, has been considered for decades the main pollutant affecting marble structure. Urban levels of SO_2 are now decreasing, however the corrosion rates of most calcite containing materials still seem to be increasing. This is likely due to the elevated levels of nitrogen compounds; levels of NO_2 have doubled in the last decade, accompanied by a concomitant increase in the concentration of the nitrate component in acid rain. In fact, in presence of water or environmental humidity, NO_2 produces HNO_2 and HNO_3, which react with $CaCO_3$ giving calcium nitrate ($Ca(NO_3)_2$), which is highly soluble (121.2 g/100 ml at 20 °C)

$$CaCO_3 + 2HNO_3 \rightarrow Ca(NO_3)_2 + CO_2 + H_2O \quad [1]$$

The same happens for SO_2, which in contact with water can give rise to the formation of sulfuric acid (H_2SO_4) through oxidation. Rain water are already slightly acid due to the presence of CO_2 in the atmosphere; the high levels of H_2SO_4 and HNO_3 lead to a further decrease in rainwater pH, promoting an acceleration of corrosion and dissolution of calcareous materials[13–16]. Moreover, several authors suggest the possible synergic action between SO_2 and NO_2 and the rapid sulfate formation resulting from the simultaneous exposure of calcite to O_3 and SO_2 at humid condition[13,17,18].

The reaction between H_2SO_4, atmospheric water and the calcite contained in stones lead to the formation of gypsum; the reaction take place as follow:

$$CaCO_3 + H_2SO_4 + H_2O \rightarrow CaSO_4 * 2H_2O + CO_2 \quad [2]$$

This is believed to be the origin of black crusts formation, which are originated from the encapsulation of dust, airborne particles, polyaromatic hydrocarbons (PAHs) and carbonaceous particulate matter (PM) present in the atmosphere during gypsum crystals formation. Examples of black crusts formation are reported in Figure 1.2. Gypsum is more soluble (~2/2.5 g/L, 25°C) and occupy more volume (molar volume 74.4 $cm^3\ mol^{-1}$) that the original calcium carbonate matrix (molar volume 36.9 $cm^3\ mol^{-1}$) [19]. As a result, either it can be eroded in rain-washed areas, causing loss of material, or can induce mechanical stress due to the molar volume increase [20–25].

The increased level of CO_2 in the atmosphere is also dangerous especially for monuments made with calcium carbonate, such as marble. The reaction between calcium carbonate and CO_2 at high humidity values give rise to the formation of calcium bicarbonate ($Ca(HCO_3)_2$), as reported in the reaction below.

$$CaCO_3 + CO_2 + H_2O \leftrightarrow Ca(HCO_3)_2 \quad [3]$$

Calcium bicarbonate, which is more soluble (16.6 g/100 mL at 20 °C) and instable with respect to $CaCO_3$ (0.013 g/L 25 °C), can be either washed out by rainwater or, when the water evaporates, it can precipitates again in form of calcite, giving rise to large areas of white crusts over the building material [25–27].

Therefore, the reaction of calcium carbonate with the atmospheric pollutants dissolved in water, lead to the formation of more soluble products, which can undergo further leaching and consequent loss of material.


a.

b.

Figure 1.2 a. and b. Presence of black crusts on two limestone sculptures due to the dry deposition of pollutants present in the atmosphere [28].

1.1.2 Damages due to soluble salts

Salt weathering is another important cause of stone deterioration. Soluble salts presence in stone can be originated from different sources: air pollution, deicing salts, soil, sea spray[29–31]. As mentioned above, air pollution is the main source of sulfates and nitrates, while some authors attributed the presence of phosphate to rainwater leaching of bat guano [24,29,32]. Water in the soil, which is rich in minerals, is able to dissolve any soluble salts present in it and carry them into masonry by capillary rise. Once in the stone, the salts will migrate at different heights depending on their solubility and will crystallize at diverse location depending on the environmental condition during evaporation [24]. The most insoluble salts, such as gypsum ($CaSO_4*2H_2O$), crystallize close to the ground generating whitish films or crusts. As the solution continues to migrate upward and with on-going evaporation other salts will crystallize out, such as potassium nitrate and magnesium and sodium sulfates, forming efflorescences. The most soluble salts, as like as nitrates and chlorides, are the last in crystallizing. Efflorescences takes place on the surface, when salt bearing water evaporates straight from the surface

of the material and crystallize (Figure 1.3), while subefflorescence takes place below the surface, inside stone bulk [33]. This latter phenomenon is the most dangerous: as they crystallize within the pores of the material, salts can cause damages. The crystallization pressure of salts can both induce mechanical stress to the building structure and reduce the cohesive force between particles, giving rise to typical damages, including surface scaling, deep cracking, expansion, granular disintegration, surface powdering and micro cracking [30,31].

There is, in general, a strong relationship between the extent of salt decay and the environmental conditions in which the heritage is placed [29,34].

For example, salt weathering is enhanced in coastal and desert environments, which are rich in sodium chloride (NaCl) and sodium sulfate (Na_2SO_4) respectively, salts are blown by the wind from the sea or the desert. However, regions characterized by the strong contrast between the rainy and dry season, typical of tropical monsoon climate, may also be affected by salt weathering[10,11,24,35,36].

Temperature is another parameter that strongly affects the alteration patterns in the case of decays associated to the presence of soluble salts. Angeli et al.[37] indeed studied the influence of temperature and salt concentration on the salt weathering of sedimentary rocks, and they could observe a strong correlation between the patterns and the weathering extent with the change they cause in the evaporation velocity, and thus in the crystallization depth of sodium sulfate.

Other parameters may affect the resistance to salt crystallization, including the mineralogical composition, texture and pore size of the stone itself [38,39].

Pore size strongly influence salt weathering; according to several studies [40,41] for stone with pore size between 0.1 and 10 μm the crystallization stress generated by salt has to be considered relevant.

In order to penetrate pores of below 0.1 μm a crystal requires a degree of saturation, which is not frequent in building stone, while pores larger than 10 μm do not contribute significantly to salt weathering. This is why stones with large pores, such as travertine and tufa are less prone to salt deterioration than sandstones and calcarenites with thin pores. As well as stone like marble and Istria stone are more resistant to salt damages thanks to their minimal porosity and tendency not to have a strong capillary suction.

 a.

Figure 1.3 Formation of salts forming efflorescence on the surface of sandstone masonry, focused at joints between masonry blocks. [28].

1.1.3 Damages due to biocolonization

Microbial growth on and in stone made cultural heritages is once again determined by the availability of water in form of rain, rising dump, condensation, moisture. The presence of individual or complex microorganism communities, such as algae, bacteria, cyanobacteria, fungi, and lichens, on monuments and buildings leads not only to aesthetical alterations, but also to severe physical as well as chemical damage to the stone material. Primarily, the presence of the microflora can be found in the biogenic pigments, such as green chlorophyll, brownish melanin, or red carotenoids on the stone surface. Cyanobacteria are very frequent stone dwellers and can cause black, bluish and violet stains .[28] Several groups of algae may also grow on and in stone depending on climate condition and stone characteristics. Sometimes the stone surface is just the solid host for the growth of these microorganisms, but in other cases, it can also represent a source of nutriments.

Once microorganisms are fastened to the substrate, they can alter its physico-chemical characteristics, modifying the mechanical properties, wettability, diffusivity, and thermohygric behavior of the original material. Finally, the microbial colony may cause a bio corrosive attack leading to the alteration of the structure and stability of materials through several processes, such as the excretion of corrosive metabolic products[42].

Some of the microorganism found on stone, such as lichens and cyanobacteria, are photoautotrophic. Thus, they can grow on stone even when no organic matter is present and, even though better climate conditions favor their proliferation; this characteristic allows them to survive even in extreme conditions, including the vertical surfaces of monuments (Figure 1.4)[43].

As for damages due to air pollutants and salt, the degree of biological colonization of a stone surface depends also on the intrinsic properties of the material and its bio receptivity [44]; for example, studies of biological colonization on travertine showed that the stone characteristics play a relevant role. A

higher degree of colonization was observed in cavities and pores with respect to the surface, thanks to the possibility of hold water in it [45].


a.

b.

Figure 1.4a. Colonization of red algae on a bas-relief sandstone sculpture and b. Biological colonization constituted of an association of algae (dark grey), lichen (light grey and orange) and mosses (green cushions)[28].

1.1.4 Other damages due to the presence of water

As mentioned above, water acts as a carrier through which several degradation pathways might take place on stone artifacts. Nevertheless, water is able to degrade stone materials even without the presence of salt, pathogens microorganisms or pollutants.[46] Water can enter the pores trough infiltrations from the roof of the building, trough rising damp from the soil, or trough superficial and/or interstitial condensation and lead to chemical and/or physical damages.

The presence of water in the pores is a direct cause of physical damages of stone materials, especially in cold regions or in severe winter condition; the alternating of freeze and thaw cycles of water inside the stone pores is responsible for cracking and loss of mechanical strength. In fact, ice crystals occupy a higher volume (up to 9% more) with respect to liquid water, inducing mechanical stresses to the material.

Once again the deterioration processes due to freeze-throw cycles are dependent on the character of the pores such as the distribution of pore sizes, pore shapes and pores' interconnection whether they are sandstone or limestone [47,48].

Moreover, the exposure of high porous stone to frequent and intense rains lead to erosion and loss of material [49,50]. This is the case of calcarenite: even in relatively unpolluted areas, rainwater can slowly but steadily lead to the dissolution of calcium carbonate, which is extremely low soluble in pure water but becomes more soluble as the dissolution of carbon dioxide increases.[51]

In addition, in stone with high contents of clay minerals, such as smectite and montmorillonite, they can absorb moisture and undergo swelling-shrinking cycles and, if salts are also present, the cycles are no longer reversible and the expansion increases significantly with each new cycle, leading to physical damages.

Table 1.1 resume the main degradation mechanisms linked to the presence of water on stone materials. It is anyway important to stress that the decay is a spontaneous and irreversible process, which is often the result of the synergic action of several of these mechanisms and thus, in many cases, it is not possible to identify a single cause of degradation.

Table 1.1 Possible interaction of water with stone materials and consequent deterioration mechanisms observed.

Water activity and form	**Degradation mechanism**
Freezing-throwing cycles inside pores	Mechanical stresses, cracking
Run-off and flowing	Physical/mechanical erosion, loss of material
Presence of liquid water inside pores	Dissolution and transport of soluble salt, and mechanical stress due to their crystallization. upon water evaporation Transport of reactive pollutants coming from the atmosphere (SO_2, NO_X, CO_2), erosion and formation of black crusts
Sorption/desorption	Swelling-shrinking of clay minerals, mechanical stress due to hydration/dehydration of unstable minerals and soluble salt hygroscopicity
Presence of adsorbed water and moisture	Development of microorganism that may cause chemical/physical degradation

1.2 Protection of natural stone: state of the art

The previous section shortly described the main problems of building and monuments exposed to outdoor conditions and due to the presence of water.

The knowledge acquired about the deterioration processes has promoted the preservation of buildings and decorative surfaces of architectural monuments using hydrophobic or superhydrophobic protective coating.

The wetting phenomena are described through the Young's, Wenzel, and Cassie–Baxter equations (Figure 1.5).

Young was the first to study the interaction between a solid surface and a water drop, and his equation define the exact shape of the liquid-water drop as reported in Figure 1.5a. γ_{SV}, γ_{LV} , and γ_{SL} are the solid-vapor (sv), liquid-vapor (lv), and solid-liquid (sl) interfacial surface tensions, respectively, and θ_Y the equilibrium-Young contact angle. In the cases where the liquid-vapor surface tension is smaller than the solid-vapor surface tension ($\gamma_{LV} < \gamma_{SV}$), the liquid-solid interface increases to minimize energy. As the water droplets wets the surface, the contact angle approaches zero. Inherent hydrophilic surfaces correspond to $\theta_Y < 90°$, while inherent hydrophobic surfaces correspond to $\theta_Y > 90°$. The Young contact angle (θ_Y) is influenced exclusively by the intermolecular interactions, while the effect of surface roughness in the wettability of the solid surface is not taken in consideration.

Wenzel and Cassie–Baxter models introduced the relationship between roughness and hydrophobicity/superhydrophobicity. A surface is considered superhydrophobic when it shows a water contact angle (CA) higher than 150° and a sliding angle (SA) less than 5°. Both models by Wenzel and Cassie–Baxter can predict large apparent contact angles θ^* on rough surfaces, even larger than 150°.In the Wenzel model, however, θ^* can become larger than 150° only when underneath inherent hydrophobic materials. According to Wenzel, in fact, roughness increases the intrinsic hydrophobic or hydrophilic characteristics of a surface. Instead, for Cassie and Baxter any material, either hydrophilic or hydrophobic, can reach θ^* higher than 150° when the roughness is increased [52–55].

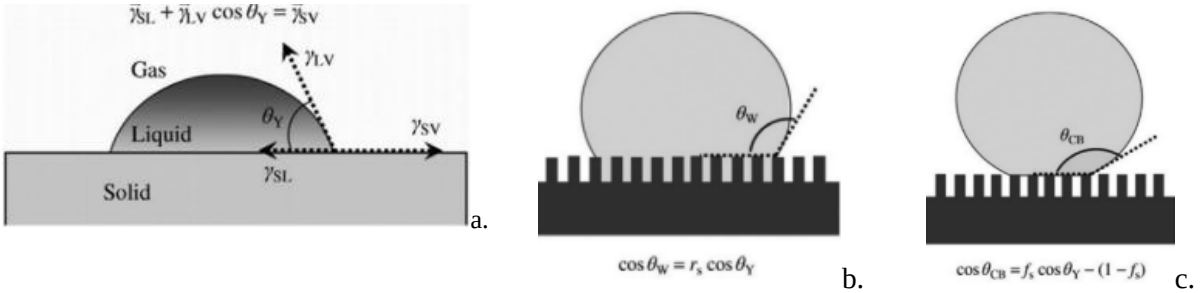

Figure 1.5 Schematic illustration of wetting states on solid surfaces. From top left to top right, wetting states are described by Young's, Wenzel, and Cassie–Baxter equations [52].

As shown in Figure 1.5a and b respective, in the Wenzel model, the liquid droplet makes contact at all points with the solid surface below it, while in the Cassie–Baxter model, the drop rests on the peaks of surface protrusions with air gaps trapped in between.

A short overview on hydrophobic and superhydrophobic coatings in stone conservation in the following paragraphs is reported. In particular synthetic, also with nanostructured additive and bio-based protective coatings available on the market and proposed in literature will be presented, evaluated and critically analyzed.

1.3 Synthetic polymers and nanostructured materials

Protective strategies are especially required to preserve stone from the action of water, ensuring at the same time the adhesion and compatibility with the substrate, avoiding significant water vapor permeability changes and color alterations. Moreover, they have to guarantee durability and retreatability of the surface, wherever the reversibility of the treatment it is not possible[56].

Most of the polymers used to protect stone monuments and buildings are of synthetic origin. Acrylates, silicon based polymers, fluoropolymers as well as mixtures of two or more components have been extensively used as protective coatings for stone protection due to their promising properties in terms of water repellency and transparency [23,51,57–64].

1.3.1.1 Acrylic polymers

Starting from 1960s, acrylates and silicon-based polymers have been widely applied for several conservation purpose. Acrylate and methacrylate polymers have been largely employed in formulation of varnishes, paints, adhesives, and for protection and consolidation of different substrates, such as wood, bricks, stones, textiles and leather[53,65,66].

Paraloid B72, obtained via free radical polymerization between ethyl methacrylate (EMA) and methyl acrylate (MA), is one of the first acrylic resin used as protective coating for stone [67]. Other acrylate and methacrylate copolymers, however, have been tested and applied for stone protection. Among them poly(metyl methacrylate) (PMMA), and poly(isobulyl methacrylate) (PiBMA), known by the commercial name of Paraloid B67, have been extensively employed in the protection of stones and frescoes[59,68]

These polymers have been used for long time in stone conservation thanks to their film forming ability, good adhesive properties, transparency and moderate water repellence. In fact, acrylics were believed to be stable against oxygen and UV radiation and able to keep their solubility when aged and therefore reversible [69].

Nevertheless, several studies demonstrated that prolonged UV-light exposure, humidity, extreme temperature variations may induce unwanted degradation of acrylic polymers [70]. In some cases they

degrade up to the total elimination of the coating [59], while other polymers undergo cross-linking and/or chain scission reactions [71,72].

Favaro et al. [73] proposed a degradation pathway for the methacrylates and acrylates units under photo-oxidative weathering. As reported in Figure 1.6a, the methacrylate unit undergoes the formation of a cyclic ester originated either by the addiction of O_2 to the radical formed by the extraction of hydrogen bonded to the tertiary carbons or by oxidation in the same position. On the other hand, the photo-oxidative weathering of the acrylate unit results in the formation of double bonds inside the chain as illustrated in Figure 1.6b.

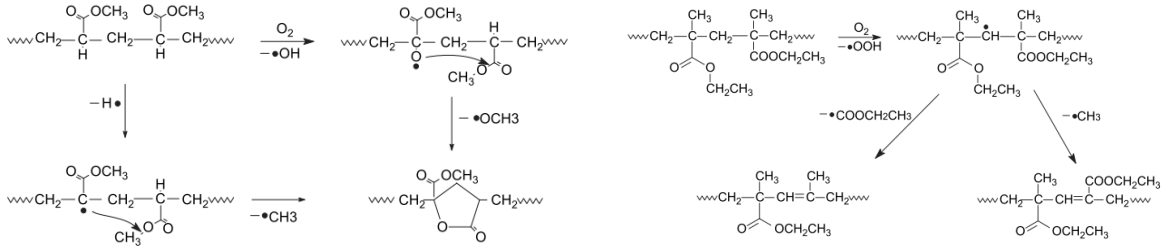

a. b.

Figure 1.6 Photo-oxidative weathering of Paraloid B72 for a. the methylacrylate and b. the acrylate units [73].

These reactions may result in reduced waterproofing behavior, yellowing and detachment of the polymeric layer. Moreover a difficult, and sometimes impossible, removability from the substrate was observed in several studies, which is a dramatic effect in case of occurrence of a new restoration [73,74].

1.3.1.2 Silicon based and nanostructured polymers

Silicone water repellent used for stone conservation belong to the family of alkyl silicon products, i.e., alkyl siliconates, alkyl silanes, siloxanes, polysiloxanes and silicone resins. The water repellency of the silanes and siloxanes products depends on their structure. They all come with a hydrophobic alkyl chains and a hydrophilic SiOR groups. The degree of hydrophobicity mainly depends on the length of the alkyl group, which also influence the resistance against alkalinity. When applied to the substrate, the alkoxy groups of these products undergoes hydrolysis in presence of water or humidity to form a silanol intermediate which will spontaneously polycondensate to form a hydrophobic film. While the reactive OH-groups from the silanols can form irreversible bonds with the mineral substrate [75,76].Table 1.2 shows the information available in the literature about silicon-based treatments for

stone protection. Most of them are applied in solvent medium, water-based emulsions were introduced in the late 1980s following the environmental concerns about solvent-based water repellents [77].

Table 1.2 Silicon-based commercial water repellent treatments tested for stone protection.

Product name	**Composition**	**Solvent**	**Ref.**
HIDRÓFUGO SH (Weber & Broutin)	Polysiloxane	Hydrocarbon	[78]
ESTEL 1100 (CTS Europe)	Oligomeric siloxanes	White Spirit	[78]
TEGOSIVÍN HL 100 (Goldshmidt)	Oligomeric siloxanes	No solvent	[78,79]
LOTEXAN/N (Keim)	Siloxanes	Mix aromatic/hydrocarbon solvents	[78,79]
BPS 7700 (BPS)	Siloxanes	Aromatic hydrocarbon	[78]
RADGUARD RADCRETE Development	Water-based alkyl silane	Solvent (not specified)	[78]
SIKAGUARD 700S (SIKA)	Siloxane	Solvent (not specified)	[78,80]
Wacker – not specified name	Oligomeric polysiloxane	White spirit	[57]
Silres BS 290 (Wacker)	silanes and siloxanes mix	White spirit	[79,81,82]
Silres BS 4004 (Wacker)	silanes and siloxanes mix	Water	[83]
Rhodosil 224 (Rhodia Silicones)	poly alkyl siloxane	White spirit	[82,84,85]
Porosil VV plus (AquaBarta)	poly alkyl siloxane	White spirit	[84]
Dri-Film 104 (General Electric)	Methyl-methoxy silane	White spirit	[73]
Silo 111 (CTS Europe)	Siloxane	White spirit	[86]
Silo 112 (CTS Europe)	Polysiloxanes	Water	[87]
Wacker OH 100 (Wacker)	cyclohexylmethyl-dimethoxysilane	Solvent (not specified)	[88]
Ethyl silicate	$(Si(OC_2H_5)_4$		[88]

VP 1805 (CHEM SPEC s.r.l)	Organicall-modified alkyl silane	Water	[89]
Acqua 1-K (Nortech GmbH)	emulsion of acrylic resin and alkyl silane	Water	[89]
BAYER LF (Bayer GMB)	Siloxane-acrylic copolymer	White spirit	[82]
FTORSAM-39 (Russian Accademy of science)	Fluoro-organosilane	Chloroform	[82]
AlphaSI30 (Sikkens)	Oligomeric polysiloxane		[90]
Silres BS29A (Wacker)	Emulsion of silane, siloxane and organic polymer	water	[91]

Despite the water repellency, stability and absence of chromatic variation observed for most of the commercially available treatments even after ageing [92], researchers have also highlighted some issues. For example, SIKAGUARD 700S and HB Siliker S 101 applied on granite were seen able to impart excellent hydrophobicity to the stone with no visible chromatic variation even after accelerated ageing tests. Nevertheless the application of these protectives caused a certain pore occlusion resulting in enhanced degradation processes with respect to non-treated granite, especially in areas interested by rising damp[80]. Moreover, Dri-Film 104 was seen to undergoes hydrolytic processes and consequent formation of cross-linked structures, processes which might interest even others products listed in Table 1.2 [73].

Moreover, during the cleaning operation on the Royal Palace in Madrid (Spain), some black stains were attributed to past protective treatments on limestone and granite with silicon-based protective products. The treatment did not allow the water inside the ashlar to evaporate and as a consequence dark stains and sub-efflorescences and crypto-efflorescences were observed in the areas with the highest moisture contents [93].

Another important aspect, which was pointed out by some authors, is the instability of silicon resins to SO_2 action, which leads to changes in their structure and, consequently, to shorter lives of these protective coatings in case of high level of SO_2 in the environment [94].

Recently, aiming at reduce the wettability and water penetration of porous building materials, research geared towards innovative methodologies, including the addiction of nanometric TiO_2 and SiO_2 to several synthetic polymers [62,87,95,96]. The addition of nanoparticle to silanes and siloxane products was tested by several authors and was seen to give rise to superhydrophobic and breathable surfaces [60,83–85,89,97]. Beside the enhanced superhydrophobicity, these nanomaterials are known for their photocatalytic activity; they are able to degrade the organic pollutants in the air through photooxidation thus preventing their accumulation on stone. Titanium dioxide (TiO_2), inorganic silica (SiO_2) and other nanoparticles are able to increase the stability of the polymer to photo-ageing thanks to the formation of organic and inorganic network, preserving the material transparency and flexibility when applied in blends but, even when used alone, impart superhydrophobicity, self-cleaning, antipollution and antibacterial properties to the treated stone [95,96,98–101]. Moreover, the use of high amount of titania results in chromatic alteration and cracking of the polymeric layer [102,103]. An important parameter to be considered for the optimization of the formulation of polymeric nanocomposites is the chemical stability after ageing, as TiO_2 nanoparticles can catalyse the degradation of the polymeric matrix [87]. Other issues related to the use of nanoparticles is their possible release in the environmental and consequent risks for human health [6,103,104].

1.3.1.3 Fluoropolymers

Fluoroplymers is the third main class of synthetic polymers used for stone protection. Infact, fluoropolyethers such as Fluoline PE, and foroelastomers, such as Tecnoflon NM (fluoroelastomer copolymer based on hexafluoropropene (HFP) and vinylidene fluoride (VDF)) or Fluoline HY, proved to be the best among protective materials because of both their higher stability (due to the relevant strength of carbon-fuorine bond) and the hydrophobic characteristics [87,105–107].

However, the use of sole fluorine-based coating in stone protection was limited by the fact that such coatings are bonded to the surface via very weak van-der-Waals forces, which causes lower adhesion to the substrates. Moreover, several studies stressed that the efficacy of these polymers is affected both by surface and bulk characteristics, such as roughness and porosity, and coating application method. In addition, in contrast to acrylic polymers, fluoropolymers have very high costs [108,109].

Since the beginning of this century, side-chain fluorination of acrylic or methacrylic-based copolymers as well as fluoro-organosilanes and silicone-acrylic resin-politetrafluoroethylene polymer systems has been tested, with the aim to improve the efficiency of protective coatings for stone substrates [60,61,82,110].

These recipes aim at combining the good physical characteristics and low price of acrylic polymers, with the enhanced water repellency, durability and transparency imparted by fluorine chains. In fact, fluorine in esteric side chain has been demonstrated to be able to increase water repellency and to reduce the water absorbed by capillarity. Anyway the efficiency of the blends need to be evaluated case by case [56,58,63].

Generally, fluorination showed a stabilizing effect on acrylic polymers properties. Benedetti et al. [105] noticed that with higher percentages of Tecnoflon NM in a blend with Paraloid B72 the degradation through ageing decrease.

Other studies highlighted that even though fluorinated monomers are able to lower the surface energy and thus give enhanced hydrophobicity, the percentage of fluorinated side chains along the macromolecule strongly influences the photo-chemical stability of the blends [111].

Recently, with the aim of overcoming the limited durability of acrylic protective polymers, Sabatini et al. [63] synthetized a new type of polymer protective via free radical polymerization between POMA (3,3,4,4,5,5,6,6,7,7,8,8,8-tridecafluoro-octyl methacrylate) and methyl methacrylate.

Despite the excellent water repellent properties, environmental and toxicity studies pointed out serious issues about the use of fluorinated polymers. They were found to be highly persistence in the environment and dangerous both for humans and animals, since they tend to accumulate in cells and tissue in animals and humans [112]. Toxicity studies performed on animals suggested that long-chain linear perfluoroalkyl derivatives containing more than six CFn units, like PFOA and PFOS, (Figure 1.7) induce serious toxic and endocrine disrupting effects [113–115].

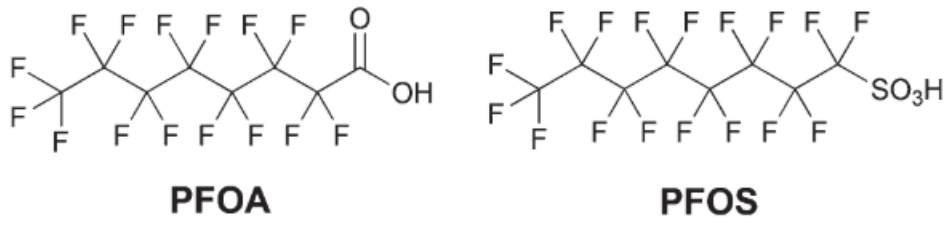

Figure 1.7 Chemical structures of perfluorooctanoic acid (PFOA) and perfluorooctanesulfonic acid (PFOS).

Due to their long-lasting persistence and toxicity, PFOS were listed as persistent organic pollutants under the Stockholm Convention, the US Environmental Protection Agency (EPA), in collaboration with the eight major companies in the fluorochemical industry, launched a Stewardship Program to commit to working towards the elimination of PFOA and its derivatives from emissions and products by 2005 [116,117].

Moreover, most of the synthetic protectives above mentioned are applied by means of volatile organic solvents, such as toluene, white spirit and chloroform, aspects which is particularly important when high volumes of solvents are required to protect extent surfaces, such as building façades ore monuments.

1.4 Biopolymers

Recently, ECHA (European Chemicals Agency) introduced restrictions on the use of conventional petroleum-based polymers that pose a risk to the environment favoring the introduction of more eco-friendly products [118].

In addition, the European Parliament and the Council of the European Union adopted the Directive (EU) 2019/904, which aims at prevent and reduce the impact of certain plastic products on the environment - in particular on aquatic environment and human health – and promotes the transition to a circular economy with innovative and sustainable business models, products and materials [119]. Thus, research is now focusing on the development of biopolymers in several field, from packaging, consumer electronics, sensors, automotive, agriculture, biomedical, toys, water remediation to textiles, coating and several other segments. The global production of biopolymers, divided by sectors, is reported in Figure 1.8. Packaging remains the main field of application for biopolymers with 47 percent (0.99 million tonnes) of the total bioplastics market in 2020 [120].

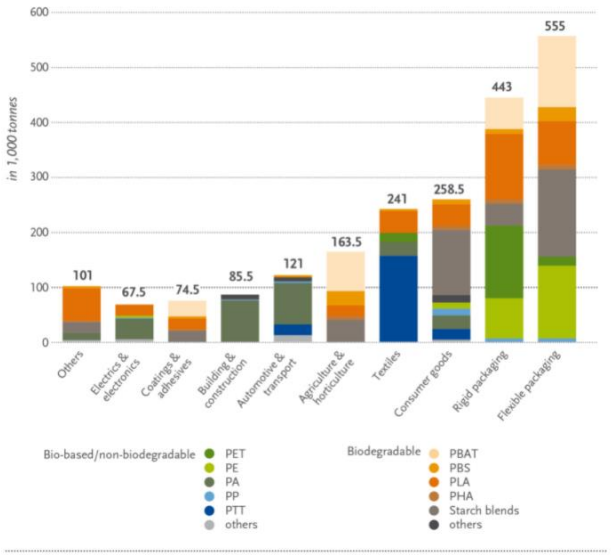

Figure 1.8 Global production capacity of biopolymers in 2021 (by market segment).

Concerning Cultural Heritage field, international organizations, such as EU, are encouraging the implementation of sustainable actions in conservation field. The importance of promotion and

conservation to maintain European cultural heritage and to favor technological advancement is highlighted in the new Horizon Europe program in "Culture, Creativity, and Inclusive Society" section [4,121].

Moreover, several national and international conferences, such as "Quale sostenibilità per il restauro?", "Restauro sostenibile 2.0" and "Green Conservation of Cultural Heritage" assessed and discussed the necessity of green and sustainable alternatives for the cultural heritage [6].

For these reasons and pushed by Europa Nostra and ICOMOS for the introduction of green materials and methodologies in cultural heritage, the use of biopolymers started to draw attention also in this field.

According to the definition given by the standard CEN/TR 15932 [122], the term *biopolymer* can assume several meanings depending on how the "bio" prefix is used. Biopolymers are polymers obtained from organic matter constituting living organisms, such as plants, animals and micro-organisms, and from their residues [123]. They can be either natural or synthetic. The first term refers to polymers "directly" synthetized by living organisms, such as polysaccharides (starch, chitin, cellulose), essentially in the form in which they are finally used. The second class of biopolymers, instead refers to polymers obtained renewable resources via synthetic routes, this is the case of poly(lactic acid) (PLA). The "bio" prefix is often used also as an abbreviation of *biodegradable* polymers. Biodegradable polymers should spontaneously disappear from the underlying stone, after their properties (namely, water barrier and repellence properties) are lost. Biodegradability is linked to the structure of the polymer; it does not depend on the origin of the raw materials. There are different fossil-based materials in the market that are biodegradable according to the specific standards, such as polycaprolactone (PCL), as well as there are polymers made from biomass and are highly resistant to biodegradation.

However, as previously illustrated, traditional organic coatings, made of synthetic polymers and used in conservation field, have been found to be hardly removable after some years of exposure to outdoor conditions and with aging. This suggests the potential replacement of non-biodegradable materials with biodegradable one.

Regarding the actual suitability of biodegradable polymers for cultural heritage conservation, the Literature does not provide a high amount of data.

Among biopolymers for potential application in stone protection, PLA was the most investigated material.

Sacchi et al. (2012) [124] investigated the performance of two lactic acid and Fluorolink D-10H (a low weight perfluoropolyether) co-polymers on different systems. Treated materials were subjected to artificial ageing, both with thermohygrometric cycles and UV exposure, aiming at proof their suitability to protect marble. Author demonstrated an enhancement of the water-repellent behavior in comparison to non-fluorinated PLA even after thermohygrometric aging. However, UV aging led, in some cases, to a detachment between the polymer layer and the marble substrate, depending on the kind of marble examined.

Performances of PLA functionalized through fluorinated alcohols as co-initiators of polymerization were also investigated by Giuntoli et al. (2012) [125]. The polymers showed an interesting stability to artificial ageing, even after a long-term exposition. The authors observed no significant differences in the structure and composition of the polymers as well as in their final performances.

Mistretta et al. (2019) [126] focused on the investigation of the mechanical and optical properties of PLA, PBAT, and a PBAT/PLA blend, concerning particularly on the behavior after exposure to UV irradiation. The mechanical properties of the blend were seen to be intermediate between those of the neat PLA and PBAT; however, the UV exposure led to different worsening of the three systems, pointing out that the blend undergoes more limited decay of the main mechanical properties, in comparison to the neat PBAT.

Ocak et al. evaluated the efficiency of four different biopolymers -chitosan, zein, polyhydroxybutyrate (PHB), high and low molecular weight poly-L-lactide (HMWPLA and LMWPLA) - as protective coatings for marble surfaces subject to sulphation processes [22]. Chitosan and zein showed high hygroscopicity and poor protection efficiency against sulphation and therefore not suitable to be applied as protective for marbles, in the specific condition use. PHB and PLA demonstrated promising properties in terms water repellency and permeability to water vapour and, among them, HMWPLA ensured best SO_2 barrier of all the tested biopolymers. Nevertheless, the study highlighted also a drawback linked to the high brittleness of HMWPLA, which may prevent its use for cultural heritage application. Moreover, both PHB and PLA are diluted in chloroform, which is a highly toxic and a recognised environmental pollutant.

Another study by Ocak et al. investigated the use of montmorillonite clays as fillers for PLA [5]. The addition of nanoclay into polymer result in increased hydrophobicity of the marble surface, nevertheless a worsening in water vapor permeability was observed. A high percentage of montmorillonite clay (<2%) caused both pores occlusion and significant color variation, as reported in Figure 1.9.

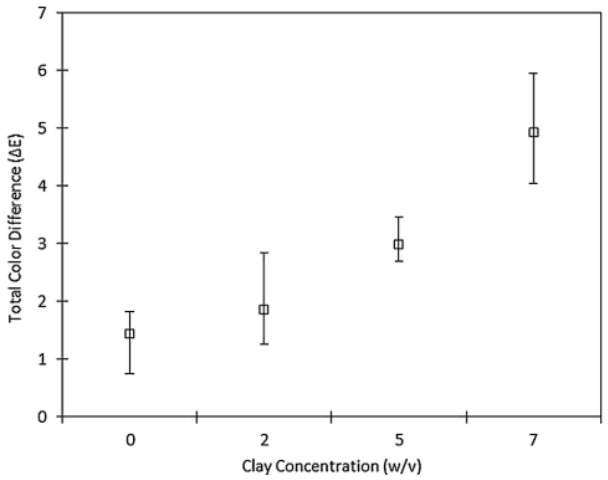

Figure 1.9 Total color difference (ΔE) of the neat PLA, and 2, 5, 7% PLA/MMT nanocomposite coated marbles[5].

Recently, another study investigated the use of poly(hydroxyalkanoate)s (PHAs) as protectives for stone. PHA is a class of naturally occurring thermoplastic linear polyesters synthesized as high molecular weight polymer chains by several species of bacterial strains. In the study carried out by Andreotti et al., PHB (polyhydroxybutyrate) and PHBVV (poly(3-hydroxybutyrate-co-3-hydroxyvalerate-co-4-hydroxyvalerate) were applied on sandstone, limestone and marble by poultice, dip coating, and spray coating [127].

The effectiveness of the treatment was seen to be strongly influenced by the application method and the stone porosity. Even though the authors obtained good results in terms of color changes and water vapor diffusion, promising results in terms of water repellency were obtained only for limestone. The main issues regarding the use of PHAs is, once again related to chloroform toxicity.

A natural, fungal protein-based coating method was also proposed as candidate for stone protection[128]. Fungal hydrophobins are small amphiphilic proteins secreted by fungi able to reduce water surface tension or to turn their surfaces hydrophobic. Winandy et al., tested the ability of hydrophobin DewA (from *Aspergillus nidulans*) and hydrophobin HFBI (from *Trichoderma reesei*) to protect three different lithotypes.

The treatment with DewA and HFBI, reduced the water absorption of different lithotypes, showing any dependence on their chemical nature and structure and without decreasing the vapor permeability of the stone samples. Removability test showed that the coating was easily removable with alcohol and detergents. Some concerns have been raised about the long-term stability.

Moreover, the comparison of water contact angles of DewA coated marble (79°) with the one obtained with the commercially available silicon-based products (140°), cast doubts on the use of hydrophobins as sole water-repellent protective for stone.

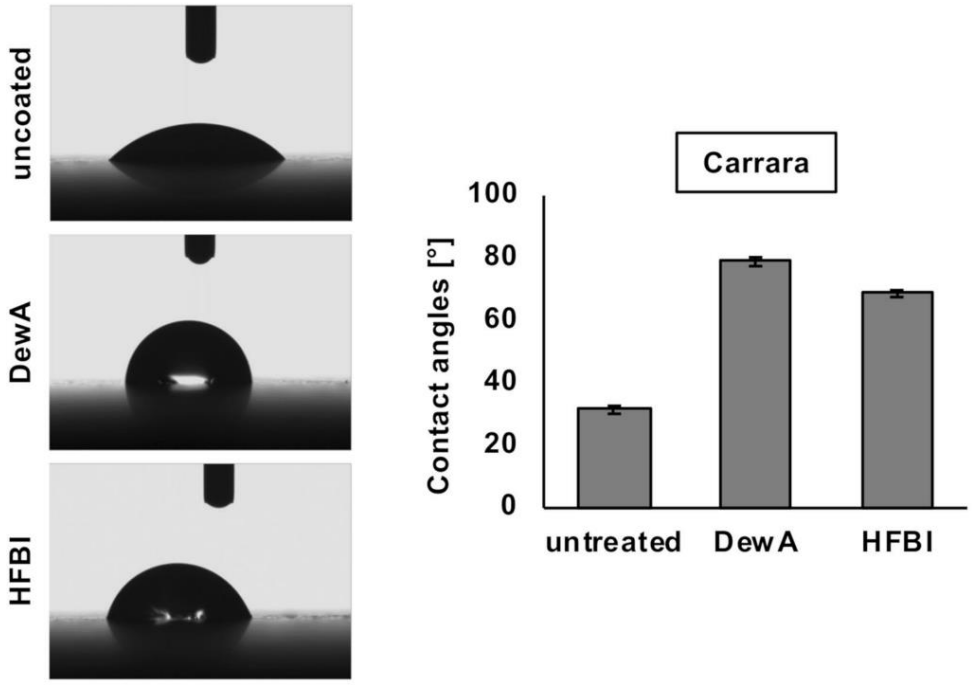

Figure 1.10 Water contact angles of DewA and HFBI treated Carrara marble[128].

In conclusion, essential issues have been highlighted regarding the effectiveness, long-term stability and impact of both synthetic polymers and nanoparticles. Moreover, most of the above mentioned protectives are often applied by means of organic solvents, such as toluene, white spirit and chloroform with possible risk for human health and the environment. Nowadays, international organizations are pushing through implementation of sustainable actions also in conservation field, thus, recently, innovative methodologies for the protection of outdoor-exposed cultural heritage assets have focused on the possible application of biopolymers as sustainable alternatives. Nevertheless, research in this

field is still in a preliminary stage, few works have been published on the topic up to now and further investigation and experimentation to find new materials and technology are needed.

In light of these considerations, the present thesis is precisely an attempt of developing and propose a new bio-based product for stone protection.

1.5 Scope of the research

The literature reported in the previous section demonstrated that traditional polymeric products with good properties are widely applied on cultural heritage, but they often show drawbacks. Acrylic and silicon-based resins instability to aging lead to both aesthetical problems and difficulties in their removal. Fluoropolymers demonstrated excellent hydrophobicity, but there are several concerns about health and environmental issues. The incorporation of nanoparticles in polymeric matrices improves the surface roughness increasing water repellency, but it also affects aesthetical properties and the lack of knowledge about their impact on human health demands further investigation.

Biopolymer coatings for stone protection may represent an alternative with good advantages in terms of eco-compatibility, reversibility and biodegradability Despite this little literature is present on this topic. Moreover, some drawbacks have been pointed out regarding the use of toxic solvents, such as chloroform for PLA and PHAs, and limited hydrophobicity.

The aim of this study is to propose and develop an innovative hydrophobic coating suitable for the protection of monuments and historical buildings exposed to outdoor environment. Environmentally friendly solvents (in this case dimethyl sulphoxide (DMSO), recyclable and readily biodegradable[129,130]) and materials were selected for the development of this innovative protective coating, based on Zein, an inexpensive, commercially available by-product of corn.

2. Development of a novel zein-based formulation

In the next paragraphs, the methodology followed for the development of the new formulation based on zein is described: the preparation, the characterization, and the study, which was carried out to understand the mechanism of hydrophobic surface formation of zein-based coating, will be illustrated.

2.1 Zein: properties, uses and possibilities in cultural heritage field

Zein belongs to the class of proteins known as prolamines, which occur specifically in cereals; it is extracted from corn endosperm and represents about 80% of the protein in corn (Figure 2.1).

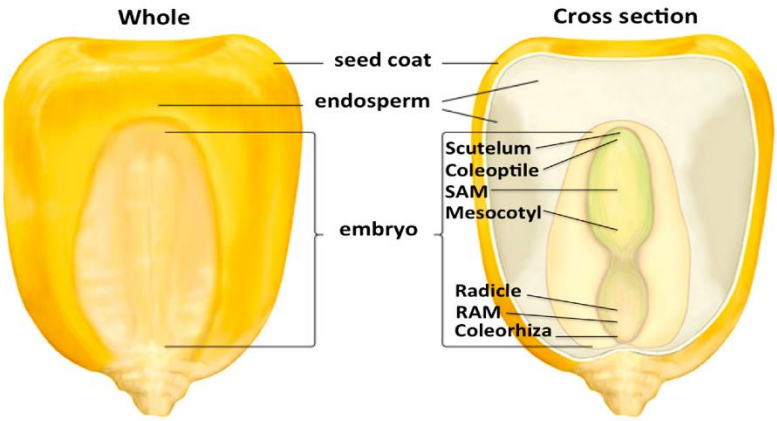

Figure 2.1 Front and cross-section of corn seed showing location of zein in the endosperm [218].

Zein has an amphiphilic character, which is due to its unusual amino acid sequence. In fact, as shown in Table 2.1 Amino acid composition of zein [92].Table 2.1, it contains over 50% hydrophobic residues, including high percentages of leucine (20%), proline (10%) and alanine (10%), while the hydrophilic component is due to the relatively high content (21%–26%) of glutamine [131].

Table 2.1 Amino acid composition of zein [92].

Class	Amino acid	Native zein Mossé (1961)	Commercial zein Pomes (1971)
Nonpolar	Glycine	0	0.7
	Alanine	10.52	8.3
	Valine	3.98	3.1
	Leucine	21.1	19.3
	Isoleucine	5	6.2
	Phenylalanine	7.3	6.8
	Tryptophane	0.16	NR*
	Proline	10.53	9.0
–OH	Serine	7.05	5.7
	Threonine	3.45	2.7
	Tyrosine	5.25	5.1
–S	Methionine	2.41	2.0
	Cysteine	0.83	0.8
Basic	Lysine	0	NR
	Arginine	4.71	1.8
	Histidine	1.32	1.1
Acidic	Aspartic acid	4.61	NR
	(as aspargine)	NR	4.5
	Glutamic acid	26.9	1.5
	(as glutamine)	Nr	21.4

* NR, not reported.

The high content of hydrophobic aminoacids makes zein insoluble in water but soluble in several organic solvents, including ethanol/water and acetic acid/water mixtures [132–135].

Its insolubility in water limits the use of the protein in human food products, while, since the mid-20th century, its potential use in industrial applications was investigated. So far, zein has been mainly used as renewable and biodegradable material for the production of adhesives for several application, for the preparation of food coating and food packaging in food industry and in tissue engineering and drug delivery systems for pharmaceutical and biomedical applications [136–142]. Due to its amphiphilic character, in fact, zein can self-assemble into various microstructures, including films, spheres, rods or fibers; allowing synthesis of materials with different properties and potentials in various applications [143].

Nevertheless, the application of zein in cultural heritage field was not investigated in depth.

As mentioned in the previous chapter, only Ocak et al., investigated the application of zein in conservation field. In that case, a solution of zein 15% (w/v) in aqueous ethanol with the addition of glycerol as a plasticizer was applied by dip-coating on marble slabs. As reported above, no satisfactory results were obtained since water contact angle was reduced from the 82° of uncoated marble to the 49° of zein coated marble [22].

Several studies in literature demonstrated that zein-based material properties can vary consistently presents depending on the solvent used, the concentration in solution, and the evaporation rate of the solvent [132,144,145]. Shi et al. [132] i.e stated that alternation of the solvents between EtOH and AcOH (acetic acid) to produce casted zein films leads to a distinct surface morphology and hydrophilicity. When AcOH /H_2O mixture (60%v/v) is used as a solvent, zein molecules tend to lie down on with the hydrophobic side wall in contact with the air; giving rise to a more hydrophobic surface. While, when EtOH/H_2O mixture (60%v/v) is used as a solvent, the zein molecules tend to position perpendicularly to the surface with the polar amino acid residues on the top; therefore, the zein film surface results more hydrophilic.

Thus the unsatisfactory results obtained by Oack et al. [146], might depend on several factors. Concentration and solvent used to dissolve zein, stone material characteristics, such as porosity and composition, as well as application method and additives used, such as glycerol, which is a hydrophilic plasticizer and might be responsible of the hygroscopicity observed.

It is believed that, by carefully tuning these parameters, a zein-based protective coating could still be developed for the protection of natural stone. The following paragraphs will describe how the formulation was prepared and characterized; moreover, a detailed study on the mechanism of hydrophobic surface formation is presented, showing how both the solvent used and the application method adopted influence the surface properties.

2.2 Preparation of zein solution

Zein protein was deeply studied, and various solvent were tested, as reported in literature: ethanol/water mixtures, benzyl alcohol (BA), ethanol/benzyl alcohol and dimethyl sulfoxide (DMSO), either with or without the addition of plasticizers [146–148].

In this study, zein concentration was taken between 5 and 20 % (w/v), knowing from literature that concentration of the protein can also play a significant role in surface morphologies [133]. Spray coating was chosen as application method since it represents the most widely used method for the application of protectives on-site. After some preliminary evaluation regarding hydrophobicity and colorimetric evaluation of the several formulations, a 5% (w/v) solution of zein in dimethyl sulfoxide was chosen because of its better performance, as reported in paragraph 2.3.

The formulation was prepared as follow. Zein (Z3625, Sigma-Aldrich, Inc. USA) powder has a typical yellow color, which is attributed to xanthophylls and b-carotene. With the aim to remove the colored impurities zein was washed in ethanol (99.7 Sigma-Aldrich, Inc.USA) following the procedure

illustrated by De Boer et al. [149]. 10 g of zein were stirred in 1.5 L of ethanol overnight and the suspension was left to sediment by gravity. The liquid phase, containing most of the impurities, was discarded, while the collected sediment was dried and used to prepare a 5% (w/v) solution of zein in DMSO (D8418, Sigma-Aldrich, Inc.USA). The mixture was maintained under stirring for 30 min at room temperature and any insoluble aggregates were removed by filtration using a 0.45 mm filter (PVDF, Millipore).

Dimethyl sulfoxide (DMSO) was chosen as solvent because, in addition to its environmental-friendly characteristics [129,130,150], it is able to solubilize a wide range of polymers and it is miscible with most of the common solvents, including water. Moreover, recently it was used to dissolve zein, and to obtain a robust film [151] and a plasticizing effect of DMSO on zein was stated.

In order to verify the purification process, UV–visible absorption spectra of purified and unpurified solutions were collected using a Cary JEOL UV- spectrophotometer. Dynamic Light Scattering (DLS) was used to determine the size distribution profile of the particles in solution before and after purification using a Zetasizer Nanoseries from a Malvern Instruments (Worcestershire, UK) technique. The temperature was set at 25°C. Five measurements were used with an automatic duration of a minimum of 10 and a maximum of 100 runs. Figure 2.2 a schematically illustrates the procedure followed for the preparation of the 5% (w/v) solution of zein in DMSO. Figure 2.2b shows the color differences between unpurified (left) and purified (right) zein solutions. The absorption spectra of solutions of unpurified and purified zein solutions are shown in Figure 2.2c. After zein purification, a lower absorption was observed in the range 300 to 500 nm, which indicates the removal of most yellow impurities that absorb in that region of the electromagnetic (EM) spectrum. DLS (dynamic light scattering) analyses performed on solutions of unpurified and purified zein powder (Figure 2.2d), showed that no significant changes in particle size in solution were detected

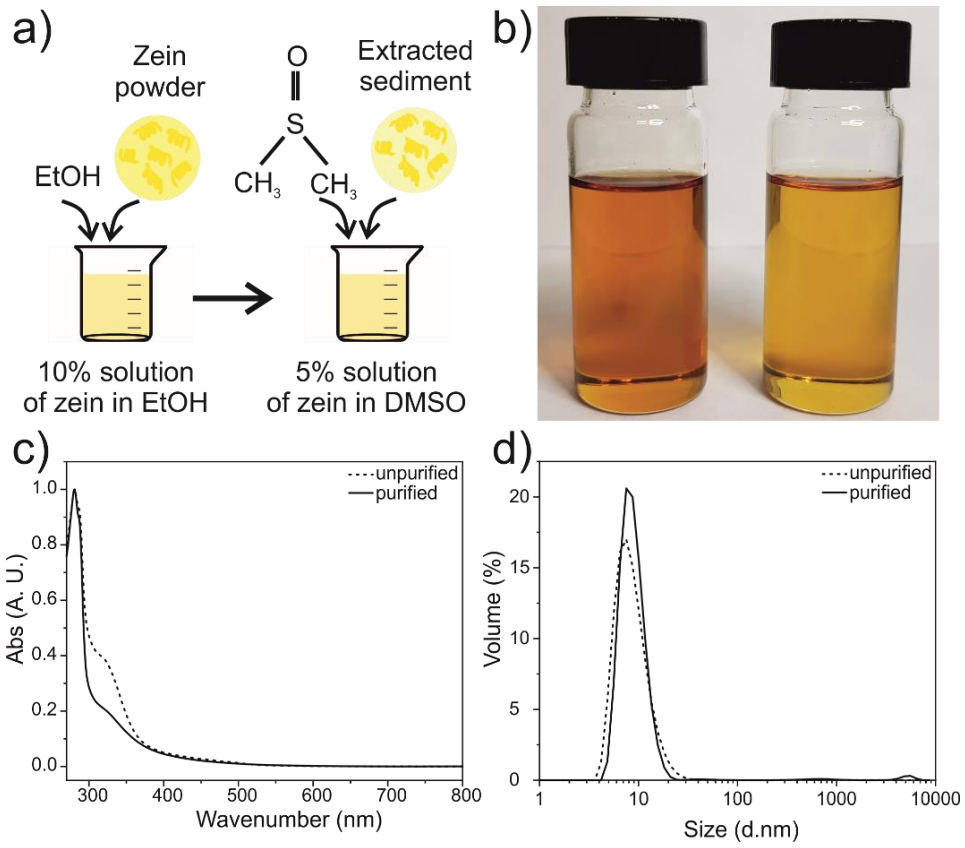

Figure 2.2a) Schematic representations of zein purification and preparation of the solution b) Photograph of DMSO solutions made with unpurified (left) and purified (right) zein. c) UV–Vis absorption spectra of unpurified (dot line) and purified (solid line) solutions of zein, d) DLS (dynamic light scattering) analyses performed on solutions of unpurified (dot line) and purified (solid line) zein powder.

2.3 Study of the influence of coating fabrication method on surface hydrophobicity

One of the main characteristics required for the developed zein-based coating is hydrophobicity. Some authors have acknowledged a relationship between proteins secondary structure and surface hydrophobicity [152]. In addition, Dong et al. [153], found a correlation between the secondary structure and the hydrophilic/hydrophobic behavior of zein casted film and zein electrospun fibers respectively.

These studies suggest that the knowledge of zein secondary structure through ATR-FTIR analysis can be suitable to understand whether the hydrophobic behavior of the here presented coating may be deemed to the spray coating application method and to the evaporation rate of the solvent.

In spray coating technique the fast evaporation of the solvent might help in forming a hydrophobic surface [154]. The study of Simovich et al. [155],which observed that the rapid evaporation of solvent during spray coating of a solution of silica nanoparticles embedded within epoxy resin, helped in fabricating a rough and superhydrophobic surface coating, supports this thesis.

In particular, the film obtained by spray coating was compared through ATR-FTIR analysis with the one obtained by casting.

To prepare the film by casting (ZF), 3 mL of zein 5% w/v solution in DMSO were poured into a Teflon Petri dish (diameter of 3 cm) and dried at room temperature under fume hood for 48 h. Subsequently the film was placed in oven at 60°C for other 24 h to remove the solvent eventually trapped.

While the sprayed coating (ZC) was prepared by spraying the same solution (zein 5% w/v solution in DMSO) onto glass slide using a spray coater (Paasche Airbrush VL with 73 mm head and 1.06 mm tip) and a thin zein coating was deposited . A total of 3 mL of solution was sprayed on the glass slide. The quantity of sprayed coatings was kept constant by controlling both spray pressure (2 bar), application time (3 s) and spraying distance from the sample (40 cm). Treated slide glass were dried at room temperature under fume hood for 48 h and, subsequently, placed in oven at 60°C for other 48 h, to remove any residual solvent from the coating.

ATR-FTIR spectra were obtained using a Fourier Transform Infrared (FTIR) spectrometer (VERTEX 70v, Bruker) equipped with an ATR (attenuated total reflection) accessory (MIRacle ATR, PIKE Technologies) with a diamond crystal. All spectra were recorded in the range from 4000 to 600 cm^{-1} with a resolution of 4 cm^{-1}, accumulating 64 scans. Three analyses were performed for each sample to ensure the reproducibility of obtained spectra. The ATR-FTIR spectra of DMSO solvent and zein powder (ZP) were also collected as references, and are reported in Figure 2.3a.

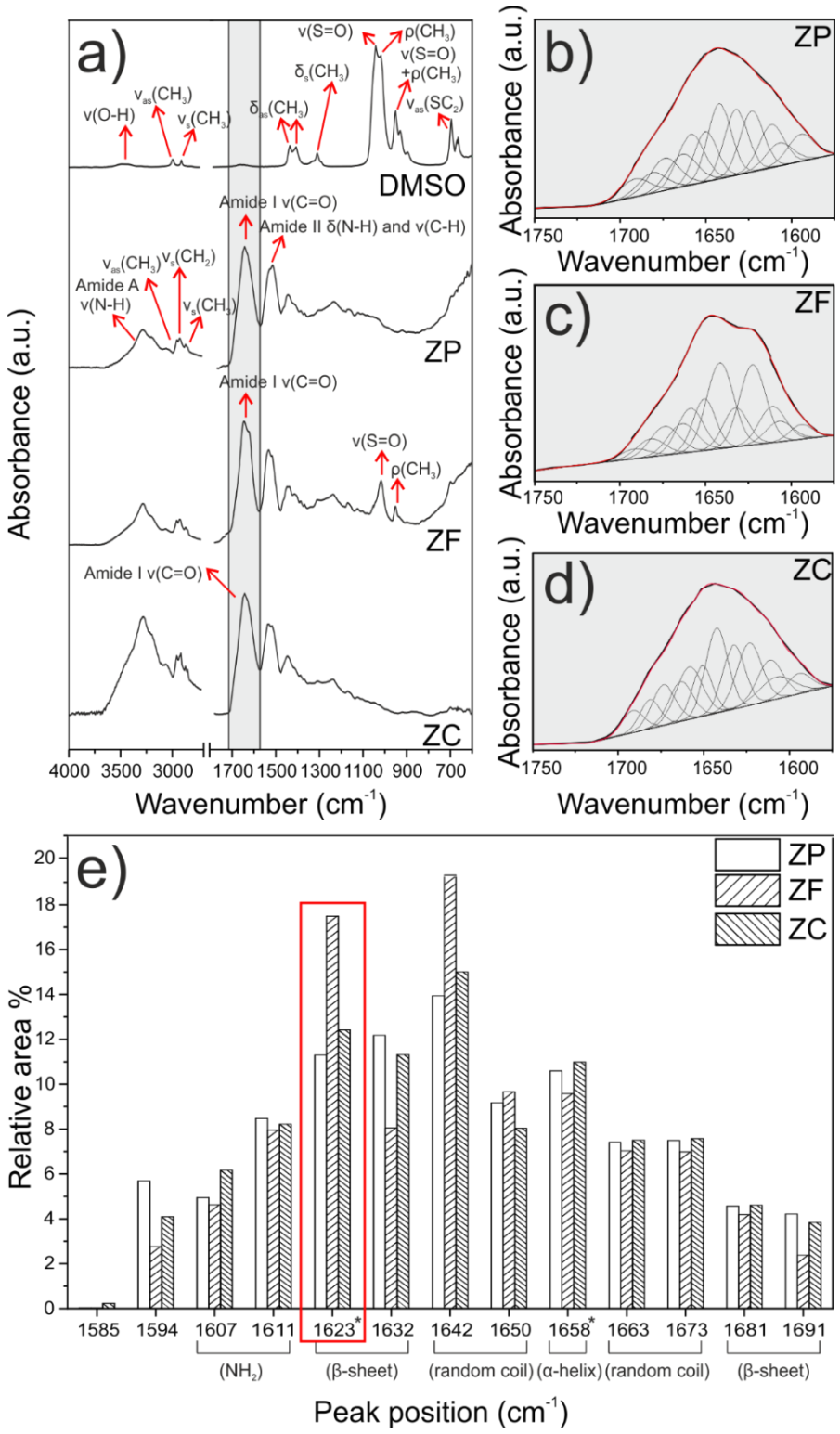

Figure 2.3a) ATR-FTIR spectra of DMSO, zein powder, zein film obtained by casting and zein coating obtained by spray coating in the 4000–600 cm−1 region. Deconvolution of amide I peak (1750–1570 cm−1) of b) zein powder c) zein film and d) zein coating. e) Changes in zein secondary structure content (%).

DMSO exhibited the typical peaks reported in literature; in particular DMSO exhibits peaks at 1438, 1405 cm^{-1}, corresponding to the antisymmetric bending of CH_3 ($\delta_{as}CH_3$), and at 1310 cm^{-1} , identified as a symmetric deformation of CH_3 (δ_sCH_3) group that is attached to the S atom. Finally, a broad peak at around 1075 cm^{-1}. is assigned as S=O stretching (νSO) [156–159].

Zein powder spectrum showed the typical protein absorption bands. The amide A band associated to the N–H and O–H bonds of the amino acids of zein appears from 3600 to 3100 cm^{-1}. The methyl group vibration (νCH_3 asymmetric and symmetric) produces the small bands at 2957 and 2872 cm^{-1}, while the peak at 2932 cm^{-1} is identified as the methylene group asymmetric stretching vibration ($\nu_{as}CH_2$). The band associated to the stretching of the carbonyl (νC=O) of the peptide groups (amide I) appears at 1640 cm^{-1}. The band at 1530 cm^{-1} (amide II) corresponds to the deformation of the N–H bond (δNH), and the band at 1235 cm^{-1} corresponds to the deformation of the C–N bond (δCN) [5,160–162].

The characteristic peaks observed in the spectrum of zein powder were found both in the zein coating (ZC) and in the zein film (ZF) spectra.

In addition, in the ZF spectrum, some of the characteristic peaks of DMSO were detected too, such as the peak at 1075 cm^{-1} assigned as S=O stretching (νSO). As mentioned above, recently Wey et al. [163] attributed the DMSO remained within zein film after the drying process to the high boiling point of the solvent (189°C).

Apart from the presence of DMSO peaks, ZF showed also a different shape in the signal around 1760-1670 cm^{-1}, with respect to ZP and ZC. That peak corresponds to the amide group, which is generally observed between 1600 and 1800 cm^{-1} and it is called the amide I band. This band is mainly attributed to the C=O stretching and vibration modes. The amide I signal contains most of the information of the protein secondary structure. Different types of secondary structures are the results of different hydrogen bonding modes and molecular geometries [160,162]. Therefore the C=O peak deconvolution of ZP, ZF, and ZC was carried out in order to understand the relationship between the secondary structure of the protein and the hydrophobic and hydrophilic nature of the coating and the film respectively. Deconvolution was carried out as previously reported by Forato et al. [162] and Bicudo et al. [164]. A linear baseline was applied to the spectrum in the region between 1600 and 1800 cm^{-1}, spectra were normalized with respect to the peak of amide I and second-order derivative analysis was performed on each spectrum using PeakFit 4.11 software [165] to confirm that each fitting peak position represented a real spectral signal from the samples.

The deconvoluted spectra of ZP, ZF, and ZC are presented in Figure 2.3b, c, and d respectively. Amide I band of ZP is symmetric, the deconvoluted spectra shows a strong signal at 1640 cm−1 (Figure 2.3b) related to the high α-helix content of zein powder as reported in literature [153,162]. In ZF spectra (Figure 2.3c), the presence of a shoulder at 1623 cm−1 is clearly evident, which, according to several authors[160,162,164], is attributed to the β-sheet structure. For ZC (Figure 2.3d), no obvious peak or shoulder at 1623 cm−1 are observed from the spectra, revealing a secondary structure similar to the one of zein in powder.

In Figure 2.3e the proportion of secondary structures (%) for ZP, ZC, and ZF are reported. Zein film shows a higher proportion of β-sheet structure at 1623 cm^{-1} (17.5%) with respect to the zein coating, where β-sheet structure only reached 10.9%, which is almost the same percentage observed for zein in powder (10.5%). Several authors [145,153] illustrated that the increase in β-sheet structure at 1623 cm^{-1} is associated to the α-helix to β-sheet transformation that occurs during solvent evaporation in ethanol-water mixed solutions of zein. This α-helix to β-sheet transformation involves a process of hydrogen bonds rearrangement, which needs the solvent as a medium to take place. DMSO is a hygroscopic solvent with strong affinity for water and high boiling point [166]. DMSO, when left drying under environmental conditions for the zein film formation, might behave like water, promoting the formation of hydrogen bonds with zein. This phenomenon could also explain the presence of DMSO in ZF observed with ATR-FTIR analysis after the drying process. During spray coating the faster evaporation of the solvent does not allow the α-helix to β-sheet transformation and, thus, in the coating, the structure is dominated by α-helix structure [153,161]. Spray coating, thus, seems to be the right technique to form a surface film without any solvent entrapped.

Regarding the hydrophilic/hydrophobic behavior, the 5% w/v in DMSO solution, which was allowed to dry slowly after casting, gave origin to a smooth hydrophilic film. Using spray coating instead, a hydrophobic surface was formed. The application method, thus, plays a central role in the wettability of the zein surface and ATR-FTIR analysis suggested that it might be a correlation between the drying process, which drives the orientation of zein molecules, and the different proportion of α-helix and β-sheet observed in the amide peak.

When applied by spray coating, the solution is ejected as small droplets in the air, forcing the solvent to evaporate from the droplets' surface at a fast rate. In a relative short period of time, before complete solvent evaporation, a radial concentration gradient of zein is formed within each droplet [153,155]. In particular, zein starts solidifying from outside, at air-liquid interface, towards inside the droplet. Due to the DMSO still present inside the droplet, the non polar hydrophobic side of zein is forced to face

the outer part of the droplets, while the hydrophilic polar side remains in contact with the solvent. As the drying process proceeds, the solvent evaporates completely also from the inner part of the droplets, while the atmospheric pressure makes the droplets to collapse one over the other, because of the pressure exerted onto the semi-solidified zein particles and the force applied to the droplets due to their impact on the stone surface. This droplets collapse gives rise to the hydrophobic coating.

3. Investigation of zein formulation performance as a protective

As previously mentioned, the properties of zein films may depends also on the interactions between the zein molecules and the substrate. In the present chapter, the performance of the developed material when applied as a protective coating for stone material are evaluated and discussed. In particular, the ability of the coating to form a continuous film able to protect the stone from the action of water have been investigated and are here presented.

3.1 Set up of the application method and stone substrate selection

The mechanism of hydrophobic surface formation illustrated in the previous chapter can be adapted to the application of the 5% w/v zein solution in DMSO on stone material as graphically illustrated in Figure 3.1.

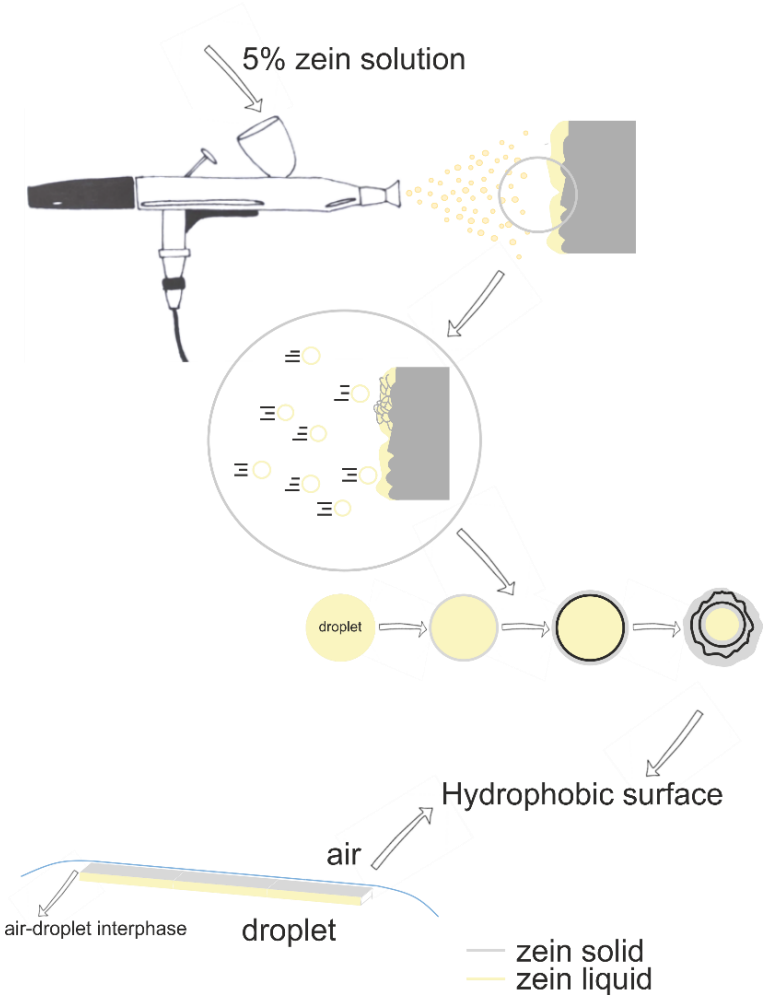

Figure 3.1 Schematic illustration of zein surface formation during spray coating.

Serena stone, a fine-medium grain sandstone characterized by a grey-bluish color, was selected to investigate the protective performances of the zein-based protective coating. This sandstone is widely used as building materials and ornamental stone mainly in Florentine and Ligurian architecture [34,167]. Moreover, Serena stone was used as support for the evaluation of coating performance by several other authors so it could represent a good support for comparing the obtained results too [62,168].

However, due to the above mentioned influence of stone composition on the performance observed, further studies might be required for an overall assessment of the developed coating performance in case of application on different litotypes.

Stone was quarried from the district of Fiorenzuola. 5 cm × 5 cm × 1 cm slabs were cut and polished with 280-grit silicon carbide paper, washed in deionized water, dried in oven at 60°C and kept in a desiccator to bring them to a constant weight.

Briefly, a set of 25 samples of Serena stone were coated by zein 5% in DMSO (w/v) solution using a spray coater (Paasche Airbrush VL with 73 mm head and 1.06 mm tip). According to other studies, spray coating application method should be the best method to allow the formation of a layer thin to not alter excessively the underneath roughness [90,155]. The solution was spryied following the same procedure described previously (Paragraph 2.3); a total of 3 mL of solution was sprayed on each slab surface (5 cm × 5 cm). The quantity of sprayed coatings was kept constant by controlling both spray pressure (2 bar), application time (3 s) and spraying distance from the sample (40 cm). Samples were dried at room temperature under fume hood for 48 h and subsequently placed in oven at 60°C for other 48 h, to remove any solvent from the coating. As shown in Figure 3.2, where a set of 6 samples is shown, transparent coating was deposited on the stone surfaces and, at first glance, no visible color variations were observed. However, colorimetric measurements were performed according to NORMAL 43/93 (as will be explained in paragraph 4.1) in order to evaluate color changes due to the application of the coating. Samples were weighted before and after the application of the coating and a weight increase of 0.13645 ± 0.011 g was observed for treated samples.

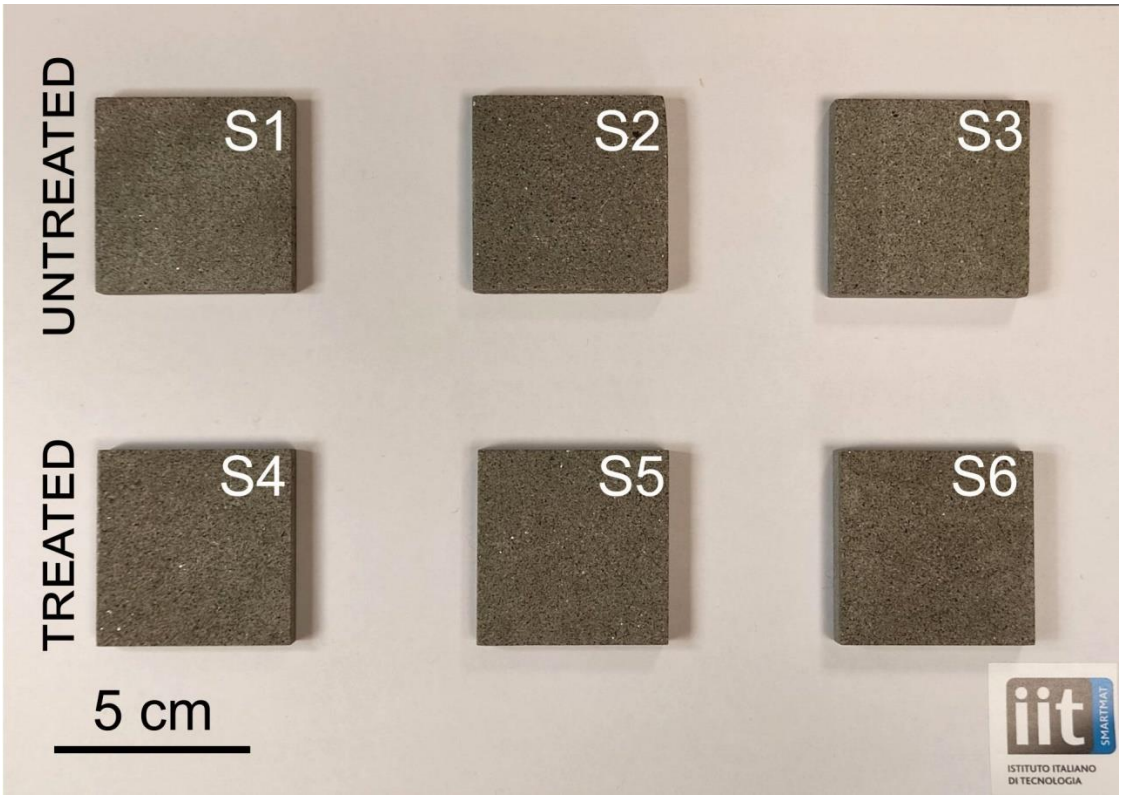

Figure 3.2 Pictures of three replicas of untreated Serena stone (S1, S2 and S3) and three replicas of Serena stone treated with the 5% solution of zein in DMSO (S4, S5 and S6), showing no significant color difference.

The chemical and physical characteristics of Serena stone could influence the behavior of the zein coatings. As chemical and physical characteristics of this kind of stone can vary depending on the quarry of origin, in the following paragraph the analyses performed to characterize the samples are presented.

3.1.1 Stone characterization

Serena stone was expected to be a low porous stone mainly made of quartz and feldspars; calcite, micas and clay minerals. Even though the relative low porosity, rainwater and the air humidity can accelerate degradation process of Serena stone, such as volumetric expansion of clay minerals of the matrix or dissolve the calcite cement, increasing the porosity inside the stone [7]. Moreover, reddish alteration were observed in stones containing high percentage of iron (from chlorites in the matrix) in presence of extent of water percolation [169]. Thus, it is important to know intrinsic parameters like composition and textural/structural characteristics in order develop protective strategies against further degradation.

The mineralogical composition of the bare stone samples was investigated through X-ray diffraction (XRD) analysis and micro-X-ray Fluorescence (μ-XRF) analysis with the aim of knowing the exact

composition [7,34]. Porosity was measured by helium picnometry and mercury intrusion porosimetry (MIP).

3.1.1.1 X-ray diffraction analysis

XRD analysis was carried out on PANanalytical Empyrean X-ray diffractometer equipped with a 1.8 kW Cu K_α ceramic X-ray tube and a PIXcel^{3D} 2 x 2 area detector, operating at 45 kV and 40 mA. The diffraction pattern was performed on small stone fragments under ambient conditions using a parallel beam geometry and in symmetric reflection mode. HighScore 4.1 software from PANalytical was employed to analyze XRD data.

Figure 3.3 shows the XRD pattern for Serena stone, revealing the presence of quartz (SiO_2), calcite ($CaCO_3$), albite ($NaAlSi_2O_8$) and Piroxene ($MgSiO_3$) as main phases.

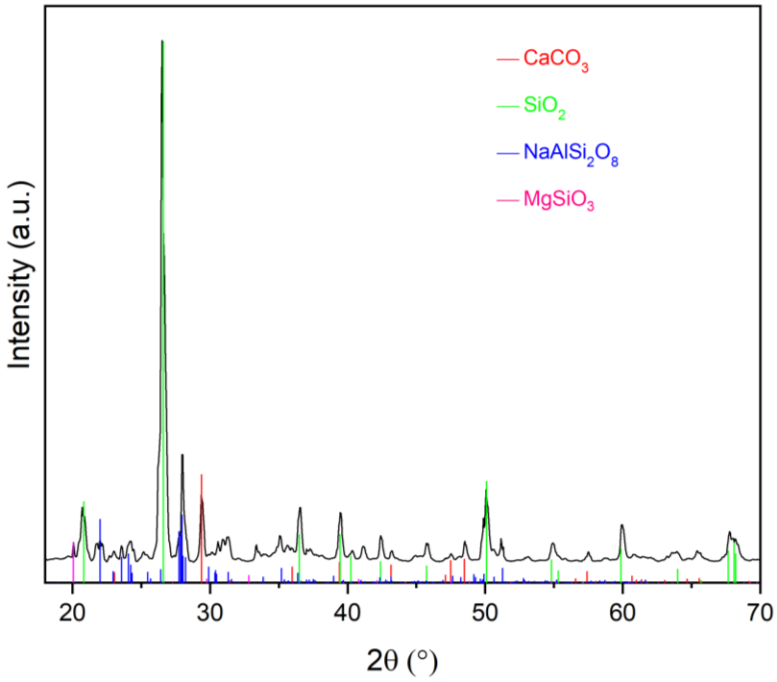

Figure 3.3 XRD pattern of Pietra Serena sandstone sample with the expected peak position references for $CaCO_3$ (calcite, ICSD code 80869), SiO_2 (quartz, ICSD code 62404), $NaAlSi_2O_8$ (albite low, ICSD code 34917) and $MgSiO_3$ (pyroxene-ideal, COD code 96-900-2909).

3.1.1.2 Micro X-ray fluorescence (µ-XRF)

Elemental distribution maps were obtained by micro X-ray fluorescence (µ-XRF) analysis using the spectrometer M4 Tornado (Bruker, Germany). The system is equipped with a Rh-anode X-ray tube cooled by air and operated at 50 kV and 199 µA. Poly-capillary optics is used to focus the

polychromatic beam to a spot size down to 25 µm for Mo K_α. Detection of fluorescence radiation is performed by an energy-dispersive silicon drift detector with 30-mm^2 sensitive area and energy resolution of <145 eV for Mn K_α. Measurements were carried out directly on the sample (1x1x1 cm) placed on the instrument platform under 20 mbar vacuum conditions. In mapping mode, sample imaging was performed on five different sides of Pietra Serena sandstone with a scan resolution of 100×70 pixel, step size of 98 µm, and a dwell time of 500 ms/pixel.

As expected, the most abundant elements (Si, Ca and Al) found with micro-XRF analysis (Figure 3.4a and b) corresponded to the characteristic minerals found by XRD analysis (quartz, calcite and albite) [34,169].

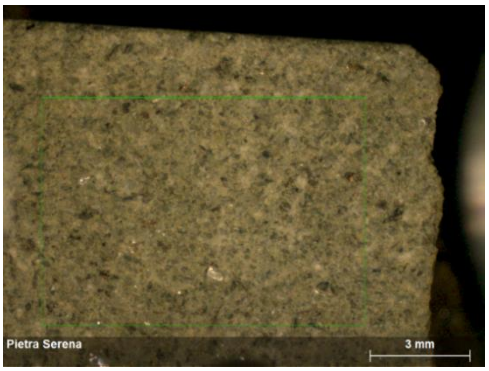

a.

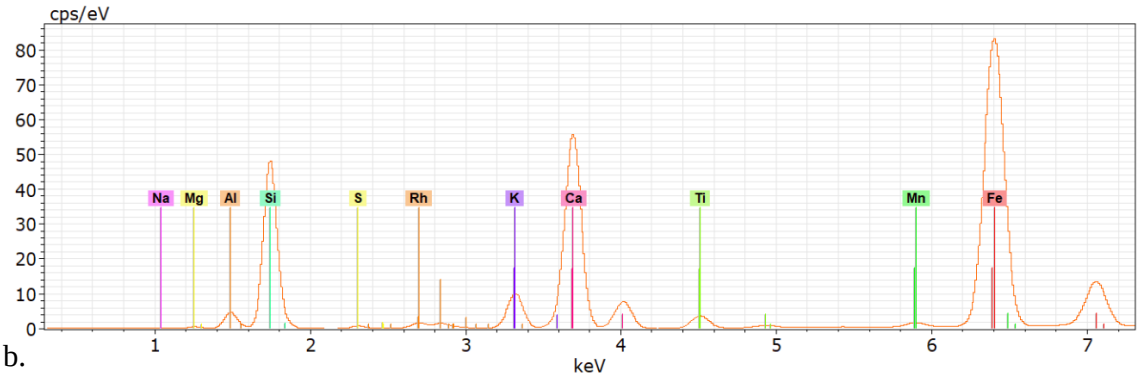

b.

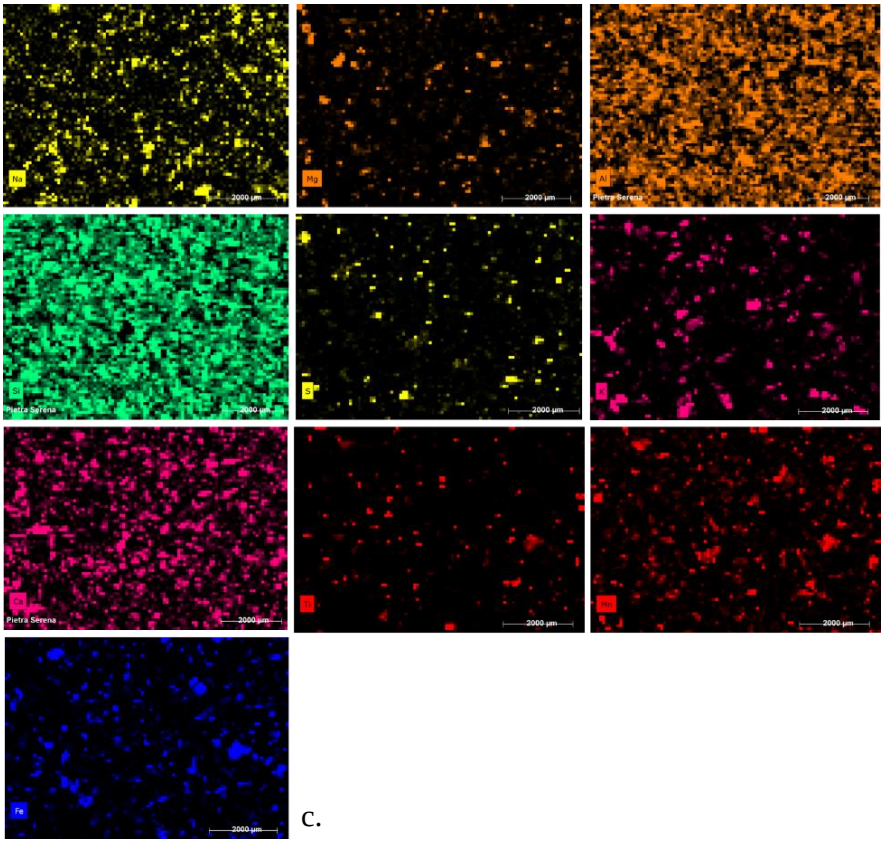

c.

Figure 3.4 Typical spectrum and element mapping by XRF of Pietra Serena sandstone sample. a. Scanned area; b. spectrum; c. element distribution maps for Na Kα (1.04 keV), Mg Kα (1.25 keV), Al Kα (1.49 keV), Si Kα (1.74 keV), S Kα (2.31 keV), K Kα (3.31 keV), Ca Kα (3.70 keV), Ti Kα (4.51 keV), Mn Kα (5.90 keV) and Fe Kα (6.40 keV).

From the elemental maps (*Figure 3.4*c) the elements resulted homogeneously distributed in the sample and this was confirmed by their low coefficient of variation (5-11%), as shown in Table 3.1.

K, Na, and Mg were found in lower amount, revealing, as expected, the presence of K-feldspar, micas and dolomite, respectively [34], detected with XRD. Besides Al, Si, and Mg, Fe was also detected with the micro-XRF analysis; this was likely due to the presence of chlorite $(MgFeAl)_8(SiAl)_8O_{20}(OH)_{16}$) and illite $(K,H_3O)(Al,Mg,Fe)_2(Si,Al)4O_{10}[(OH)_2,(H_2O)]$ in addition to kaolinite $Al_2Si_2O_5(OH)_4$ as constituents of the clay matrix [169].

Table 3.1 Elemental concentration (norm. at. %) on five scanned areas on different sides of Pietra Serena sandstone sample using XRF.

	Na	*Mg*	*Si*	*Al*	*K*	*Ca*	*Ti*	*Fe*	*S*	*Mn*
1	2.6	3.1	59.4	10.1	4.3	14.6	0.6	4.7	0.4	0.1
2	2.7	3.0	60.0	10.0	4.4	14.4	0.6	4.5	0.4	0.1
3	2.5	3.0	57.2	10.0	4.4	17.1	0.7	4.7	0.4	0.1
4	3.1	2.4	62.2	9.0	3.5	15.5	0.5	3.8	0.1	0.1
5	3.1	2.1	65.4	8.7	3.9	12.3	0.5	3.7	0.2	0.1
Average	2.8	2.7	60.8	9.6	4.1	14.8	0.6	4.3	0.3	0.1
Dev. St.	0.3	0.4	3.1	0.7	0.4	1.7	0.1	0.5	0.1	0.0
*C.V.**	10.7	14.8	5.1	7.3	9.8	11.5	16.7	11.6	33.3	0.0

* Coefficient of variation (C.V.) expressed as a percentage

3.1.1.3 Porosimetric measurements

Porosity of Serena stone was measured by helium picnometry and mercury intrusion porosimetry (MIP). The skeletal density was measured by Thermoscientific Pycnomatic Evo helium pycnometry, furnishing a 4 cm^3 chamber. Measurements were performed at 20 °C. The skeletal volume of the sample represents the volume of the sample when pores are not accessible to the gas. It was measured by detecting the change in pressure due to the volume of helium that is displaced by the sample within the sealed and pressure- equilibrated chamber. It is assumed that helium atoms are able to penetrate all open pores within the stone. Ten measurements of the same sample were averaged. The skeletal density was 2.69 $g/cm^{3,}$ calculated by dividing the sample mass by the skeletal volume. Porosity was determined by mercury intrusion porosimetry (MIP) performed with Pascal 140 Evo and Pascal 240 Evo mercury porosimeters (Thermo Fisher Scientific). The pressure of mercury intrusion was set at 0.0136 MPa and continuously increased up to 200 MPa, with a rate of 6−14 MPa min^{-1}. The contact angle of mercury with the samples and the surface tension of pure mercury were assumed to be 140° and 0.48 N m^{-1}, respectively [170,171].

Total open porosity was found 3.11%, which is a value similar to the one reported in literature [62,172], and a bimodal pore size distribution was measured, with median pore size in the ranges 0.03–0.02 μm and 6.30–3.98 μm, as shown in Figure 3.5.

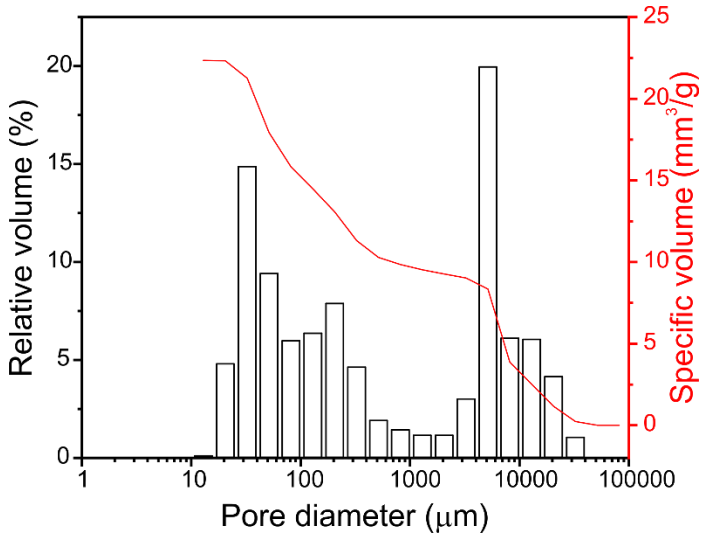

Figure 3.5 Pore diameter distribution (bars) and total porosity as the volume of mercury intruded (curves) measured by mercury intrusion porosimetry for Serena stone

Results obtained from XRD, micro-XRF and porosimetric measurements revealed the relatively heterogeneous composition and low porosity of the selected Serena stone.

3.2 Evaluation of protective performance of the developed coating

The aim of the project was the development of a hydrophobic layer able to limit water penetration into the stone bulk. As mentioned in the previous chapter, in fact, water is the main responsible of the several degradation phenomena that can interest stone building materials. Thus, a good protective coating for stone material should show enhanced water repellency, limiting at the same time the moisture penetration into the stone pores, maintaining simultaneously permeability to water vapor [173,174]. In cultural heritage field, protective efficacy against water in liquid form and vapor can be evaluated by means of several test: from hydrophobicity evaluation through water contact angle measurements [175] and water vapor permeability test [176], to water absorbance measurements by capillary rise test [177], by total immersion test [178], or at low pressure by means of "pipette" method [179].

In the present thesis, the effects of the developed polymeric film on treated stone was evaluated in terms of hydrophobicity, water uptake and water vapor permeability tests, as described in the following section. Hydrophobicity was measured through water contact angle aiming at evaluate the coating ability to increase the surface run-off of water and to avoid its penetration in the stone bulk. Water vapor uptake measurements were carried out both before and after the application of the treatment to verify whether the coatings had a blocking effect with respect to the water moisture absorption. Water

vapor permeability test instead was carried out in order to make sure that the permeability of the moisture eventually present in the bulk is maintained even after coating application. Other analysis, aimed at evaluate the coating behavior in case of prolonged contact with water, such as capillary rise test, will be carried out in a future evaluation of the zein coating performance *in situ* and on other stone materials.

3.2.1 Hydrophobicity evaluation

The wettability of the treated stone surface was measured with a contact angle instrument (OCAH-200 DataPhysics, Germany); measurements of static water contact angle (WCA) were acquired at room temperature (~23°C). As reported in paragraph 1.2, the static angle between a liquid drop and a solid surface is named Young's contact angle. A gas-tight 500 mL Hamilton precision syringe with blunt needle of 0.52 mm internal diameter was used to deposit milli-Q water droplets of 5 μL on the stone sample placed on a sample holder, with the testing surface placed in a horizontal position. 10 measurements were acquired on each sample surface, the obtained values were averaged, and standard deviation was calculated. The measurements were performed both on untreated and treated stone samples [180]. WCAs were acquired also in continuous mode for 5 min (1 acquisition/s) to track the droplet behavior in time.

3.2.2 Water uptake evaluation

Dry samples weighed with the electronic balance (0.0001 g accuracy) were placed in the humidity chamber at 100% R.H. for 14 days, until stabilization of weight (daily measures); the amount of adsorbed water vapor was calculated based on the initial dry weight, according to the following formula:

$$Water\ vapor\ adsorption\ (\%) = \frac{m_f - m_0}{m_0} \times 100$$

where m_f is the sample weight at 100% RH condition and m_0 is the sample weight at 0% RH [181].

3.2.3 Water vapor permeability

Water vapor permeability (WVP) of the untreated and treated stone was determined at 25 °C and 100% RH according to the ASTM E96 standard method [176]. 100% humidity gradient was reached by placing 400 μL of deionized water in the permeation chambers of 7 mm inner diameter and 10 mm height. In order to be able to place the samples in the chambers, samples were cutted in slices of 5.0 mm × 5.0 mm × 0.8 mm. 3 slices were treated with zein coating, while the other 3 were used as

reference of the untreated stone. The samples were placed on the top of the permeation chambers and sealed. The chambers were placed in a desiccator, maintained at RHZ5% RH by anhydrous silica gel desiccant at room temperature (20°C and ~ 40% RH). The mass loss over time was registered by weighting samples every hour for 8 consecutive hours, with an electronic balance (0.0001 g accuracy). The water mass loss of permeation chambers was plotted as a function of time and the slope of each line was calculated by linear regression. Then, the water vapor transmission rate (WVTR) was determined as below:

$$WVTR(g(m^2d)^{-1} = \frac{slope}{area\ of\ the\ sample}$$

The water vapor permeability (WVP) of the samples was calculated as follows:

$$WVP\ (g(mdPa)^{-1}) = \frac{WVTR \times L \times 100}{p_s \times \Delta RH}$$

where *L*(m) is the thickness of the sample, measured with a 0.001mm accuracy micrometer, ΔRH (%) is the percentage relative humidity gradient, and ps (Pa) is the saturation water vapor pressure at 25°C Every measurement was repeated 3 times.

Results obtained from the evaluation of the water-linked properties are reposted in *Figure 3.6*.

Water-linked properties results discussion

Water contact angle (WCA) measurements over time were acquired for untreated and zein-treated stone (Figure 3.6). A total absorption of the water droplets was observed within the first minute after droplet deposition for untreated stone. With the application of the zein coating on the stone, the water contact angles increased, giving rise to a hydrophobic surface, with values varying between 100° and 120°. According to Cassie-Baxter [55] and Wenzel [54] models, roughness can affect the wettability of a surface, enhancing the underneath hydrophilicity/hydrophobicity respectively. Thus, our hypothesis is that the WCA's variation is to be ascribed to the high heterogeneity and roughness of the underneath stone[182,183]: where underneath surface roughness was higher, higher WCA were reached. The contact angle behavior shown in Figure 3.6a is referred to the most hydrophobic areas where 120° were reached for the just deposited water drops.

In Figure 3.6b the water drop volume reduction over time is also reported: the drop volume was reduced by 90% after 5 min from its deposition on untreated stone (absorption). When applied on treated surface, instead, the drop volume only decreased by 10% after 5 min (evaporation).

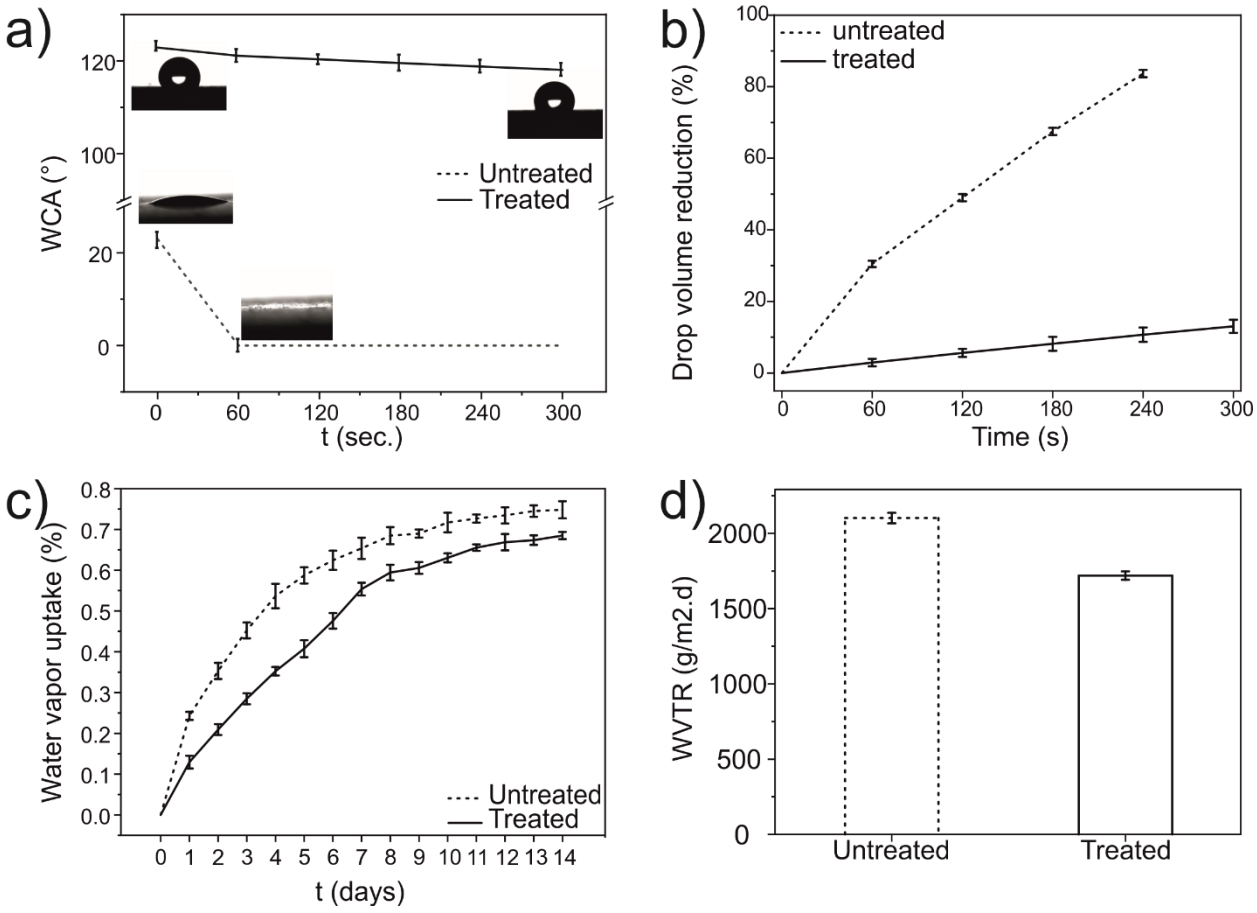

Figure 3.6 Water-related properties of Serena stone before (dot line) and after (solid line) the treatment with zein solution. a) Water contact angle over time. Static WCAs are reported at 0 s, 60 s, 120 s, 180 s, 240 s and 300 s. b) Drop volume reduction over time (%). c) Water vapor uptake of untreated and zein-treated stone at 100% RH over time. d) Water vapor permeability of untreated and zein-treated stone.

Figure 3.6c shows the water vapor uptake at 100% RH (relative humidity) for untreated (dot line) and treated (solid line) stone respectively. Due to intrinsic low porosity of Serena stone, the amount of water vapor absorbed by the untreated stone was not high (0.24% after 24 h); still, with the application of the coating a reduction of 8.4% in water vapor uptake was observed for 15 days.

Regarding the breathability of the stone, a slight reduction in water vapor transmission rate (WVTR), was observed in presence of zein coating, as shown in Figure 3.6d. A decrease of 18 ±2% in water vapor permeability was calculated, which it can be ascribed to the low gas permeability of zein [146,184]. However, the permeability decrease, i.e., RVP %, does not exceed the acceptable threshold of 20%, and it is comparable to the one observed for many siloxane-based coatings, suggesting that the coating fit the requirement for hydrophobic coatings [185–187].

According to the results presented, zein applied by spray coating technique seems to confer a good degree of water repellency to the stone. Water contact angle is comparable to the one obtained with other natural-based coating, such as poly(hydroxyalkanoate)s [127] or fungal hydrophobines [128]. Results obtained in terms of water repellency are even improved with respect to commercially available polysiloxanes coatings [90], which gave a water contact angle of 90–100°. Moreover, the reduction in water vapor permeability does not exceed the acceptable threshold of 20%.

3.3 Evaluation of coating distribution and its interaction with stone surface

The surface distribution of the coating and the relative interaction with the adopted stones were evaluated using different surfaces analyses. The mechanism of coating formation proposed in Figure 3.1, in fact, does not consider the contribution of stone morphology and roughness in forming the hydrophobic layer. Whereas, it has to be considered that the different surface morphologies for zein coating may depends also on the interactions between zein molecules and the substrate, resulting in a different organization patterns of zein molecules during the film formation process and, thus, in the formation of either a hydrophobic or hydrohylic layer too.

The micro-morphology of the samples was analyzed through SEM analysis before and after the application of the zein coating. SEM images were acquired using a JEOL JSM-6490LA (Japan), operating at 10 kV acceleration voltage. Prior to imaging, the samples' surfaces were sputtered with a 10 nm thick film of gold (Cressington 208HR sputter coater, UK) and then SEM images were collected at different magnifications [1]. Knowing the influence of the roughness on the wettability of the surface, the stone substrate was investigated before and after the application of the coating by 3D Optical Profilometry. Different magnifications, ranging from 2.5× to 20× were used corresponding to a Z profile resolution ranging from 25.0 μm to 0.5 μm respectively [188]. Moreover, the adherence of the coating to the stone surface was evaluated by performing a peeling test using Scotch® MagicTM tape (3 M). The changes in stone surface morphology were observed by SEM. The test was carried out according to previously reported methods [98,189,190].

Chemical characterization of the coated stone was performed through X-ray photoelectron analysis (XPS) aiming at investigating the surface chemistry and the possible zein-stone chemical interactions. Moreover, due to the intrinsic characteristics of Serena stone and chemical composition of the coating itself, measurements of the coating thickness were hard to acquire with conventional techniques such as profilometer or scanning electron microscopy. The use of XPS was the only technique which allowed us to give an indication of the coating thickness.

X-ray photoelectron spectra were acquired before and after coating application by a SPECS XPS spectrometer, using a monochromatic Mg Kα source operating at 12 kV and 7 mA and a pass energy of 90 eV for the survey and 30 eV for the high resolution. Sample charging was compensated by a flood of low-energy electrons, and energy scale calibration was performed setting the main carbon C 1s peak at 284.8 eV. The spectra were analyzed using CasaXPS software [191,192].

Results are presented and commented below.

Firstly, SEM (scanning electron microscopy) images of untreated and treated slabs were acquired. Untreated stone showed the characteristic aspect of Serena stone, with many irregularities due to the presence of different minerals with their specific morphology (Figure 3.7a, b). In the treated samples, the presence of a layer of zein is detectable (Figure 3.7c, d).

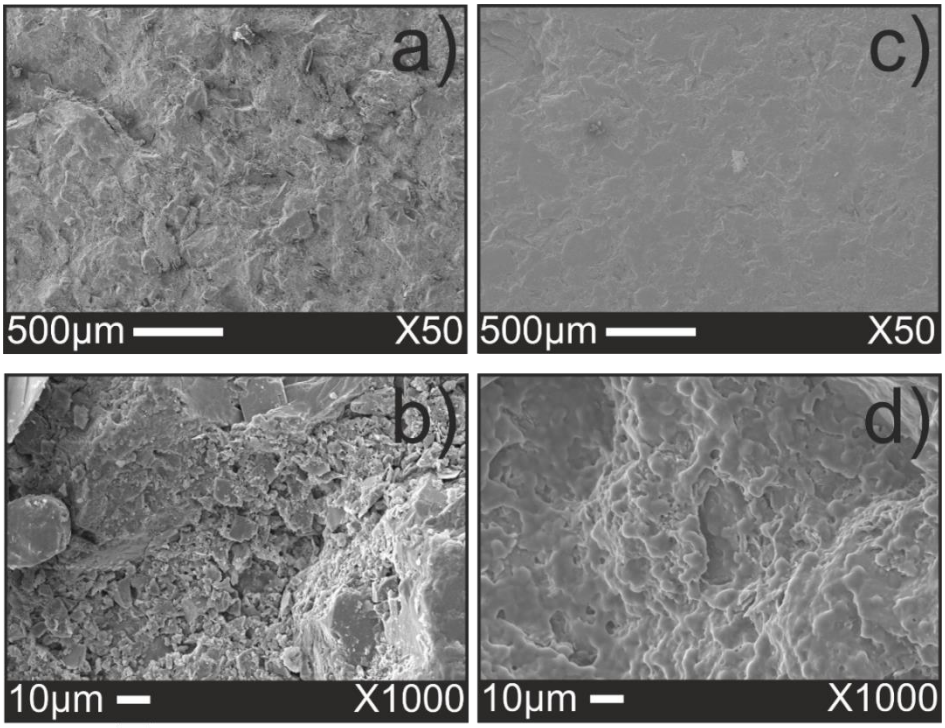

Figure 3.7 SEM images of (a,b) uncoated and (c,d) zein-coated Serena stone.

The application of the zein coating resulted in the formation of a compact film on the stone's surface with a continuous structure showing micro-scale roughness.

As mentioned previously, different factors influence the wettability of inorganic materials treated with organic compounds. Roughness is one of the surface properties most affecting the hydrophobicity since typically, hydrophobicity increases by increasing the surface roughness [126,182,193,194].

Therefore, roughness observed with SEM analysis was measured by optical profilometry. The topography of non-treated and treated samples was compared using 3D surface images, as shown in Figure 3.8 (a not treated and b treated).

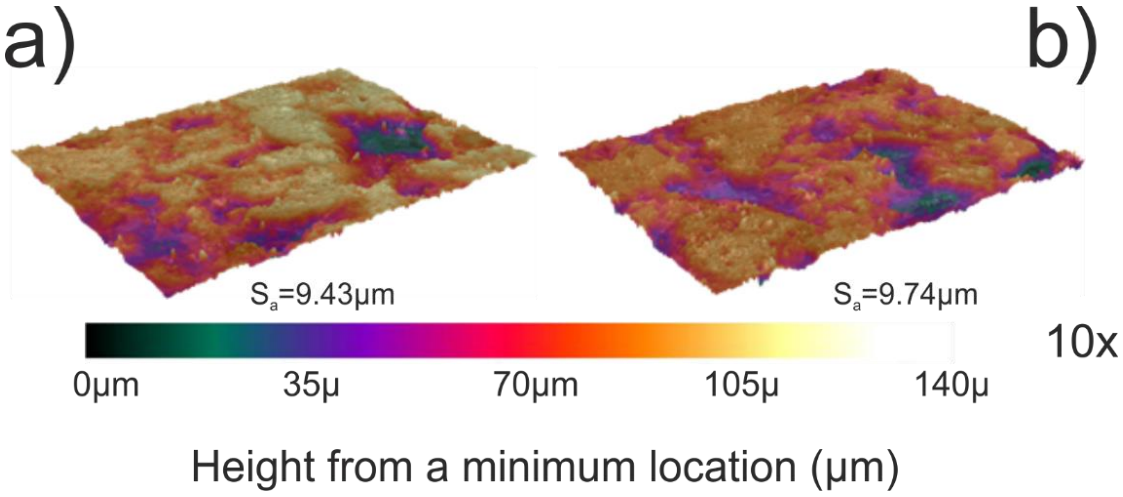

Figure 3.8 Optical profilometer topography: 3D surface images of Serena stone before (a) and after (b) the application of the zein 5% coating.

The average roughness (S_a) and root mean square roughness (S_q) parameters were calculated and are reported in Table 3.2. No statistically significant roughness differences were detected between the untreated sample and the treated one. This suggested the formation of a thin conformal layer of zein onto the stone's surface that did not mask the stone's intrinsic roughness. Other studies in literature stated that spray coating techniques allows to deposit a thin film that follows the features of the samples, avoiding the smoothing of the surface observed for coatings applied with other techniques [90].

Table 3.2 Average roughness (S_a) and root mean square roughness (S_q) measurements obtained with 3D optical profilometer.

SAMPLE	S_a (µm ± µm)	S_q (µm ± µm)
Untreated	9.747 ± 0.7858	12.25 ± 0.9711
Treated	9.434 ± 0.9748	12.36 ± 0.9346

The degree of adhesion of the coatings synthesized to the stone was evaluated with a peeling test and results were evaluated through SEM images. Figure 3.9 shows the surface morphology before (left side) and after (right side) the peeling test. The removal of a very small amount of material from the

sample surface was observed after peeling test, indicating an overall satisfactory adhesion of the coating to the stone. No significant loss of mass were observed after the tape removal (1.8 ± 0.4 mg).

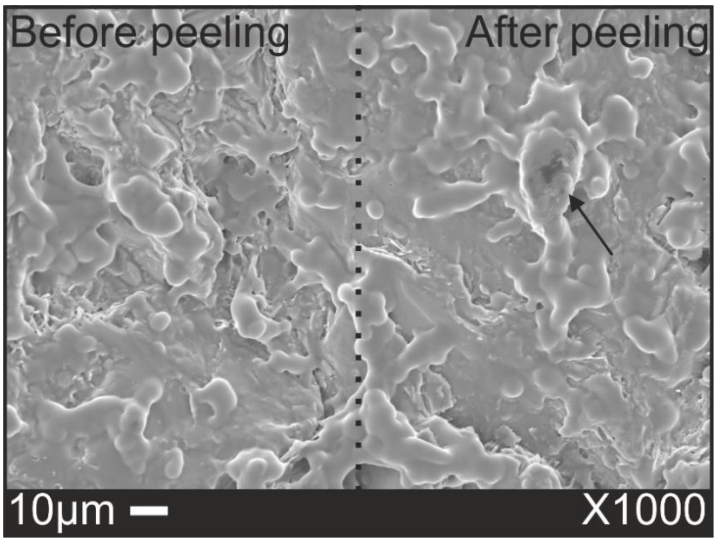

Figure 3.9 SEM images of Serena stone before (left) and after (right) peeling test. The right part of the image (after peeling) shows that only a slight portion of coating was removed after peeling test.

Figure 3.10a and b show the full spectra of untreated Serena stone and Serena stone with zein coating respectively.

In the XPS spectrum of Serena stone (Figure 3.10a) the characteristic elements of the stone were detected. After the application of the zein coating (Figure 3.10b), the peaks attributed to the stone disappeared, except for Si 2p and Ca 2p peaks, whose intensity however decreased considerably. In Table 3.3 are reported the differences in elemental compositions (%) between treated and untreated stone obtained from the survey spectra. In particular, N 1s peak (398.5 eV) was detected only in the spectra of treated stone and it demonstrates the presence of a zein coating of at least 10 nm. Moreover, the treated stone was found to be rich in C 1s (284.8 eV) and O 1 s (530.9 eV).

Table 3.3 Surface Chemical Composition obtained through XPS analysis for treated and untreated Serena stone.

	Elemental composition (At %)							
	C 1s	O 1s	N 1s	Si 2p	Ca 2p	Al 2p	Fe 2p	K 2p
Serena Stone	7.9	57.4	-	19.1	1.6	11.2	0.6	1.7
Serena Stone + coating	59.5	24.0	11.5	4.2	0.6	-	-	-

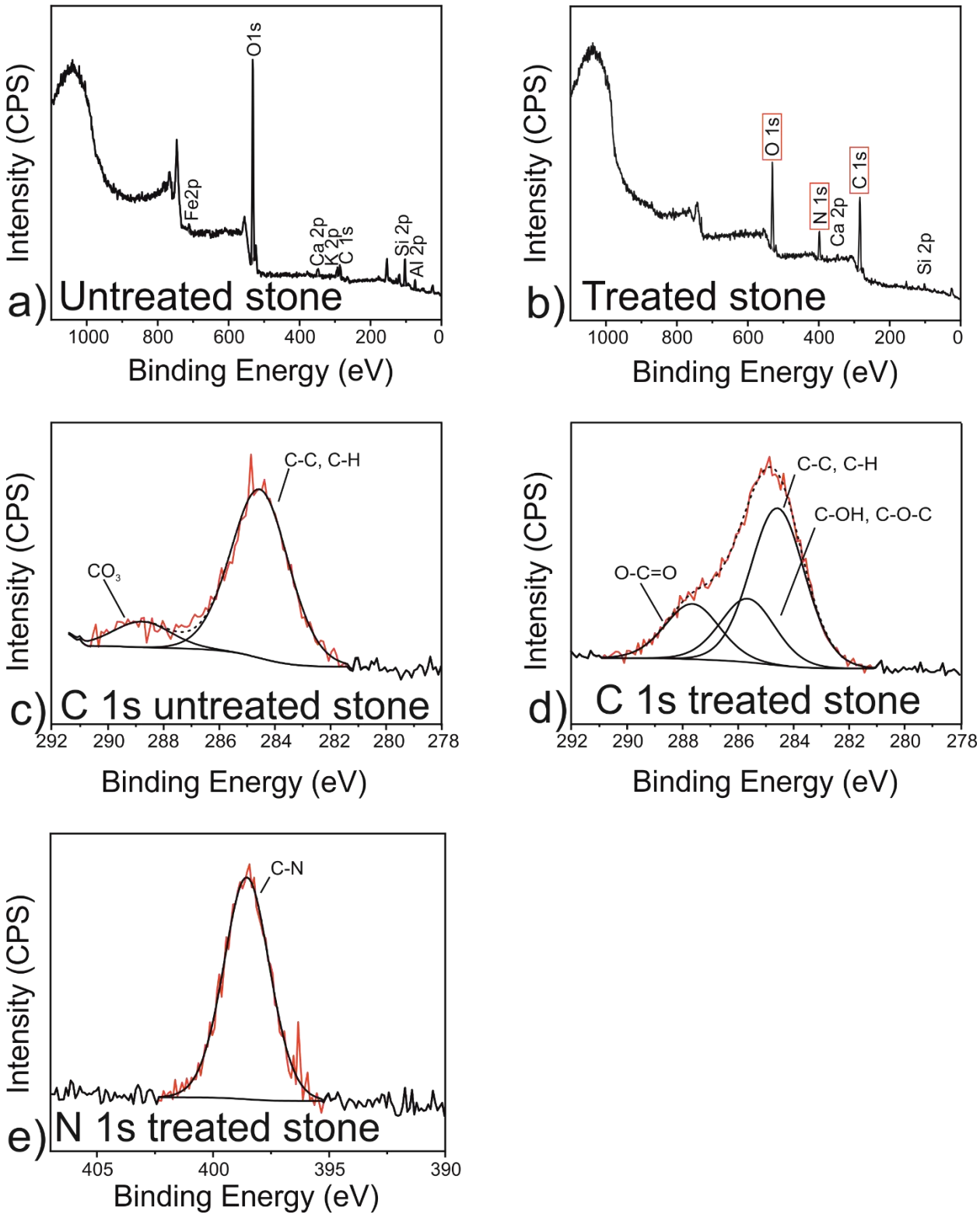

Figure 3.10 Full XPS scanning spectrum of a) Serena stone untreated and b) Serena stone treated with zein coating. XPS high-resolution spectra of C 1s for c) untreated Serena stone and d) Serena stone treated with zein coating. e) XPS high-resolution spectra.

However, to better understand the origin of the peaks, the high-resolution C1s XPS spectra of untreated and zein-treated stone peak were acquired and compared. Figure 3.10c and d show the high-resolution XPS survey spectra of untreated and treated stone respectively: the difference in the shape of the peaks is evident. In the high resolution spectra of C 1s of untreated Serena stone only two peaks were observed: the peak at 284.5 eV, related to the C–C and/or C–H (aliphatic carbons), due to the adventitious carbon, while the minor peak at 289.2 eV is attributed the carbonate group of the small amount of calcite present in the stone. C 1s peak of zein-treated stone, instead, was deconvoluted in three fitted peaks: the component located at 284.5 eV corresponded to C–C and/or C–H (aliphatic carbons), the component at 285.6 corresponded to C–O–C and/or C–OH, while the component at 287.7 eV corresponded to C–C=O [132,137,161,195].

SEM and XPS and analysis, combined with profilometric measurements and peeling test, confirmed that a thin conformal coating having nanoscale thickness (at least 10nm) and strong adhesion to the stone was deposited[196].

3.4 Conclusion

This chapter deal with the study of a zein-based protective coating for stone. The set up used for the application of the coating on stone material was illustrated and the characteristics of the selected stone evaluated. Then, the chapter focused mainly on the evaluation of the protective effectiveness against the action of water and on the evaluation of coating distribution when applied on stone material.

The coating was able to confer a good degree of water repellency, and a reduced absorption of moisture in humid environment. Moreover, it is thin enough to maintain a high surface roughness, which enhance the coating hydrophobicity. The application of surfaces techniques such as XPS, SEM AND profilometric measurements allowed observing a uniform of the coating over the treated stone, with strong adhesion to the stone substrate.

Nevertheless, as already mentioned, other requirements need to be fulfilled in other to be sure of the suitability of a polymer system as protective for stone materials. Criteria such as durability, transparency, stability and reversibility have to be evaluated in order to establish the suitability of the coating proposed for stone protection. The next chapter concerns on the evaluation of these requirements.

4. Applicability of the zein-based coating

Aiming at predicting the potential long-term serviceability of the developed material under its expected conditions of use, several test concerning the durability were performed.

Due to the previously outlined issues regarding the removability of past interventions on historical buildings, reversibility and retreatability are becoming more and more crucial in conservation[93,197]. Zein is known to be extracted from renewable sources and biodegradable. Nevertheless, there is no logical assumption that the material developed in this work is also fully biodegradable. There is a general expectation that novel biopolymers designed from renewable and biodegradable resources must be also biodegradable. Changes in functional groups, formation of cross-linked structures and copolymerization eventually occurring during the fabrication of new materials can lead to a product that do not necessarily exhibit significant or relevant biodegradability [198]. Therefore, several tests have been performed: artificial ageing and resistance to biodegradation tests were carried out; moreover, a biodegradability assessment was performed with the aim to assess the long-term environmental impact of the developed zein-based material under environmental conditions, and removability tests were performed with the aim of verify the effective treatment reversibility.

4.1 Stability of zein coating by artificial aging

The behavior of the treated stone over time by accelerated aging is essential to evaluate the effectiveness of the treatments and their stability. Through ageing it is possible to predict the change of properties such as residual hydrophobicity and color variation [199].

Thus, a four-week aging test was carried out on treated and untreated stone samples. Briefly, 3 replicas of treated and untreated stones were placed in a Memmert Climate chamber with three cold light fluorescent lamps (D65, 6500 K) and two UV lamps (320–400 nm), at 25°C and 60% R.H., simulating an accelerated aging of 7.5 Mlxh (million lux hours) [74,127,180]. After aging, static contact angle was measured in order to verify the residual protective effectiveness of treatment and a colorimetric analysis was performed in order to state any possible color changes due to ageing [200,201].

The evaluation of colorimetric parameter in conservation science is of great concern. The proposed treatment is deemed to be applied on valuable building façades and historical monuments and, thus, it should guarantee the preservation of the original color avoiding any aesthetical change on the treated surface. The color of the stone was measured before and after applying the protective coating, and before and after performing accelerated aging tests. The total chromatic variation upon application of

the product was evaluated according to NORMAL 43/93[202]. A portable spectrophotometer and colorimeter Konica Minolta CM 26d with a D65 illuminant and 10◦ standard observer was used. The instrument has a 3-mm diameter measurement area, and it is set to quantify the potential specular component included (SCI). The measurement points were localized by a reference spatial grid to ensure precise repeated measurements in the same location before and after the treatment as well as before and after the artificial aging. Reflectance measurements were analyzed according to the CIEL*a*b color parameters. The Cartesian (L*a*b*) coordinates, where L* is the brightness vector on a gray scale from 0 to 100 (from black to white, respectively), a* is the red/green color component (positive for red and negative for green), and b* is the yellow/blue component (positive for yellow and negative for blue), were obtained [203,204]. The color space in which the coordinates are placed is represented in Figure 4.1.

The total color change ΔE*, which represents the deviation from the original value due to the presence of the coating, was calculated for each sample according to the formula:

$$\Delta E^* = \sqrt{(\Delta L^*)^2 + (\Delta a^*)^2 + (\Delta b^*)^2}$$

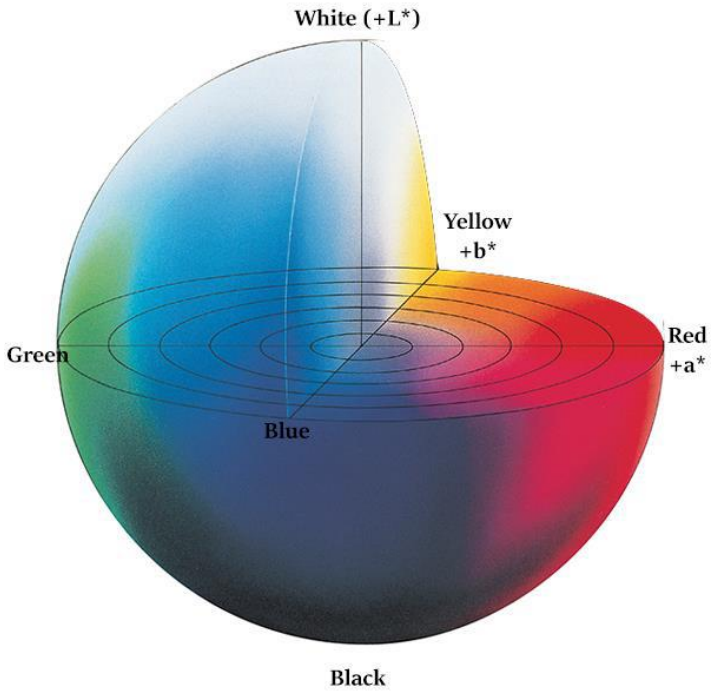

Figure 4.1 CIE 1976 Lab Color space [219].

The static water contact angle (WCA) was calculated after accelerated ageing tests. To obtain average values, 10 measurements were acquired on each of the 3 aged samples and standard deviation was calculated.

Results of artificial ageing test are shown in Figure 4.2.

After aging of the zein-treated stone a decrease in water contact angle was observed, nevertheless, a water contact angle around 100° was maintained. Moreover, from the WCAs tracking in time it is evident that aged samples exhibit the same trend observed for unaged sample (Figure 4.2a).

Figure 4.2b shows the measured colorimetric variations ΔE* due to the aging. A ΔE* of 1.21 ± 0.06 and 1.29 ± 0.08 was observed for unaged and aged stone, respectively. Checking the colorimetric variation is fundamental in order to evaluate whether the treatment and the aging have an aesthetical impact on the stone. In fact, both after being treated and being aged, the stone should maintain the color variation under the threshold value of 3 in terms of ΔE [205].

Hence, the measured values are much below the limit value even after accelerate aging. This means that the color changes are always maintained lower than the threshold value beneath which the variations are accepted by conservators.

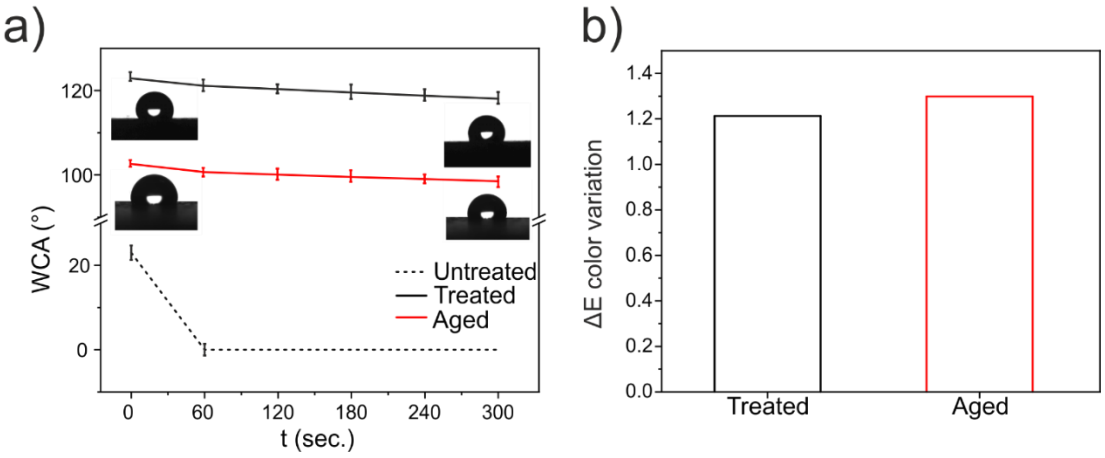

Figure 4.2a) Water contact angle over time of untreated (dot line), treated (black solid line) and aged (red solid line) samples. Static WCA are reported at 0 s, 60 s, 120 s, 180 s, 240 s and 300 s; b) ΔE color variation for unaged zein-treated (black) and aged zein-treated (red) samples with respect to untreated stones. (For interpretation of the references to color in this figure legend, the reader is referred to the web version of this article).*

Overall, the zein coating showed a good resistance to aging, a satisfactory water repellency was maintained, and no significant color variations were observed in the specific experimental conditions.

4.2 Resistance to biodeterioration by microbial colonization test

Considering the bio-based origin of the coating, to exclude any potential pro-vegetative effect on the treated stones the effect of zein coating on microbial colonization was assessed. Samples were analyzed by a semi- quantitative method observing the growth of either *Agrocybe aegerita* (Aae) mycelium or naturally occurring microorganisms on the stone surface. Biological growth was classified as follows: − when no colonization was observed on the stone; + in case of mild colonization on the stone; ++ to +++ for stone partially covered by colonies; ++++ when high colonization was observed on the stone. The mycelium from the fungal strain *Agrocybe aegerita* (Aae), was chosen as a test microorganism because of its ability to grow even on inert substrates, which is related to the outstanding oxidizing properties of its secretome (Patent No. IT102020000016798) [206]. The fungal strain growth was monitored for 2 weeks on both treated and untreated Serena stone, previously sterilized with UV radiation. Sterilization of the stone through UV radiation was aimed at avoiding the alteration of the zein film during the thermal process. Briefly, 5 cm × 5 cm × 1 cm treated and untreated samples were exposed for 20 min to the radiation of a UV lamp with emission peak at 253,7 nm (U.V.C.). This wavelength is optimal to ensure sterilization by damaging microorganisms' nucleic acids (absorbance maximum at 260 nm), while minimizing the potential effects on zein (the UV absorbance spectrum of photosensitive aminoacids tryptophan and tyrosine shows a minimum around 250–260 nm and maximum at 280 nm) [207]. Each sample was then placed in a glass jar (diameter 10 cm) previously sterilized by autoclave and filled with 30 mL of either Potato Dextrose Broth (PDB) nutrient medium or water. Samples were inoculated with a disk (8 mm diameter) of mycelium on the top surface of the stone and incubated for 15 days in climatic chamber at 78% RH and 27°C. In parallel, a second set of experiments was performed in order to monitor potential growth of naturally occurring microorganisms on stone. Samples without the mycelium were thus subjected to the same process above illustrated. In this second case, two samples (G and H) did not undergo the sterilization procedure to ensure that UV treatment was not modifying the zein coating. Two replicates were prepared for each sample and, for a semi-quantitative evaluation of the fungal colonization, samples were monitored on a daily basis [200,201,208].

The growth of microorganisms on treated and untreated stone was monitored on a daily base and results are summarized in Table 4.1.

Figure 4.3, instead, shows the degree of colonization for each experimental condition after 15 days. In presence of PDB medium, the selected mycelium (*Agrocybe aegerita* - *Aae*) colonized the top surface

of both treated and untreated samples (Figure 4.3C and D respectively) and the surrounding medium, irrespective of the zein coating. On the contrary, when the test was repeated using pure MilliQ water as growth medium, negligible colonization was detected (Figure 4.3A and B). These results proved that zein does not seem to serve as nourishment for the fungal mycelium. During a second set of experiments, no mycelium was added while treated and untreated stone samples were incubated in PDB. In absence of the competing mycelium, some microorganisms resident on stone grew in PDB but did not colonize the stone samples (Figure 4.3E and F), just a mild adhesion was observed for the untreated stone in presence of PDB medium (see Table 4.1). The growth of microorganisms in the medium was more intense when the samples did not undergo UV sterilization before incubation (Figure 4.3G* and H*), nevertheless, even in these cases only a mild colonization was observed. These results confirm that zein does neither limit nor promote the growth of common microorganisms naturally occurring in the environment.

Table 4.1 Temporal evolution of the growth of Aae (myc) or naturally occurring microorganisms on stone samples.

	DESCRIPTION	**TIME (DAYS)**			
		2	5	10	15
A	Treated - myc- H_2O	+	+	+	+
B	Untreated - myc- H_2O	+	+	+	+
C	Treated - myc- PDB	+	++	+++	++++
D	Untreated - myc- PDB	+	++	+++	++++
E	Treated - no myc- PDB	–	–	–	–
F	Untreated - no myc- PDB	–	–	–	+
G*	Treated - no myc- PDB	–	–	–	–
H*	Untreated - no myc- PDB	–	–	–	+
	*not UV sterilized samples				

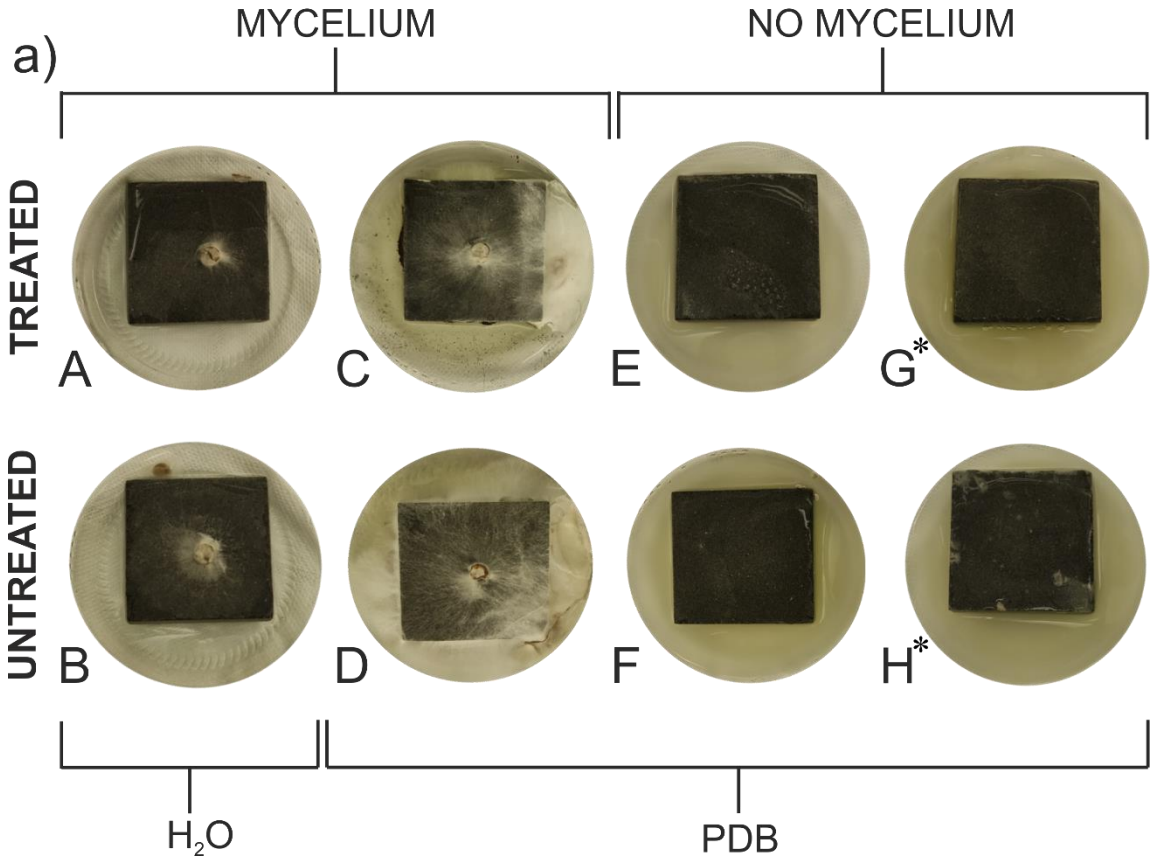

Figure 4.3 Fungal and microbial degradation test on stone samples after 15 days. Treated (A) and untreated (B) Serena stone, UV treatment, mycelium in H2O; treated (C) and untreated (D) Serena stone, UV treatment, mycelium in PDB; treated (E) and untreated (F) Serena stone, UV treatment, no mycelium in PDB; treated (G) and untreated (H*) Serena stone no UV treatment, no mycelium.*

4.3 Biodegradability assessment

The biodegradability assessment aimed at verifying the effective biodegradability of the developed film. This is of great concern in case of any accidental loss of material in the environment. For this assessment the ISO 14851 methodology was used, which estimates the biodegradation in aqueous medium by measuring O_2 consumption [209]. Biochemical Oxygen Demand (BOD) was determined by monitoring the oxygen consumption in a closed respirometer. Respirometric methodologies are a direct and reliable estimation of biodegradability of materials. 100mg of samples were weighted and incubated in 432 ml of river water collected from the environment, which already contains the real microbial population and the nutrients needed for their growth. The experiment was conducted inside dark glass bottles hermetically closed with the OxiTop® in order to monitor pressure variations inside them. The tested material represents the sole carbon source. During biodegradation, oxygen is

consumed while carbon dioxide is released. NaOH was added to the system, not in contact with the water, in order to sequestrate carbon dioxide produced during the biodegradation therefore biotic consumption of the oxygen present in the free volume of the system can be measured as a function of the decrease in pressure. The experiment was conducted at room temperature for 28 days under continuous magnetic stirring. The 28 days of incubation time was considered sufficient from preliminary studies to allow almost entire expression of the biodegradation [210]. Raw data of oxygen consumption (mg O_2/L) are corrected subtracting the mean values of the blanks, obtained by measuring the oxygen consumption of the river water in absence of any test material. After this subtraction, values get normalized on the mass of the individual samples and referred to 100 mg of material (mg O_2/100mg material). Finally, means of the replicates are calculated and the detected values of BOD were plotted as a function of time. As result sigmoidal curves, describing the progressive microbial growth, which directly depends on the biodegradability of the tested material, were obtained.
Starch was used as reference material to compare results obtained because as zein it is obtained from maize grain and it is commonly used as biodegradable component in composites.

The curves of the Biochemical Oxygen Demand (BOD) analysis in Figure 4.4, shows that the oxygen consumption obtained for the tested samples are of the same order of magnitude.

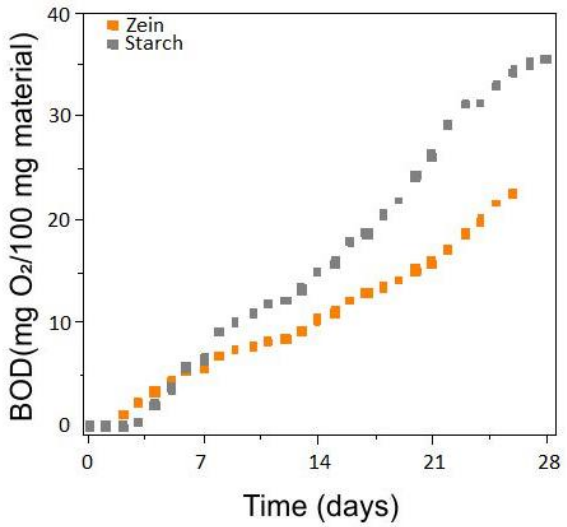

Figure 4.4 . Biochemical oxygen consumption (mg O_2/100 g material) as a function of time (days) for for zein (orange dots) and starch (gray dots) composites.

Both materials undergo biodegradation; however none of the two materials reach the plateau after 28 days, indicating the maximum amount of oxygen is not consumed within the end of the analysis. Zein undergoes faster degradation during the first 7 days of experiment, while as the experiment proceed the degradation rate slow down with respect to starch composite.

Longer experiments could be necessary to reach the more complete biodegradability of the developed material; however, it can be stated that no issues dispersion of polymer in the environment should be present.

4.4 Removability tests

Although biopolymers cannot be properly defined as reversible or retreatable, since they do not necessarily exhibit any improved solubility with respect to current protectives, if they are biodegradable, they are expected to completely disappear from the stone once their water repellency action is lost. For this reason, biopolymers might be considered intrinsically reversible, as they do not leave any permanent residue in the stone and do not cause any unforeseen consequences in subsequent conservation work.

However, their removability should not be taken for granted. No regulation is present in cultural heritage conservation field to evaluate the removability of the coating, thus, several tests have been performed.

A first solubility test was conducted by dipping the zein 5%-DMSO film in four different solvents: water, water-Tween 20(2%v/v), EtOH (80%) and DMSO.

Then, the removability test was conducted both in vitro, on slide glasses treated by spray coating with the 5% solution of zein in DMSO, and on stone material. Since when applied on stone material the coating adhesion might be related to its roughness and porosity, the test on slide glasses was used as a reference to establish if the coting was removed effectively. The test was conducted by means of cotton wool sticks saturated with the above-mentioned solvents.

Removal test on stone samples, instead, was performed by immerging the treated stone in 20 mL of EtOH and DMSO respectively for 1 hour. Samples were then washed several times with fresh solvent and dried in an oven at 60°C for 24 hours [211].

After removal test, WCAs and SEM images were acquired as described in the previous paragraphs.

Results of the solubility test are reported in Figure 4.5; as expected zein film is still soluble in DMSO and EtOH 80% while it is not soluble in water, even when 2% of Tween 20 is added as surfactant.

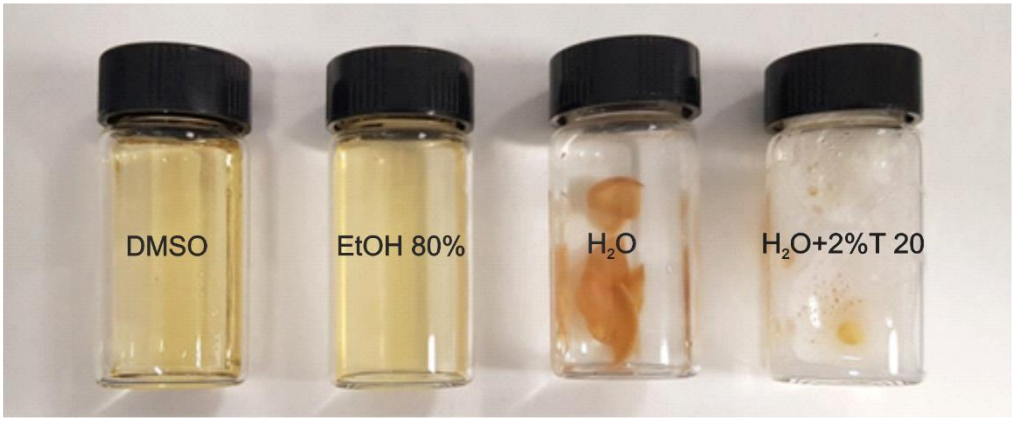

Figure 4.5 Solubility test of zein5%-DMSO film in dimethyl sulphoxide (DMSO), ethanol 80%(v/v) (EtOH), water (H_2O) and H_2O + Tween 20 (2% v/v) (H2O+2%T20).

The removability test performed in vitro gave the same results: a complete removal of the coating was obtained only when EtOH 80% and DMSO were used as solvents. While using sole water and the mixture of water-Tween 20 (2%) surfactant the coating was not removed effectively.

As shown in Table 4.2 after the removability test with DMSO and EtOH 80%, surface turns out to be hydrophilic again, indicating a certain degree of coating removal. Nevertheless, WCAs measured (85±2° and 78±3° for DMSO and EtOH 80% respectively) are higher than the one observed for untreated stone (~30°); this might indicate a non-complete removability possibly due to the penetration of the coating inside the stone pores during the treatment. SEM images confirmed that the coating was removed effectively from the surface and, especially when EtOH 80% was used as solvent, the surface morphology observed after washing is similar to the one of untreated stone.

Table 4.2 Results of removal test after washing the samples in DMSO or in EtOH 80%.

	WCA (°) after 1 hour washing		SEM image before washing	SEM image after 1 hour washing
PS after immersion in DMSO	85 ± 2°		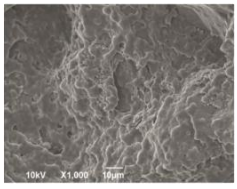	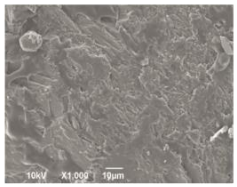
PS after immersion in EtOH 80%	78 ± 3°			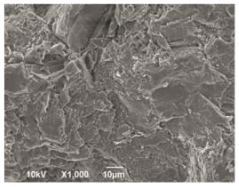

Several other washing cycles could be necessary to assess a complete removability of zein-based coating from the stone, nevertheless, with the surface removal of the coating at least the retreatability is guaranteed.
Moreover, further studies might be necessary in order to exclude any other issues in term of biodegradability and removability during the eventual intermediate phase of polymer degradation.

4.5 Preliminary implementation for a Lifa Cycle Analysis (LCA)

As reported previously, the here developed coating demonstrated to fulfill the requirements needed for its application as protective coating for exposed stone materials. However, the quantification of environmental burned might give a more complete idea of its application in real cases. In fact, besides the issues regarding their degradation with ageing, one of main problem related to the production and use of traditional synthetic products is that most of them have a relatively high environmental footprint. Moreover, often their application requires the use of potentially carcinogenic solvents.

Life Cycle Assessment (LCA) is a standardized method [212] which aims exactly at quantify all the energy requirements, the resources consumed, and the relevant emissions to the environment, and to evaluate the related environmental impacts that are associated with life cycle of a given material.

According to ISO standards, the methodology to evaluate the LCA is structured in several phases:

- Goal and scope definition;
- System boundries;
- Definition of the functional unit;
- Life cycle inventory;
- Impact assessment
- Results interpretation.

One of the main problems related to the application of LCA in the field of the protection of the cultural heritage, is the lack of literature data, thus any assessment regarding the potential impact of the developed material can serve mainly as a source of comparative data for future LCA studies [104,213,214]

Moreover, this lack of knowledge results often also in difficulties in finding data in data base inventories, regarding some specific processes. In the specific case of zein, for examples, several data were missing regarding processes such as its extraction from maize gluten meal and its purification.

Further study is necessary in order to collect data and implement the life cycle inventory, however, in the following paragraphs the preliminary phases for the implementation of the life cycle assessment of the developed zein-based coating are presented. Some considerations and concerns, which have been encountered while planning the impact assessment, are raised.

4.5.1 Definition of goal and scope

The aim of this study was to evaluate the environmental performance of the developed zein 5% solution in DMSO in order to assess if the material can be really proposed as a sustainable alternative, at least from the environmental point of view. Then, other aspects, such as impact of the intervention on society and the economy might be further investigated [6,215].

4.5.2 Definition of system boundaries

Study of potential environmental impact in all the relevant life cycle stages is defined cradle-to-grave; it includes the production stage, the construction process stage, the use stage and the end-of-life stage.

This preliminary study instead focused on the manufacturing of the materials; therefore, the cradle-to-gate system boundaries were considered in planning the LCA. The following processes were included in this first phase:

- The production of constituent materials (including the treatment of dry-milled maize to obtain maize gluten meal, from which zein is extracted)
- The transport of chemicals and constituents materials to the laboratory in which the material is manufactured
- The manufacturing of the final material

4.5.3 Definition of functional unit

The surface treatment of 1 m^2 of Serena stone was used as functional unit. The amount of protective material, which is applied per square meter of a cultural heritage structure, is 1.2 L (one layer).

However, the actual consumption of conservation materials, based on the treatment of 1 m^2 depends on the type of surface being treated, and especially on the porosity of the substrate, also related to its state of conservation.

For this reason, the amount of product applied can vary depending on the decision of the restorers, who need to evaluate each case separately.

4.5.4 Life cycle inventory (LCI)

Figure 4.6 Schematic description of the processes involved in zein-based protective coating development.shows a diagram in which resume all the processes involved to produce the zein-based coating.

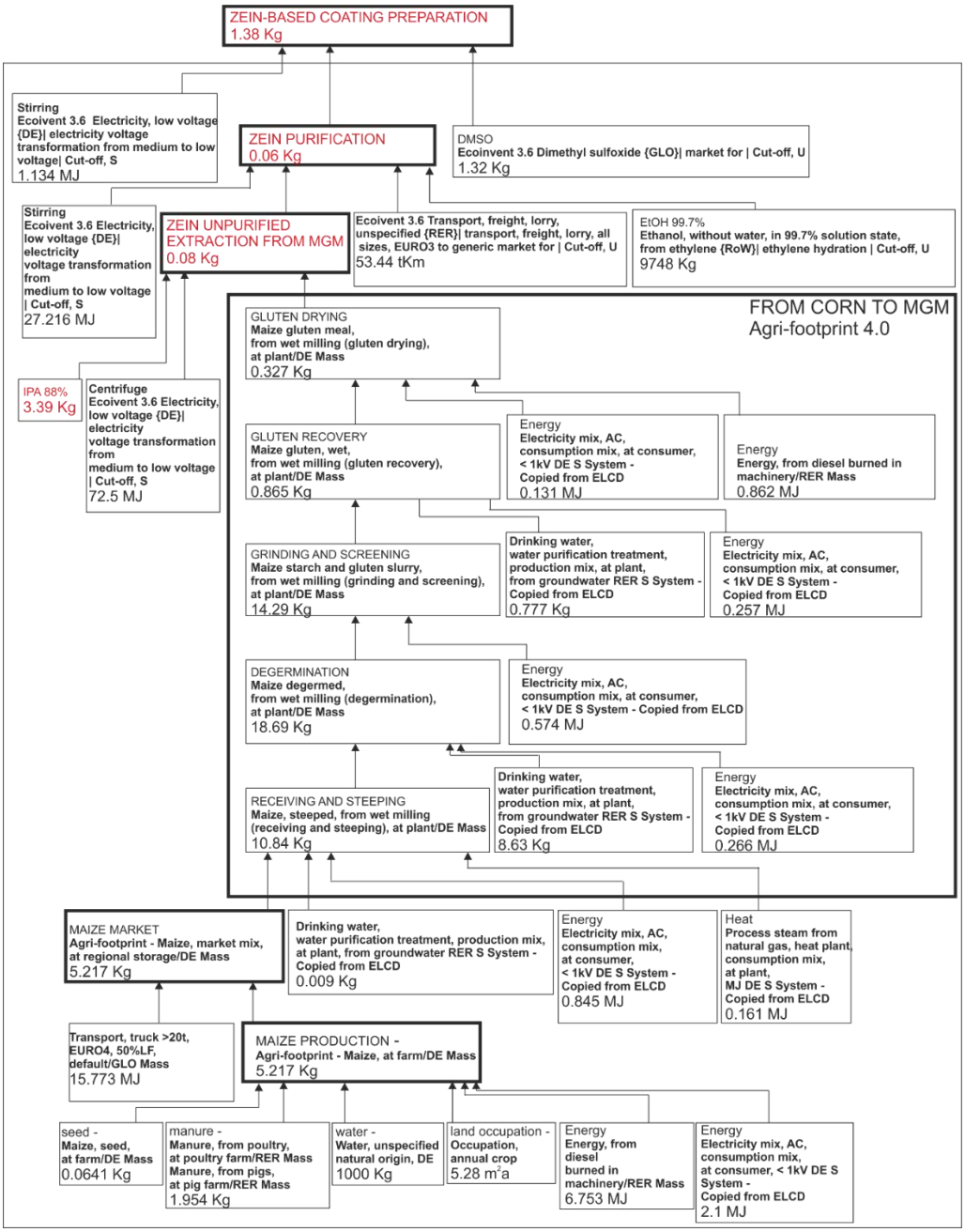

Figure 4.6 Schematic description of the processes involved in zein-based protective coating development.

LCI data from Agri-footprint database can be used to evaluate the environmental impacts related to (i) the cultivation of maize, (ii) the transformation of maize in maize gluten meal, from which sein is extracted. These processes are indicated with bold black boxed in the diagram. Regarding zein extraction from MGM (Maize gluten meal) and purification of zein no LCI data were available in the database, thus, at the moment some of these data are just conceiveble. For zein extraction procedure was obtained from the literature [135,216], nevertheless some data are still missing to proceed in the implementation of the life cycle assessment. However, due to the presence of several uncertain parameter, a sensitivity analysis should be carried out, in order to study the robustness of the results and their sensitivity to data, assumptions and models [217].

4.6 Conclusion

The present chapter aimed to predict the developed material's behavior when applied as a protective coating for stone substrates. Besides the promising results of protection against water, good adhesion and uniform distribution over the stone surface, a polymer must satisfy several other requirements to be applied in the cultural heritage protection field.

Artificial ageing test aimed at predicting the long term durability of the coating; hydrophobicity was maintained after accelerated ageing, showing WCAs around 100°, and no visible color changes due to ageing were detected. Considering the natural origin of zein, a microbial colonization test was performed aiming at excluding any pro-vegetative effect on the treated stone. From the experiment, it was clear that zein neither avoids or promotes the treated stone’s biocolonization.

As previously mentioned the bio-based origin of the developed material does not necessarily ensure its biodegradability. Thus, an assessment of the zein-based material biodegradability was carried out aiming at exclude environmental issues in case of accidental dispersion of material in the environment, either due to external factors or due to the natural long-term behavior under environmental conditions. From the results obtained the biodegradability of the here developed material was confirmed.

Aiming at meeting the requirement of reversibility of the treatment solubility and removability test were performed and, according to the results obtained, the superficial removability is ensured.

Finally, through the LCA, which is still ongoing, it will be estimated the overall environmental impact of the proposed treatment.

5. Conclusions and future prospectives

This thesis was born from the need to develop an innovative and sustainable treatment for the conservation of valuable outdoor architecture and monument. Stone in fact, is prone to several degradation phenomena such as dissolution, erosion, biodeterioration, formation of crusts and patina and cracking due to the exposure to water and humidity. Chapter 1 illustrated that water acts as a carrier of air pollutants and salts present in the atmosphere and in the soil, and promote the growth of microorganism both on stone surface and in the bulk, causing chemical and physical damages.

The literature investigation, also presented in Chapter 1, revealed the presence of several synthetic commercial products for protection treatments. However, most of these commercially available polymers, with ageing undergo to degradation, with reducing of waterproofing behavior, yellowing and detachment of the polymeric layer, and other degradation forms resulting often in a difficult, and sometimes impossible, removability. Others, such as fluoropolymers, are heading towards elimination due to their known long-lasting persistence and toxicity.

For these reasons, in the attempt to respond to a literature lack of knowledge concerning biopolymers and pushed by several international organization, which are now driving towards the introduction of green materials and methodologies in cultural heritage, this research focused on proposing an innovative bio-based and biodegradable treatment, paying particular attention to sustainability and reversibility needs.

The developed hydrophobic zein-based coating was presented in Chapter 2. Solvents with no environmental hazards were used for zein purification and for biopolymer manufacturing, and the hydrophobic surface formation obtained through spray-coating technique was deeply studied. The obtained coating was then successfully tested as protective for stone material.

Chapter 3 showed that the developed material can form a thin uniform layer with excellent adhesion to the stone substrate and, taking advantage of the intrinsic roughness of the stone high hydrophobicity was conferred. Moreover, our analysis demonstrated that even the spray technique used for the application of the zein coating contributed to the formation of a hydrophobic coating on the stone surface. The zein-based treatments also conferred high resistance to water and, at the same time, maintained a good water vapor permeability, despite the known high gas barrier properties of zein. The colorimetric properties were unaltered after the treatments and their stability to accelerated aging was also confirmed.

Chapter 4 illustrated the tests performed with the aim to predict the behavior of the zein-based material under its expected conditions of use.

After accelerated ageing test, the protective coating maintained a good hydrophobicity and aesthetical properties were unchanged. Biodeterioration test demonstrated that zein does not enhance the microbial growth on stone material. Biodegradability and removability assessments confirmed the fulfillment of the conservation requirements.

The promising hydrophobic characteristics, good adhesion, transparency, durability, sustainability and retreatability make thus the proposed treatment suitable for the protection of valuable buildings and monuments. Future prospectives of this work concerns the application of the treatment on other stone materials, such as marble and travertine, as well as *in situ* application in order to evaluate its performance as protective in real conditions. Moreover, the possible addition of a proper anti-fouling system to the developed material will be considered in order to address the problems related to the biological growth observed on the stone. Moreover, the quantification of environmental burned might give a more complete idea of the impact of the treatment when applied in real cases.

Bibliography

[1] A. Moropoulou, E. Zendri, P. Ortiz, E.T. Delegou, I. Ntoutsi, E. Balliana, J. Becerra, R. Ortiz, Scanning microscopy techniques as an assessment tool of materials and interventions for the protection of built cultural heritage, Scanning. 2019 (2019). https://doi.org/10.1155/2019/5376214.

[2] E.M. Winkler, Stone: Properties, Durability in man's Environment, (1973).

[3] Icomos, European Cultural Heritage Green Paper, Value. 1 (2020) i–v.

[4] F. Di Turo, L. Medeghini, How green possibilities can help in a future sustainable conservation of cultural heritage in Europe, Sustain. 13 (2021) 1–14. https://doi.org/10.3390/su13073609.

[5] Y. Ocak, A. Sofuoglu, F. Tihminlioglu, H. Böke, Sustainable bio-nano composite coatings for the protection of marble surfaces, J. Cult. Herit. 16 (2015) 299–306. https://doi.org/10.1016/j.culher.2014.07.004.

[6] E. Balliana, G. Ricci, C. Pesce, E. Zendri, Assessing the value of green conservation for cultural heritage: Positive and critical aspects of already available methodologies, Int. J. Conserv. Sci. 7 (2016) 185–202.

[7] T. Salvatici, S. Calandra, I. Centauro, E. Pecchioni, E. Intrieri, Monitoring and Evaluation of Sandstone Decay Adopting Non-Destructive Techniques : On-Site Application on Building Stones, (2020) 1287–1301.

[8] E. Zendri, G. Biscontin, I. Nardini, S. Riato, Characterization and reactivity of silicatic consolidants, Constr. Build. Mater. 21 (2007) 1098–1106. https://doi.org/10.1016/j.conbuildmat.2006.01.006.

[9] M. Zucchelli, F.D. Villarruel, P. David-Gara, M.R. Costante, M. Tascon, F. Marte, F.S. García Einschlag, F.M. Cabrerizo, Photophysics and photochemistry of carminic acid and related natural pigments, Phys. Chem. Chem. Phys. 22 (2020) 9534–9542. https://doi.org/10.1039/d0cp01312a.

[10] D. Eric, Price Clifford A., Research in Conservation, 2010. https://doi.org/10.1007/s10531-016-1233-4.

[11] A.E. Charola, E. Wendler, An Overview of the Water-Porous Building Materials Interactions, 21 (2015) 55–65. https://doi.org/10.1515/rbm-2015-0006.

[12] C. Esposito Corcione, R. Striani, M. Frigione, Novel hydrophobic free-solvent UV-cured hybrid organic-inorganic methacrylic-based coatings for porous stones, Prog. Org. Coatings. 77 (2014) 803–812. https://doi.org/10.1016/j.porgcoat.2014.01.008.

[13] S.W. Massey, The effects of ozone and NO(x) on the deterioration of calcareous stone, Sci. Total Environ. 227 (1999) 109–121. https://doi.org/10.1016/S0048-9697(98)00409-4.

[14] H.A. Al-Hosney, V.H. Grassian, Water, sulfur dioxide and nitric acid adsorption on calcium carbonate: A transmission and ATR-FTIR study, Phys. Chem. Chem. Phys. 7 (2005) 1266–1276. https://doi.org/10.1039/b417872f.

[15] M. Camaiti, S. Bugani, E. Bernardi, L. Morselli, M. Matteini, Effects of atmospheric NOx on biocalcarenite coated with different conservation products, Appl. Geochemistry. 22 (2007) 1248–1254. https://doi.org/10.1016/j.apgeochem.2007.03.035.

[16] S. Eyssautier-Chuine, B. Marin, C. Thomachot-Schneider, G. Fronteau, A. Schneider, S. Gibeaux, P. Vazquez, Simulation of acid rain weathering effect on natural and artificial carbonate stones, Environ. Earth Sci. 75 (2016) 1–19. https://doi.org/10.1007/s12665-016-5555-z.

[17] S.J. Haneef, J.B. Johnson, G.E. Thompson, G.C. Wood, Effects of dry deposition of pollutant gases on the degradation of pentelic marble, Corros. Sci. 35 (1993) 743–747. https://doi.org/10.1016/0010-938X(93)90211-X.

[18] L.G. Johansson, Synergistic effects of air pollutants on the atmospheric corrosion of metals and calcareous stones, Mar. Chem. 30 (1990) 113–122. https://doi.org/10.1016/0304-4203(90)90065-K.

[19] A. Putnis, Experimental study of the replacement of calcite by calcium sulphates, 156 (2015) 75–93. https://doi.org/10.1016/j.gca.2015.02.012.

[20] M. Hartman, O. Trnka, K. Svoboda, V. Veselý, Thermal Dissociation and H2S Reactivity of Czech Limestones, Chem. Pap. 57 (2003) 309–316.

[21] S. Keener, S.-J. Khang, T. Keener, A calcination and sulfation reaction model for calcium carbonate with sulfur dioxide, J. Environ. Manage. 2 (1998) 251–268.

[22] Y. Ocak, A. Sofuoglu, F. Tihminlioglu, H. Böke, Protection of marble surfaces by using biodegradable polymers as coating agent, Prog. Org. Coatings. 66 (2009) 213–220. https://doi.org/10.1016/j.porgcoat.2009.07.007.

[23] A. Artesani, F. Di Turo, M. Zucchelli, A. Traviglia, Recent advances in protective coatings for cultural heritage-an overview, Coatings. 10 (2020). https://doi.org/10.3390/coatings10030217.

[24] A.E. Charola, STONE DETERIORATION CHARACTERIZATION FOR ITS CONSERVATION, 24 (2016) 16–20. https://doi.org/10.18285/geonomos.v24i2.836.

[25] M.P. Campanella, L. Casoli, A. Colombini, M.P. Marini Bettolo, R. Matteini, M. Migneco, L.M. Montenero, A. Nodari, L. Piccioli, C. Plossi Zappalà, M. Portalone, G. Russo, U. Sammartino, Chimica per l'arte, 2007.

[26] V. Fassina, I. Santa, P. Mantova, THE INTERACTIONS BETWEEN THE STONE AND THE ATMOSPHERIC POLLUTANTS . THE FORMATION OF BLACK CRUSTS, (2020).

[27] H. Morillas, M. Maguregui, E. Gallego-Cartagena, I. Marcaida, N. Carral, J.M. Madariaga, The influence of marine environment on the conservation state of Built Heritage: An overview study, Sci. Total Environ. 745 (2020) 140899. https://doi.org/10.1016/j.scitotenv.2020.140899.

[28] ICOMOS, ISCS, Illustrated glossary on stone deterioration patterns, 2008. http://www.icomos.org/publications/monuments_and_sites/15/pdf/Monuments_and_Sites

_15_ISCS_Glossary_Stone.pdf.

[29] E. Doehne, Salt weathering: A selective review, Geol. Soc. Spec. Publ. 205 (2002) 51–64. https://doi.org/10.1144/GSL.SP.2002.205.01.05.

[30] A.E. Charola, Salts in the deterioration of porous materials: An overview, J. Am. Inst. Conserv. 39 (2000) 327–343. https://doi.org/10.1179/019713600806113176.

[31] A.E. Charola, C. Bläuer, Salts in Masonry: An Overview of the Problem, Restor. Build. Monum. 21 (2015) 119–135. https://doi.org/10.1515/rbm-2015-1005.

[32] E. Uchida, Y. Ogawa, N. Maeda, T. Nakagawa, Deterioration of stone materials in the Angkor Monuments, Cambodia, Dev. Geotech. Eng. 84 (2000) 329–340. https://doi.org/10.1016/S0165-1250(00)80027-9.

[33] V. Lopez-Acevedo, C. Viedma, V. Gonzalez, A. La Iglesia, Salt crystallization in porous construction materials II. Mass transport and crystallization processes, 0248 (1997).

[34] E. Cantisani, C.A. Garzonio, M. Ricci, S. Vettori, Relationships between the petrographical, physical and mechanical properties of some Italian sandstones, Int. J. Rock Mech. Min. Sci. 60 (2013) 321–332. https://doi.org/10.1016/j.ijrmms.2012.12.042.

[35] Q. Sun, Z. Dong, H. Jia, Decay of sandstone subjected to a combined action of repeated freezing–thawing and salt crystallization, Bull. Eng. Geol. Environ. 78 (2019) 5951–5964. https://doi.org/10.1007/s10064-019-01490-6.

[36] C. Cardell, F. Delalieux, K. Roumpopoulos, A. Moropoulou, F. Auger, R. Van Grieken, Salt-induced decay in calcareous stone monuments and buildings in a marine environment in SW France, Constr. Build. Mater. 17 (2003) 165–179. https://doi.org/10.1016/S0950-0618(02)00104-6.

[37] M. Angeli, R. Hébert, B. Menéndez, C. David, J.P. Bigas, Influence of temperature and salt concentration on the salt weathering of a sedimentary stone with sodium sulphate, Eng. Geol. 115 (2010) 193–199. https://doi.org/10.1016/j.enggeo.2009.06.001.

[38] M.H. Ghobadi, R. Babazadeh, Experimental Studies on the Effects of Cyclic Freezing–Thawing, Salt Crystallization, and Thermal Shock on the Physical and Mechanical Characteristics of Selected Sandstones, Rock Mech. Rock Eng. 48 (2015) 1001–1016. https://doi.org/10.1007/s00603-014-0609-6.

[39] C. Alves, C. Figueiredo, A. Maurício, M.A.S. Braga, L. Aires-Barros, Limestones under salt decay tests: Assessment of pore network-dependent durability predictors, Environ. Earth Sci. 63 (2011) 1511–1527. https://doi.org/10.1007/s12665-011-0915-1.

[40] D. Benavente, Why pore size is important in the deterioration of porous stones used in the built heritage, Macla. 15 (2011) 41–42. https://doi.org/10.1007/s12665-010-0815-9.transported.

[41] D. Benavente, N. Cueto, J. Martínez-Martínez, M.A. García Del Cura, J.C. Cañaveras, The influence of petrophysical properties on the salt weathering of porous building rocks, Environ. Geol. 52 (2007) 197–206. https://doi.org/10.1007/s00254-006-0475-y.

[42] E. Charola, O. Salvadori, Methods to prevent biocolonization and recolonization: An overview of current research for architectural and archaeological heritage, Biocolonization Stone Control Prev. Methods, Proc. from MCI Work. Ser. (2011) 38–39.

[43] A.Z. Miller, P. Sanmartín, L. Pereira-Pardo, A. Dionísio, C. Saiz-Jimenez, M.F. Macedo, B. Prieto, Bioreceptivity of building stones: A review, Sci. Total Environ. 426 (2012) 1–12. https://doi.org/10.1016/j.scitotenv.2012.03.026.

[44] O. Guillitte, Bioreceptivity: a new concept for building ecology studies, Sci. Total Environ. 167 (1995) 215–220. https://doi.org/10.1016/0048-9697(95)04582-L.

[45] G. Caneva, D. Di Stefano, C. Giampaolo, S. Ricci, D. Kwiatkowski, R. Löfvendahl, Stone Cavity and Porosity as a Limiting Factor for Biological Colonisation: the Travertine of Lungotevere (Rome), Proc. 10th Int. Congr. Deterior. Conserv. Stone. (2004) 227–232.

[46] T. Szymura, D. Barnat-hunek, Protection of Stone Building Structures Against Corrosion Caused by Moisture, (2013).

[47] G. Khanlari, R.Z. Sahamieh, Y. Abdilor, The effect of freeze–thaw cycles on physical and mechanical properties of Upper Red Formation sandstones, central part of Iran, Arab. J. Geosci. 8 (2015) 5991–6001. https://doi.org/10.1007/s12517-014-1653-y.

[48] C. Walbert, J. Eslami, A.L. Beaucour, A. Bourges, A. Noumowe, Evolution of the mechanical behaviour of limestone subjected to freeze–thaw cycles, Environ. Earth Sci. 74 (2015) 6339–6351. https://doi.org/10.1007/s12665-015-4658-2.

[49] A. Bonazza, P. Messina, C. Sabbioni, C.M. Grossi, P. Brimblecombe, Mapping the impact of climate change on surface recession of carbonate buildings in Europe, Sci. Total Environ. 407 (2009) 2039–2050. https://doi.org/10.1016/j.scitotenv.2008.10.067.

[50] S. Ist, B. Bianche, R. March, Decay of Sandstone in Urban Areas C O R R E L a T E D With, (1991) 305–316.

[51] P. Rizzarelli, C. La Rosa, A. Torrisi, Testing a fluorinated compound as a protective material for calcarenite, J. Cult. Herit. 2 (2001) 55–62. https://doi.org/10.1016/S1296-2074(01)01109-8.

[52] I.S. Bayer, Superhydrophobic Coatings from Ecofriendly Materials and Processes: A Review, Adv. Mater. Interfaces. 7 (2020) 1–25. https://doi.org/10.1002/admi.202000095.

[53] I. Karapanagiotis, M. Hosseini, Superhydrophobic coatings for the protection of natural stone, in: Adv. Mater. Conserv. Stone, Springer International Publishing, 2018: pp. 1–25. https://doi.org/10.1007/978-3-319-72260-3_1.

[54] R.N. Wenzel, RESISTANCE OF SOLID SURFACES TO WETTING BY WATER, Ind. Eng. Chem. 28 (1936) 988–994. https://doi.org/10.1021/ie50320a024.

[55] B.D. Cassie, Wettability of porous surfaces, Trans. Faraday Soc. (1944) 546–551.

[56] G. Alessandrini, M. Aglietto, V. Castelvetro, F. Ciardelli, R. Peruzzi, L. Toniolo, Comparative evaluation of fluorinated and unfluorinated acrylic copolymers as water-repellent coating materials for stone, J. Appl. Polym. Sci. 76 (2000) 962–977.

https://doi.org/10.1002/(SICI)1097-4628(20000509)76:6<962::AID-APP24>3.0.CO;2-Z.

[57] G. Biscontin, P. Maravelaki, E. Zendri, A. Glisenti, Siliconic and Acrylic Resins Dispersed in Water as Protectives for Stone Surface, MRS Proc. 267 (1992) 935–941. https://doi.org/10.1557/proc-267-935.

[58] T. Poli, L. Toniolo, O. Chiantore, The protection of different Italian marbles with two partially flourinated acrylic copolymers, Appl. Phys. A Mater. Sci. Process. 79 (2004) 347–351. https://doi.org/10.1007/s00339-004-2530-4.

[59] M.J. Melo, S. Bracci, M. Camaiti, O. Chiantore, F. Piacenti, Photodegradation of acrylic resins used in the conservation of stone, Polym. Degrad. Stab. 66 (1999) 23–30. https://doi.org/10.1016/S0141-3910(99)00048-8.

[60] M. Zielecka, E. Bujnowska, Silicone-containing polymer matrices as protective coatings: Properties and applications, Prog. Org. Coatings. 55 (2006) 160–167. https://doi.org/10.1016/j.porgcoat.2005.09.012.

[61] H. Ling, N. Maiqian, L. Guozheng, Preparation and feasibility analysis of fluoropolymer to the sandstone protection, Prog. Org. Coatings. 62 (2008) 206–213. https://doi.org/10.1016/j.porgcoat.2007.11.002.

[62] L. Bergamonti, F. Bondioli, I. Alfieri, S. Alinovi, A. Lorenzi, G. Predieri, P.P. Lottici, Weathering resistance of PMMA/SiO2/ZrO2 hybrid coatings for sandstone conservation, Polym. Degrad. Stab. (2018). https://doi.org/10.1016/j.polymdegradstab.2017.12.012.

[63] V. Sabatini, C. Cattò, G. Cappelletti, F. Cappitelli, S. Antenucci, H. Farina, M.A. Ortenzi, S. Camazzola, G. Di Silvestro, Protective features, durability and biodegration study of acrylic and methacrylic fluorinated polymer coatings for marble protection, Prog. Org. Coatings. 114 (2018) 47–57. https://doi.org/10.1016/j.porgcoat.2017.10.003.

[64] V. Sabatini, E. Pargoletti, M. Longoni, H. Farina, M.A. Ortenzi, G. Cappelletti, Stearyl methacrylate co-polymers: Towards new polymer coatings for mortars protection, Appl. Surf. Sci. 488 (2019) 213–220. https://doi.org/10.1016/j.apsusc.2019.05.097.

[65] O. Chiantore, M. Lazzari, Characterization of acrylic resins, Int. J. Polym. Anal. Charact. 2 (1996) 395–408. https://doi.org/10.1080/10236669608033358.

[66] R.L. Feller, New solvent-type varnishes, Stud. Conserv. 6 (1961) 171–175. https://doi.org/10.1179/sic.1961.s040.

[67] T. Nishiura, M. Fukuda, S. Miura, Treatment of stone with synthetic resins for its protection against damage by freeze-thaw cycles, Stud. Conserv. 29 (1984) 156–159. https://doi.org/10.1179/sic.1984.29.Supplement-1.156.

[68] G.G. Amoroso, V. Furlan, Utilisation de rÉsines acryliques pour la protection superficielle de grÉs tendres, Stud. Conserv. 20 (1975) 2–7. https://doi.org/10.1179/sic.1975.20.1.001.

[69] M.L. Tabasso, Acrylic Polymers for the Conservation of Stone: Advantages and Drawbacks, APT Bull. 26 (1995) 17. https://doi.org/10.2307/1504445.

[70] E. Zendri, Protettivi acrilici nella conservazione della pietra, (1991).

[71] M. Lazzari, O. Chiantore, Thermal-ageing of paraloid acrylic protective polymers, Polymer (Guildf). 41 (2000) 6447–6455. https://doi.org/10.1016/S0032-3861(99)00877-0.

[72] O. Chiantore, M. Lazzari, Photo-oxidative stability of paraloid acrylic protective polymers, Polymer (Guildf). 42 (2001) 17–27. https://doi.org/10.1016/S0032-3861(00)00327-X.

[73] M. Favaro, R. Mendichi, F. Ossola, U. Russo, S. Simon, P. Tomasin, P.A. Vigato, Evaluation of polymers for conservation treatments of outdoor exposed stone monuments. Part I: Photo-oxidative weathering, Polym. Degrad. Stab. 91 (2006) 3083–3096. https://doi.org/10.1016/j.polymdegradstab.2006.08.012.

[74] M. Favaro, R. Mendichi, F. Ossola, S. Simon, P. Tomasin, P.A. Vigato, Evaluation of polymers for conservation treatments of outdoor exposed stone monuments . Part II : Photo-oxidative and salt-induced weathering of acrylic e silicone mixtures, 92 (2007) 335–351. https://doi.org/10.1016/j.polymdegradstab.2006.12.008.

[75] M. Roos, F. König, S. Stadtmüller, B. Weyershausen, Evolution of silicone based water repellents for modern building protection, 5th Int. Conf. Water Repel. Treat. Build. Mater. 16 (2008) 3–16.

[76] G. Wheeler, Alkoxysilanes and the Consolidation of Stone, 2005. http://www.jstor.org/stable/40025051.

[77] A.E. Charola, Water Repellents and Other 'Protective' Treatments: A Critical Review, Restor. Build. Monum. 9 (2003) 3–22.

[78] C. Domingo, M. Alvarez de Buergo, S. Sánchez-Cortés, R. Fort, J. V. García-Ramos, M. Gomez-Heras, Possibilities of monitoring the polymerization process of silicon-based water repellents and consolidants in stones through infrared and Raman spectroscopy, Prog. Org. Coatings. 63 (2008) 5–12. https://doi.org/10.1016/j.porgcoat.2008.03.002.

[79] B. Simionescu, M. Olaru, M. Aflori, F. Doroftei, Siloxane-based polymers as protective coatings against SO2 dry deposition, High Perform. Polym. 23 (2011) 326–334. https://doi.org/10.1177/0954008310397635.

[80] A.C. De Oliveira Tavares Fojo, Estudo da aplicação de consolidantes e hidrófugos em pedras graníticas de Igreja Matriz de Caminha, (2006).

[81] D. Lampakis, P.N. Manoudis, I. Karapanagiotis, Monitoring the polymerization process of Si-based superhydrophobic coatings using Raman spectroscopy, Prog. Org. Coatings. 76 (2013) 488–494. https://doi.org/10.1016/j.porgcoat.2012.11.002.

[82] A. Tsakalof, P. Manoudis, I. Karapanagiotis, I. Chryssoulakis, C. Panayiotou, Assessment of synthetic polymeric coatings for the protection and preservation of stone monuments, J. Cult. Herit. 8 (2007) 69–72. https://doi.org/10.1016/j.culher.2006.06.007.

[83] A. Chatzigrigoriou, P.N. Manoudis, I. Karapanagiotis, Fabrication of water repellent coatings using waterborne resins for the protection of the cultural heritage, Macromol. Symp. 331–332 (2013) 158–165. https://doi.org/10.1002/masy.201300063.

[84] P.N. Manoudis, I. Karapanagiotis, A. Tsakalof, I. Zuburtikudis, B. Kolinkeová, C.

Panayiotou, Superhydrophobic films for the protection of outdoor cultural heritage assets, Appl. Phys. A Mater. Sci. Process. 97 (2009) 351–360. https://doi.org/10.1007/s00339-009-5233-z.

[85] M.Y. Yüce, A.L. Demirel, The effect of nanoparticles on the surface hydrophobicity of polystyrene, Eur. Phys. J. B. 64 (2008) 493–497. https://doi.org/10.1140/epjb/e2008-00042-0.

[86] J. Kapolos, N. Bakaoukas, A. Koliadima, G. Karaiskakis, Evaluation of acrylic polymeric resin and small siloxane molecule for protecting cultural heritage monuments against sulfur dioxide corrosion, Prog. Org. Coatings. 59 (2007) 152–159. https://doi.org/10.1016/j.porgcoat.2007.03.001.

[87] F. Gherardi, S. Goidanich, L. Toniolo, Improvements in marble protection by means of innovative photocatalytic nanocomposites, Prog. Org. Coatings. 121 (2018) 13–22. https://doi.org/10.1016/J.PORGCOAT.2018.04.010.

[88] M. Y. Abdellah, A. F. Gelany, A. F. Mohamed, A. Bakr Khoshaim, Protection of Limestone Coated with Different Polymeric Materials, Am. J. Mech. Eng. 5 (2017) 51–57. https://doi.org/10.12691/ajme-5-2-3.

[89] C. Esposito Corcione, N. De Simone, M.L. Santarelli, M. Frigione, Protective properties and durability characteristics of experimental and commercial organic coatings for the preservation of porous stone, Prog. Org. Coatings. 103 (2017) 193–203. https://doi.org/10.1016/j.porgcoat.2016.10.037.

[90] P. Fermo, G. Cappelletti, N. Cozzi, G. Padeletti, S. Kaciulis, M. Brucale, M. Merlini, Hydrophobizing coatings for cultural heritage. A detailed study of resin/stone surface interaction, Appl. Phys. A Mater. Sci. Process. 116 (2014) 341–348. https://doi.org/10.1007/s00339-013-8127-z.

[91] D. Aslanidou, I. Karapanagiotis, C. Panayiotou, Tuning the wetting properties of siloxane-nanoparticle coatings to induce superhydrophobicity and superoleophobicity for stone protection, Mater. Des. 108 (2016) 736–744. https://doi.org/10.1016/j.matdes.2016.07.014.

[92] iccrom, ed., Methods of evaluating products for the conservation of porous building materials in monuments, 1995.

[93] M.J. Varas, M. Alvarez de Buergo, R. Fort, The influence of past protective treatments on the deterioration of historic stone façades: A case study, Stud. Conserv. 52 (2007) 110–124. https://doi.org/10.1179/sic.2007.52.2.110.

[94] G. Mavrov, Aging of silicone resins, Stud. Conserv. 28 (1983) 171–178. https://doi.org/10.1179/sic.1983.28.4.171.

[95] E. Ntelia, I. Karapanagiotis, Superhydrophobic Paraloid B72, Prog. Org. Coatings. 139 (2020) 105224. https://doi.org/10.1016/j.porgcoat.2019.105224.

[96] P.N. Manoudis, I. Karapanagiotis, Modification of the wettability of polymer surfaces using nanoparticles, Prog. Org. Coatings. 77 (2014) 331–338. https://doi.org/10.1016/j.porgcoat.2013.10.007.

[97] L. De Ferri, P.P. Lottici, A. Lorenzi, A. Montenero, E. Salvioli-Mariani, Study of silica nanoparticles - polysiloxane hydrophobic treatments for stone-based monument protection, J. Cult. Herit. 12 (2011) 356–363. https://doi.org/10.1016/j.culher.2011.02.006.

[98] L. Pinho, M.J. Mosquera, Titania-silica nanocomposite photocatalysts with application in stone self-cleaning, J. Phys. Chem. C. 115 (2011) 22851–22862. https://doi.org/10.1021/jp2074623.

[99] A. Licciulli, A. Calia, M. Lettieri, D. Diso, M. Masieri, S. Franza, R. Amadelli, G. Casarano, Photocatalytic TiO 2 coatings on limestone, J. Sol-Gel Sci. Technol. 60 (2011) 437–444. https://doi.org/10.1007/s10971-011-2574-9.

[100] E. Quagliarini, F. Bondioli, G.B. Goffredo, A. Licciulli, P. Munafò, Smart surfaces for architectural heritage: Preliminary results about the application of TiO2-based coatings on travertine, J. Cult. Herit. 13 (2012) 204–209. https://doi.org/10.1016/j.culher.2011.10.002.

[101] E. Quagliarini, F. Bondioli, G.B. Goffredo, A. Licciulli, P. Munafò, Self-cleaning materials on Architectural Heritage: Compatibility of photo-induced hydrophilicity of TiO2 coatings on stone surfaces, J. Cult. Herit. 14 (2013) 1–7. https://doi.org/10.1016/j.culher.2012.02.006.

[102] E. Quagliarini, L. Graziani, D. Diso, A. Licciulli, M. D'Orazio, Is nano-TiO2 alone an effective strategy for the maintenance of stones in Cultural Heritage?, J. Cult. Herit. 30 (2018) 81–91. https://doi.org/10.1016/j.culher.2017.09.016.

[103] R. Kaegi, A. Ulrich, B. Sinnet, R. Vonbank, A. Wichser, S. Zuleeg, H. Simmler, S. Brunner, H. Vonmont, M. Burkhardt, M. Boller, Synthetic TiO2 nanoparticle emission from exterior facades into the aquatic environment, Environ. Pollut. 156 (2008) 233–239. https://doi.org/10.1016/j.envpol.2008.08.004.

[104] A.M. Ferrari, M. Pini, P. Neri, F. Bondioli, Nano-TiO 2 coatings for limestone: Which sustainability for cultural heritage?, Coatings. 5 (2015) 232–245. https://doi.org/10.3390/coatings5030232.

[105] E. Benedetti, A. D'Alessio, M.F. Zini, E. Bramanti, N. Tirelli, P. Vergamini, G. Moggi, Characterization of acrylic resins and fluoroelastomer blends as potential materials in stone protection, Polym. Int. 49 (2000) 888–892. https://doi.org/10.1002/1097-0126(200008)49:8<888::AID-PI514>3.0.CO;2-E.

[106] Y. Cao, A. Salvini, M. Camaiti, One-step fabrication of robust and durable superamphiphobic, self-cleaning surface for outdoor and in situ application on building substrates, J. Colloid Interface Sci. 591 (2021) 239–252. https://doi.org/10.1016/j.jcis.2021.02.001.

[107] M. Mazzola, P. Frediani, S. Bracci, A. Salvini, New strategies for the synthesis of partially fluorinated acrylic polymers as possible materials for the protection of stone monuments, Eur. Polym. J. 39 (2003) 1995–2003. https://doi.org/10.1016/S0014-3057(03)00110-1.

[108] M. Sadat-Shojai, A. Ershad-Langroudi, Polymeric Coatings for Protection of Historic Monuments: Opportunities and Challenges, J. Appl. Polym. Sci. 116 (2010) 2658–2667.

https://doi.org/10.1002/app.

[109] E. Casazza, L. Ricco, S. Russo, A. Mariani, Synthesis, characterization, and properties of a novel acrylic terpolymer with pendant perfluoropolyether segments, Polymer (Guildf). 43 (2002) 1207–1214. https://doi.org/10.1016/S0032-3861(01)00722-4.

[110] R.A. Iezzi, S. Gaboury, K. Wood, Acrylic-fluoropolymer mixtures and their use in coatings, Prog. Org. Coatings. 40 (2000) 55–60. https://doi.org/10.1016/S0300-9440(00)00117-X.

[111] L. Toniolo, C. Della Volpe, M. Brugnara, T. Poli, Partially fluorinated acrylic copolymers as coatings for stone protection: Characterization and surface properties, Mater. Res. Soc. Symp. - Proc. 712 (2002) 91–97. https://doi.org/10.1557/proc-712-ii3.3.

[112] T. Report, J. Nipsect, E. Assessment, S. Alternative, M. View, Survey and environmental / health assessment of fluorinated substances in impregnated consumer products and ... Survey and environmental / health assessment of fluorinated substances in impregnated consumer products and, (2016).

[113] A. Blum, Perspectives | Brief Communication The Madrid Statement on Poly- and, Environ. Health Perspect. 123 (2015) A107–A111. https://doi.org/10.1021/es201662b.Fei.

[114] V. Dichiarante, R. Milani, P. Metrangolo, Natural surfactants towards a more sustainable fluorine chemistry, Green Chem. 20 (2018) 13–27. https://doi.org/10.1039/c7gc03081a.

[115] M. Niegowska, P. Pretto, E. Porcel-rodriguez, D. Marinov, L. Ceriani, T. Lettieri, Per- and polyfluoroalkyl substances (PFAS) of possible concern in the aquatic environment, 2021. https://doi.org/10.2760/377564.

[116] United Nations Environment Programme, Stockholm Convention, (n.d.). http://www.pops.int/TheConvention/ThePOPs/TheNewPOPs/tabid/2511/Default.aspx.

[117] M.M. Reddy, Acid Rain Damage To Carbonate Stone : a Quantitative Assessment Based on the Aqueous, Earth Surf. Process. Landforms. 13 (1988) 335–354. https://onlinelibrary.wiley.com/doi/epdf/10.1002/esp.3290130406.

[118] ECHA to consider restrictions on the use of oxo-plastics and microplastics, (n.d.). https://echa.europa.eu/it/-/echa-to-consider-restrictions-on-the-use-of-oxo-plastics-and-microplastis.

[119] European Council, Directive (Eu) 2019/904 of the European Parliament and of the Council of 5 June 2019 on the reduction of the impact of certain plastic products on the environment, Www.Plasticseurope.De. 2019 (2019) 1–19. https://www.plasticseurope.org/en/resources/publications/1689-working-together-towards-more-sustainable-plastics%0Ahttps://www.plasticseurope.org/en/resources/publications%0Ahttps://eur-lex.europa.eu/legal-content/EN/TXT/PDF/?uri=CELEX:32019L0904&from=EN.

[120] European boplastics, (n.d.). https://www.european-bioplastics.org/market/.

[121] M. Conde, Horizon Europe. The next EU Research & Innovation Investment Programme (2021–2027), (2019). https://ec.europa.eu/info/research-and-innovation/funding/funding-

opportunities/funding-programmes-and-open-calls/horizon-europe_en.

[122] CEN European Committee for Standardization, CEN/TR 15932. Plastics—recommendation for terminology and characterization of biopolymers and bioplastics., 2010.

[123] Y. Zhong, P. Godwin, Y. Jin, H. Xiao, Biodegradable polymers and green-based antimicrobial packaging materials : A mini-review, Adv. Ind. Eng. Polym. Res. 3 (2020) 27–35. https://doi.org/10.1016/j.aiepr.2019.11.002.

[124] B. Sacchi, E. Cantisani, G. Giuntoli, S. Salvini, L. Rosi, M. Frediani, P. Frediani, Bio-Polymers as Stone Protectives, 12th Int. Congr. Deterior. Conserv. Stone Columbia Univ. New York, 2012 BIO-POLYMERS. (2012) 1–10.

[125] G. Giuntoli, L. Rosi, M. Frediani, B. Sacchi, P. Frediani, Fluoro-Functionalized PLA Polymers as Potential Water-Repellent Coating Materials for Protection of Stone Giulia, J. Appl. Polym. Sci. 116 (2011) 2658–2667. https://doi.org/10.1002/app.

[126] M.C. Mistretta, F.P. La Mantia, V. Titone, B. Megna, L. Botta, M. Morreale, Durability of biodegradable polymers for the conservation of cultural heritage, Front. Mater. 6 (2019) 1–12. https://doi.org/10.3389/fmats.2019.00151.

[127] S. Andreotti, E. Franzoni, P. Fabbri, Poly(hydroxyalkanoate)s-based hydrophobic coatings for the protection of stone in cultural heritage, Materials (Basel). 11 (2018) 9–11. https://doi.org/10.3390/ma11010165.

[128] L. Winandy, O. Schlebusch, R. Fischer, Fungal hydrophobins render stones impermeable for water but keep them permeable for vapor, Sci. Rep. 9 (2019) 1–8. https://doi.org/10.1038/s41598-019-42705-w.

[129] M. Martí, L. Molina, C. Alemán, E. Armelin, Novel epoxy coating based on DMSO as a green solvent, reducing drastically the volatile organic compound content and using conducting polymers as a nontoxic anticorrosive pigment, ACS Sustain. Chem. Eng. 1 (2013) 1609–1618. https://doi.org/10.1021/sc400271k.

[130] W. Xie, T. Li, C. Chen, H. Wu, S. Liang, H. Chang, B. Liu, E. Drioli, Q. Wang, J.C. Crittenden, Using the Green Solvent Dimethyl Sulfoxide to Replace Traditional Solvents Partly and Fabricating PVC/PVC- g-PEGMA Blended Ultrafiltration Membranes with High Permeability and Rejection, Ind. Eng. Chem. Res. 58 (2019) 6413–6423. https://doi.org/10.1021/acs.iecr.9b00370.

[131] R. Shukla, M. Cheryan, Zein: The industrial protein from corn, Ind. Crops Prod. 13 (2001) 171–192. https://doi.org/10.1016/S0926-6690(00)00064-9.

[132] K. Shi, J.L. Kokini, Q. Huang, Engineering zein films with controlled surface morphology and hydrophilicity, J. Agric. Food Chem. 57 (2009) 2186–2192. https://doi.org/10.1021/jf803559v.

[133] Y. Li, Q. Xia, K. Shi, Q. Huang, Scaling behaviors of α-zein in acetic acid solutions, J. Phys. Chem. B. 115 (2011) 9695–9702. https://doi.org/10.1021/jp203476m.

[134] Y. Li, J. Li, Q. Xia, B. Zhang, Q. Wang, Q. Huang, Understanding the dissolution of α-

zein in aqueous ethanol and acetic acid solutions, J. Phys. Chem. B. 116 (2012) 12057–12064. https://doi.org/10.1021/jp305709y.

[135] T.J. Anderson, B.P. Lamsa, Zein extraction from corn, corn products, and coproducts and modifications for various applications: A review, Cereal Chem. 88 (2011) 159–173. https://doi.org/10.1094/CCHEM-06-10-0091.

[136] E. Corradini, P.S. Curti, A.B. Meniqueti, A.F. Martins, A.F. Rubira, E.C. Muniz, Recent advances in food-packing, pharmaceutical and biomedical applications of zein and zein-based materials, Int. J. Mol. Sci. 15 (2014) 22438–22470. https://doi.org/10.3390/ijms151222438.

[137] U. Dashdorj, M.K. Reyes, A.R. Unnithan, A.P. Tiwari, B. Tumurbaatar, C.H. Park, C.S. Kim, Fabrication and characterization of electrospun zein/Ag nanocomposite mats for wound dressing applications, Int. J. Biol. Macromol. 80 (2015) 1–7. https://doi.org/10.1016/j.ijbiomac.2015.06.026.

[138] Y. Zhang, W.Y. Li, R. Lan, J.Y. Wang, Quality Monitoring of Porous Zein Scaffolds: A Novel Biomaterial, Engineering. 3 (2017) 130–135. https://doi.org/10.1016/J.ENG.2017.01.001.

[139] C. Xia, W. Wang, L. Wang, H. Liu, J. Xiao, Multilayer zein/gelatin films with tunable water barrier property and prolonged antioxidant activity, Food Packag. Shelf Life. 19 (2019) 76–85. https://doi.org/10.1016/j.fpsl.2018.12.004.

[140] Y. Wei, J. Yao, Z. Shao, X. Chen, Water-Resistant Zein-Based Adhesives, (2020). https://doi.org/10.1021/acssuschemeng.0c01179.

[141] M. Oh, Q. Ma, S. Simsek, D. Bajwa, L. Jiang, Comparative study of zein- and gluten-based wood adhesives containing cellulose nanofibers and crosslinking agent for improved bond strength, Int. J. Adhes. Adhes. 92 (2019) 44–57. https://doi.org/10.1016/j.ijadhadh.2019.04.004.

[142] H. Tian, G. Guo, X. Fu, Y. Yao, L. Yuan, A. Xiang, Fabrication, properties and applications of soy-protein-based materials: A review, Int. J. Biol. Macromol. 120 (2018) 475–490. https://doi.org/10.1016/j.ijbiomac.2018.08.110.

[143] Q. Wang, L. Yin, G.W. Padua, Effect of hydrophilic and lipophilic compounds on zein microstructures, Food Biophys. 3 (2008) 174–181. https://doi.org/10.1007/s11483-008-9080-9.

[144] Y. Wang, G.W. Padua, Formation of zein microphases in ethanol-water, Langmuir. 26 (2010) 12897–12901. https://doi.org/10.1021/la101688v.

[145] Y. Wang, G.W. Padua, Nanoscale Characterization of Zein Self-Assembly, Langmuir. 28 (2012) 2429–2435. https://doi.org/10.1021/la204204j.

[146] M.I. Beck, I. Tomka, E. Waysek, Physico-chemical characterization of zein as a film coating polymer. A direct comparison with ethyl cellulose, Int. J. Pharm. 141 (1996) 137–150. https://doi.org/10.1016/0378-5173(96)04630-3.

[147] K. Shi, H. Yu, S. Lakshmana Rao, T.C. Lee, Improved mechanical property and water

resistance of zein films by plasticization with tributyl citrate, J. Agric. Food Chem. 60 (2012) 5988–5993. https://doi.org/10.1021/jf3001444.

[148] A. Jones, PROTEIN-BASED PLASTICS AND THEIR POTENTIAL USE IN MEDICAL AND FOOD PACKAGING APPLICATIONS, Pap. Knowl. . Towar. a Media Hist. Doc. (2020) 12–26.

[149] F.Y. De Boer, R.N.U. Kok, A. Imhof, K.P. Velikov, White zein colloidal particles: Synthesis and characterization of their optical properties on the single particle level and in concentrated suspensions, Soft Matter. 14 (2018) 2870–2878. https://doi.org/10.1039/c7sm02415k.

[150] Echa-European Chemical Agency, (n.d.). https://echa.europa.eu/ (accessed 12 April 2020).

[151] Y. Wei, L. Hu, J. Yao, Z. Shao, X. Chen, Facile Dissolution of Zein Using a Common Solvent Dimethyl Sulfoxide, Langmuir. (2019) 1–5. https://doi.org/10.1021/acs.langmuir.9b00670.

[152] Z. Wang, Y. Li, L. Jiang, B. Qi, L. Zhou, Relationship between secondary structure and surface hydrophobicity of soybean protein isolate subjected to heat treatment, J. Chem. 2014 (2014). https://doi.org/10.1155/2014/475389.

[153] F. Dong, M. Zhang, W.W. Tang, Y. Wang, Formation and mechanism of superhydrophobic/hydrophobic surfaces made from amphiphiles through droplet-mediated evaporation-induced self-assembly, J. Phys. Chem. B. 119 (2015) 5321–5327. https://doi.org/10.1021/acs.jpcb.5b00011.

[154] F. Petronella, A. Pagliarulo, A. Truppi, M. Lettieri, M. Masieri, A. Calia, M.L. Curri, R. Comparelli, TiO2 nanocrystal based coatings for the protection of architectural stone: The effect of solvents in the spray-coating application for a self-cleaning surfaces, Coatings. 8 (2018) 1–23. https://doi.org/10.3390/COATINGS8100356.

[155] T. Simovich, A.H. Wu, R.N. Lamb, Hierarchically rough, mechanically durable and superhydrophobic epoxy coatings through rapid evaporation spray method, Thin Solid Films. 589 (2015) 472–478. https://doi.org/10.1016/j.tsf.2015.05.065.

[156] V.M. Wallace, N.R. Dhumal, F.M. Zehentbauer, H.J. Kim, J. Kiefer, Revisiting the Aqueous Solutions of Dimethyl Sulfoxide by Spectroscopy in the Mid- and Near-Infrared: Experiments and Car-Parrinello Simulations, J. Phys. Chem. B. 119 (2015) 14780–14789. https://doi.org/10.1021/acs.jpcb.5b09196.

[157] N. Mozhzhukhina, L.P. Méndez De Leo, E.J. Calvo, Infrared spectroscopy studies on stability of dimethyl sulfoxide for application in a Li-air battery, J. Phys. Chem. C. 117 (2013) 18375–18380. https://doi.org/10.1021/jp407221c.

[158] M.Y. Skripkin, P. Lindqvist-Reis, A. Abbasi, J. Mink, I. Persson, M. Sandström, Vibrational spectroscopic force field studies of dimethyl sulfoxide and hexakis(dimethyl sulfoxide)scandium(III) iodide, and crystal and solution structure of the hexakis(dimethyl sulfoxide)scandium(III) ion, Dalt. Trans. (2004) 4038–4049. https://doi.org/10.1039/b413486a.

[159] M.T. Forel, M. Tranquille, Spectres de vibration du diméthylsulfoxyde et dn diméthylsulfoxyde-d6, Spectrochim. Acta Part A Mol. Spectrosc. 26 (1970) 1023–1034. https://doi.org/10.1016/0584-8539(70)80004-6.

[160] L.A. Forato, R. Bernardes-Filho, L.A. Colnago, Protein structure in KBr pellets by infrared spectroscopy, Anal. Biochem. 259 (1998) 136–141. https://doi.org/10.1006/abio.1998.2599.

[161] S. Ali, Z. Khatri, K.W. Oh, I.S. Kim, S.H. Kim, Zein/cellulose acetate hybrid nanofibers: Electrospinning and characterization, Macromol. Res. 22 (2014) 971–977. https://doi.org/10.1007/s13233-014-2136-4.

[162] L.A. Forato, T.D.C. Bicudo, L.A. Colnago, Conformation of α Zeins in Solid State by Fourier Transform IR, Biopolym. - Biospectroscopy Sect. 72 (2003) 421–426. https://doi.org/10.1002/bip.10481.

[163] Y. Wei, L. Hu, J. Yao, Z. Shao, X. Chen, Facile Dissolution of Zein Using a Common Solvent Dimethyl Sulfoxide, Langmuir. 35 (2019) 6640–6649. https://doi.org/10.1021/acs.langmuir.9b00670.

[164] T.C. Bicudo, L.A. Forato, L.A.R. Batista, L.A. Colnago, Study of the conformation of γ-zeins in purified maize protein bodies by FTIR and NMR spectroscopy, Anal. Bioanal. Chem. 383 (2005) 291–296. https://doi.org/10.1007/s00216-005-0003-z.

[165] C. Pignatelli, G. Perotto, M. Nardini, R. Cancedda, M. Mastrogiacomo, A. Athanassiou, Electrospun silk fibroin fibers for storage and controlled release of human platelet lysate, Acta Biomater. 73 (2018) 365–376. https://doi.org/10.1016/j.actbio.2018.04.025.

[166] R.G. Lebel, D.A.I. Goring, Density, Viscosity, Refractive Index, and Hygroscopicity of Mixtures of Water and Dimethyl Sulfoxide, J. Chem. Eng. Data. 7 (1962) 100–101. https://doi.org/10.1021/je60012a032.

[167] F. Fratini, S. Rescic, The stone materials of the historical architecture of Tuscany, Italy, Geol. Soc. Spec. Publ. 391 (2014) 71–92. https://doi.org/10.1144/SP391.5.

[168] P. Frediani, C. Manganelli, D. Fa, U. Matteoli, P. Tiano, C. Manganelli, Maney Publishing Use of Perfluoropolyethers as Water Repellents : Study of Their Behaviour on Pietra Serena , a Florentine Building Stone AS WATER REPELLENTS : USE OF PERFLUOROPOLYETHERS STUDY OF THEIR BEHAVIOUR ON PIETRA SERENA , A FLORENTINE BUILDING ST, 27 (2015) 31–37.

[169] E.L. Pecchioni, S.I. Vettori, E.M.M.A. Cantisani, F.A. Fratini, M.A. Ricci, Chemical and mineralogical studies of the red chromatic alteration of Florentine Pietra Serena sandstone, (2016) 449–458. https://doi.org/10.1127/ejm/2015/0027-2504.

[170] L. Vásquez, L. Campagnolo, A. Athanassiou, D. Fragouli, Expanded Graphite-Polyurethane Foams for Water-Oil Filtration, ACS Appl. Mater. Interfaces. 11 (2019) 30207–30217. https://doi.org/10.1021/acsami.9b07907.

[171] M.E. Antinori, L. Ceseracciu, G. Mancini, J.A. Heredia-Guerrero, A. Athanassiou, Fine-Tuning of Physicochemical Properties and Growth Dynamics of Mycelium-Based Materials, ACS Appl. Bio Mater. 3 (2020) 1044–1051.

https://doi.org/10.1021/acsabm.9b01031.

[172] P.P. Malesani, S.A. Vannucci, Decay of pietra serena and pietraforte, florentine building stones: Petrographic observations, Stud. Conserv. 19 (1974) 36–50. https://doi.org/10.1179/sic.1974.003.

[173] D. Colangiuli, A. Calia, N. Bianco, Novel multifunctional coatings with photocatalytic and hydrophobic properties for the preservation of the stone building heritage, Constr. Build. Mater. 93 (2015) 189–196. https://doi.org/10.1016/j.conbuildmat.2015.05.100.

[174] A. Calia, L. Matera, M. Lettieri, COMPACT LIMESTONES AS HISTORICAL BUILDING MATERIAL: PROPERTIES OF THE TRANI STONE (APULIA, SOUTHERN ITALY) AND PRELIMINARY STUDY FOR SELF CLEANING TREATMENTS, in: 2012: pp. 1–9.

[175] Raccomandazione NORMAL 33/89 1989. 'Misura dell'angolo di contatto'., in: Raccomandazioni Norm. Alterazioni Dei Mater. Lapidei e Tratt. Conserv. Propos. per l'unificazione Dei Metod. Sper. Di Stud. e Di Control., C.N.R – I.C.R.., Rome, Italy, n.d.

[176] ASTM. E96/E96M-10 Standard test methods for water vapor transmission of materials. In Annual book of ASTM standards Vol. 04.06., West Conshohocken, PA, 2010.

[177] UNI 10859:2000, Beni Culturali. Materiali lapidei naturali ed artificiali - Determinazione dell'assorbimento dell'acqua per capillarità, (n.d.).

[178] Raccomandazione NORMAL 7/81 1981. 'Assorbimento d'acqua per immersione totale – capacità di imbibizione'., in: Raccomandazioni Norm. Alterazioni Dei Mater. Lapidei e Tratt. Conserv. Propos. per l'unificazione Dei Metod. Sper. Di Stud. e Di Control., C.N.R – I.C.R.., Rome, Italy, 1981.

[179] Normal 44/93 : assorbimento d'acqua a bassa pressione, in: Raccomandazioni Norm. Alterazioni Dei Mater. Lapidei e Tratt. Conserv. Propos. per l'unificazione Dei Metod. Sper. Di Stud. e Di Control., CNR : ICR, Rome, Italy, 1993.

[180] G. Mazzon, M. Zahid, J.A. Heredia-Guerrero, E. Balliana, E. Zendri, A. Athanassiou, I.S. Bayer, Hydrophobic treatment of woven cotton fabrics with polyurethane modified aminosilicone emulsions, Appl. Surf. Sci. 490 (2019) 331–342. https://doi.org/10.1016/j.apsusc.2019.06.069.

[181] G. Tedeschi, S. Guzman-puyol, U.C. Paul, M.J. Barthel, Thermoplastic cellulose acetate oleate fi lms with high barrier properties and ductile behaviour, Chem. Eng. J. 348 (2018) 840–849. https://doi.org/10.1016/j.cej.2018.05.031.

[182] C. Della Volpe, A. Penati, R. Peruzzi, S. Siboni, L. Toniolo, C. Colombo, Combined effect of roughness and heterogeneity on contact angles: The case of polymer coating for stone protection, J. Adhes. Sci. Technol. 14 (2000) 273–299. https://doi.org/10.1163/156856100742555.

[183] A. Chantada, J. Penide, A. Riveiro, J. del Val, F. Quintero, M. Meixus, R. Soto, F. Lusquiños, J. Pou, Increasing the hydrophobicity degree of stonework by means of laser surface texturing: An application on Zimbabwe black granites, Appl. Surf. Sci. 418 (2017) 463–471. https://doi.org/10.1016/j.apsusc.2016.12.196.

[184] N. Parris, L.C. Dickey, M.J. Kurantz, R.O. Moten, J.C. Craig, Water Vapor Permeability and Solubility of Zein/Starch Hydrophilic Films Prepared from Dry Milled Corn Extract, J. Food Eng. 32 (1997) 199–207. https://doi.org/10.1016/S0260-8774(97)00015-0.

[185] D. Aslanidou, I. Karapanagiotis, Waterborne Superhydrophobic and Superoleophobic Coatings for the Protection of Marble and Sandstone, (2018). https://doi.org/10.3390/ma11040585.

[186] M. Frigione, Oleo / Hydrophobic Coatings Containing Nano-Particles for the Protection of Stone Materials Having Different Porosity, (2018). https://doi.org/10.3390/coatings8120429.

[187] S. Siegfried, S. Rolf, Stone in Architecture Properties, Durability, n.d.

[188] M. Clausi, S. Grasselli, A. Malchiodi, I.S. Bayer, Thermally conductive PVDF-graphene nanoplatelet (GnP) coatings, Appl. Surf. Sci. 529 (2020) 147070. https://doi.org/10.1016/j.apsusc.2020.147070.

[189] L. Pinho, F. Elhaddad, D.S. Facio, M.J. Mosquera, A novel TiO 2 -SiO 2 nanocomposite converts a very friable stone into a self-cleaning building material, Appl. Surf. Sci. 275 (2013) 389–396. https://doi.org/10.1016/j.apsusc.2012.10.142.

[190] X.Y. Ling, I.Y. Phang, G.J. Vancso, J. Huskens, D.N. Reinhoudt, Stable and transparent superhydrophobic nanoparticle films, Langmuir. 25 (2009) 3260–3263. https://doi.org/10.1021/la8040715.

[191] S. Naderizadeh, S. Dante, P. Picone, M. Di Carlo, R. Carzino, A. Athanassiou, I.S. Bayer, Bioresin-based superhydrophobic coatings with reduced bacterial adhesion, J. Colloid Interface Sci. 574 (2020) 20–32. https://doi.org/10.1016/j.jcis.2020.04.031.

[192] G. Cappelletti, P. Fermo, M. Camiloni, Smart hybrid coatings for natural stones conservation, in: Prog. Org. Coatings, Elsevier, 2015: pp. 511–516. https://doi.org/10.1016/j.porgcoat.2014.05.029.

[193] D. Quéré, Wetting and roughness, Annu. Rev. Mater. Res. 38 (2008) 71–99. https://doi.org/10.1146/annurev.matsci.38.060407.132434.

[194] D.M. Spori, T. Drobek, S. Zürcher, M. Ochsner, C. Sprecher, A. Mühlebach, N.D. Spencer, Beyond the lotus effect: Roughness influences on wetting over a wide surface-energy range, Langmuir. 24 (2008) 5411–5417. https://doi.org/10.1021/la800215r.

[195] U.A. Qureshi, Z. Khatri, F. Ahmed, M. Khatri, I.S. Kim, Electrospun Zein Nanofiber as a Green and Recyclable Adsorbent for the Removal of Reactive Black 5 from the Aqueous Phase, ACS Sustain. Chem. Eng. 5 (2017) 4340–4351. https://doi.org/10.1021/acssuschemeng.7b00402.

[196] M. Zucchelli, G. Mazzon, L. Bertolacci, R. Carzino, E. Zendri, A. Athanassiou, Stone sustainable protection and preservation using a zein-based hydrophobic coating, Prog. Org. Coatings. 159 (2021) 106434. https://doi.org/10.1016/j.porgcoat.2021.106434.

[197] S. Voltolina, L. Nodari, C. Aibéo, E. Egel, M. Pamplona, S. Simon, E. Verga, P. Scopece, A. Gambirasi, M. Favaro, A. Patelli, Assessment of plasma torches as innovative tool for

cleaning of historical stone materials, J. Cult. Herit. 22 (2016) 940–950. https://doi.org/10.1016/j.culher.2016.05.001.

[198] T.F. Garrison, A. Murawski, R.L. Quirino, Bio-Based Polymers with Potential for Biodegradability, Polymers (Basel). (2016).

[199] R.L. Feller, Accelerated Aging: Photochemical and Thermal Aspects, The J. Paul Getty Trust, Marina del Rey, CA, 1994. https://doi.org/10.1016/B0-12-370870-2/00002-0.

[200] V. Sabatini, C. Cattò, G. Cappelletti, F. Cappitelli, S. Antenucci, H. Farina, M.A. Ortenzi, S. Camazzola, G. Di Silvestro, Protective features, durability and biodegration study of acrylic and methacrylic fluorinated polymer coatings for marble protection, Prog. Org. Coatings. 114 (2018) 47–57. https://doi.org/10.1016/j.porgcoat.2017.10.003.

[201] M.A. Aldosari, S.S. Darwish, M.A. Adam, N.A. Elmarzugi, S.M. Ahmed, Using ZnO nanoparticles in fungal inhibition and self-protection of exposed marble columns in historic sites, Archaeol. Anthropol. Sci. 11 (2019) 3407–3422. https://doi.org/10.1007/s12520-018-0762-z.

[202] NORMAL 43/93 Misure Colorimetriche di Superfici Opache (Italian Normative on Stone Material—Colorimetric Measurement of Opaque Surfaces), 1994.

[203] M. Zuena, P. Tomasin, D. Costa, J. Delgado-Rodrigues, E. Zendri, Study of calcium ethoxide as a new product for conservation of historical limestone, Coatings. 8 (2018). https://doi.org/10.3390/coatings8030103.

[204] G. Mazzon, M. Contardi, A. Quilez-Molina, M. Zahid, E. Zendri, A. Athanassiou, I.S. Bayer, Antioxidant and hydrophobic Cotton fabric resisting accelerated ageing, Colloids Surfaces A Physicochem. Eng. Asp. 613 (2021) 126061. https://doi.org/10.1016/j.colsurfa.2020.126061.

[205] J.D. Rodrigues, A. Grossi, Indicators and ratings for the compatibility assessment of conservation actions, 8 (2007) 32–43. https://doi.org/10.1016/j.culher.2006.04.007.

[206] A. Athanassiou, L. Bertolacci, PROCESSO PER IL MIGLIORAMENTO DELLA BIODEGRADABILITÀ DEI MATERIALI POLIOLEFINICI. IT102020000016798, 2020.

[207] F.-X. Schmid, Biological Macromolecules: UV-visible Spectrophotometry, Encycl. Life Sci. (2001) 1–4. https://doi.org/10.1038/npg.els.0003142.

[208] S.A. Ruffolo, M.F. La Russa, M. Malagodi, C. Oliviero Rossi, A.M. Palermo, G.M. Crisci, ZnO and ZnTiO3 nanopowders for antimicrobial stone coating, Appl. Phys. A Mater. Sci. Process. 100 (2010) 829–834. https://doi.org/10.1007/s00339-010-5658-4.

[209] I. Standard, Iso 14851, 1999 (1999).

[210] R. Bayard, H. Benbelkacen, R. Gourdon, P. Buffière, Characterization of selected municipal solid waste components to estimate their biodegradability, (n.d.).

[211] V. Sabatini, E. Pargoletti, V. Comite, M.A. Ortenzi, P. Fermo, D. Gulotta, G. Cappelletti, Towards novel fluorinated methacrylic coatings for cultural heritage: A combined

polymers and surfaces chemistry study, Polymers (Basel). 11 (2019). https://doi.org/10.3390/polym11071190.

[212] F. Matthias, I. Atsushi, R.B.H. Tan, C. Kim, K. Hans-Jürgen, International Organisation for Standardisation (ISO). (2006). Environmental Management–Life Cycle Assessment–Requirements and Guidelines (ISO 14044)., (n.d.).

[213] A. Mauko Pranjić, J. Ranogajec, L. Škrlep, A. Sever Škapin, S. Vučetić, K. Malovrh Rebec, J. Turk, Life cycle assessment of novel consolidants and a photocatalytic suspension for the conservation of the immovable cultural heritage, J. Clean. Prod. 181 (2018) 293–308. https://doi.org/10.1016/j.jclepro.2018.01.087.

[214] J. Turk, A.M. Pranjić, P. Tomasin, L. Škrlep, J. Antelo, M. Favaro, A.S. Škapin, A. Bernardi, J. Ranogajec, M. Chiurato, Environmental performance of three innovative calcium carbonate-based consolidants used in the field of built cultural heritage, Int. J. Life Cycle Assess. 22 (2017) 1329–1338. https://doi.org/10.1007/s11367-017-1260-8.

[215] D.B. Settembre, F. Anna Maria, F. del H. Alfonso, G.M. Maria Pia, Riccardi Fernando E., Improving sustainable cultural heritage restoration work through life cycle assessment based model, J. Cult. Herit. (2017).

[216] T.J. Anderson, B.P. Lamsal, Development of new method for extraction of a-zein from corn gluten meal using different solvents, Cereal Chem. 88 (2011) 356–362. https://doi.org/10.1094/CCHEM-08-10-0117.

[217] W. Wei, P. Larrey-Lassalle, T. Faure, N. Dumoulin, P. Roux, J.D. Mathias, How to conduct a proper sensitivity analysis in life cycle assessment: Taking into account correlations within LCI data and interactions within the LCA calculation model, Environ. Sci. Technol. 49 (2015) 377–385. https://doi.org/10.1021/es502128k.

[218] M.N.S. Rodríguez, G.I. Cassab, Primary root and mesocotyl elongation in maize seedlings: Two organs with antagonistic growth below the soil surface, Plants. 10 (2021). https://doi.org/10.3390/plants10071274.

[219] K. Minolta, https://sensing.konicaminolta.asia/what-is-cie-1976-lab-color-space/, (n.d.).